

Characterization and optimization of a medical XY positioning platform

Pedro Miguel Lima Pinto

Master Dissertation

FEUP's Advisor: Prof. José Ferreira Duarte

Company's Advisor: Eng. Pedro Costa



Mestrado Integrado em Engenharia Mecânica

June 2020

Abstract

The present dissertation reports on work performed in conjunction with Interventional-Systems, a medical technology company. At the start of this project their newest robotic targeting platform, Micromate™, was design-locked and ready for market entry; this XY positioning platform, internal model name iONE (designation used from here on), is a small footprint “personal robotic assistant” for fluoroscopy guided interventional radiology procedures that aims at guiding medical instruments for high precision entry point and trajectories during minimally (image-guided) invasive procedures. With the product development effort for this equipment nearing completion, the legacy mechanical construction, resultant from a past generation product and partially revamped from cooperation projects with external companies, is in need for an overall, deeper, understanding regarding performance and manufacturability.

Having manufacturing activities and advanced testing already uncovered potential improvement points, others are sure to be discovered if a caution analysis of the system is to be carried. With this in mind, it was proposed for this project that, on one end, the mechanical construction should be studied with performance and manufacturability in mind to compile a list of possible system improvement, and, on the other end, that some of the identified opportunities should be tackled for improvement solutions.

Along this document a narrative and detailed explanation of the iONE system, problematic, challenges and product development stage can be found. In a first step, an equipment cost and performance analysis was done considering the application and key relevant requirements for the system; these analyses allowed for the identification of improvement possibilities that should provide value to both the company and customers.

In a second step, the identified points for improvement were addressed leading to improvement concepts (some of which were actually implemented). For all these concepts, evidence is provided to sustain the claim that either performance or manufacturability (system assembling included) were improved.

The activities carried during this project ultimately resulted in a cost optimization of the system, with material and manufacturing process changed for some components/sub-systems and in performance or assembly improvement concepts that make use of standard parts and assembly tools. Performance wise, a complete system (theoretical) static characterization was carried, and a breakdown on the root-cause for medical instrument deviation is detailed – this allowed for the identification of the sub-systems/equipment/components most affecting the system’s positioning accuracy and position retention capacity.

Topics mentioned in this document include, but are not limited to: the iONE system, the main components responsible for precise position and position retention, system play and rigidity, system use conditions and solicitations, the miniaturization challenge, system assembly concerns, system cost analysis, components/sub-systems manufacturability and optimization opportunities. The whole work has been developed according to Interventional-Systems quality management system and integrated into the company’s design improvement roadmap.

Resumo

Esta dissertação sumariza o trabalho realizado em conjunto com a Interventional-System, uma empresa de tecnologia médica. No início deste projeto a sua nova plataforma robótica, Micromate™, designada doravante por iONE (nome interno do modelo), encontrava-se pronta para lançamento no mercado. Esta plataforma consiste num assistente robótico pessoal de proporções bastante reduzidas que faz uso de um sistema de visão de modo a guiar instrumentos médicos para pontos e trajetórias de incisão precisos, sendo indicada para procedimentos minimamente invasivos de intervenção radiológica (fluoroscopia). Com o ciclo de desenvolvimento do produto a terminar, a construção mecânica que foi sendo renovada em alguns projetos de cooperação com empresas externas, tendo sempre por base os modelos anteriores, beneficiaria de um conhecimento aprofundado da globalidade do seu desempenho e da sua capacidade de fabrico.

Tendo testes e atividades de produção já descoberto alguns pontos de melhoria, outros serão certamente identificados se uma análise cuidadosa do sistema for realizada. Tendo isto em mente, foi proposto para este projeto que, por um lado, a construção mecânica fosse estudada do ponto de vista do desempenho e da facilidade de fabrico e que uma lista de potenciais pontos de melhoria fosse compilada, e, por outro lado, que algumas dessas oportunidades fossem abordadas em busca de uma solução de melhoria.

Ao longo deste documento é exposto o sistema iONE, a sua problemática, desafios e estado de desenvolvimento do produto. Num primeiro passo, foi realizada uma análise de custo e desempenho do equipamento tendo em vista a aplicação final e os principais requisitos do sistema, tendo estas análises permitido identificar possibilidades de melhoria que deverão trazer valor quer para a empresa quer para o consumidor.

Num segundo passo, os pontos de melhoria identificados foram abordados, originando conceitos de melhoria (alguns dos quais implementados neste projeto). Para todos estes conceitos, provas são apresentadas para suportar as alegações de que o desempenho ou a facilidade de produção (incluindo a facilidade de montagem) foram melhoradas.

As atividades realizadas durante este projeto resultaram, em última instância, numa otimização do custo do sistema, com materiais e processos de manufatura alterados para alguns componentes/subsistemas, e em conceitos de melhoria de desempenho ou montagem que fazem uso de partes *standard* e de ferramentas de apoio à montagem. Em relação ao desempenho, uma caracterização estática (teórica) do sistema foi realizada e são detalhadas as causas base para desvios no instrumento médico – isto permitiu identificar os subsistemas/equipamentos/componentes que mais afetam a precisão de posicionamento do sistema e também a capacidade de retenção dessa mesma posição.

Tópicos mencionados neste documento incluem (entre outros) o sistema iONE, os principais componentes responsáveis pelo preciso posicionamento e retenção de posição, as folgas e rigidez do sistema, as condições de uso e solicitações, o desafio de miniaturização, as preocupações de montagem, uma análise de custos, uma análise da facilidade de produção de certos componentes/subsistemas e ainda as oportunidades de otimização. Todo o trabalho foi desenvolvido de acordo com o sistema de gestão de qualidade da Interventional-Systems e integrado no seu plano de melhoria.

Acknowledgements

I would like to thank everyone at Interventional-Systems who I had the opportunity and pleasure to contact with. I thank them for doing me some favors along the way (like coordinating component deliveries, getting me into contact with suppliers, etc.), for their patience in instructing me about the system and answering my questions, and for making me feel part of the team during the last few months. I would also like to thank for the confidence that was deposited in me for some activities, hope I was able to rise to the challenge.

A special thanks to Pedro Costa, my advisor at Interventional-Systems, who was always available to answer my questions and to check up on me even when filled with work of his own. I thank you also for the freedom with which you allowed me to work during the last few months, for guaranteeing readily available data on the system (as it revealed necessary for these activities), for entrusting me with some impactful work and for the opinionated discussions; hope I was worthy of the deposited confidence.

Thanks also to Ferreira Duarte, my advisor at FEUP, for the discussions we have had the chance to have regarding this project and for always offering himself as available for contact should any problem arise.

Another thoughtful thanks to my family, for putting up with me for quite a few years already, and for supporting me all the way to this point; you have been absolutely essential (even you Carol, even you...).

A heart-warmed thanks to Francisca Duarte for the shared memes during the procrastination times, right before I was told to get back to work, but also for the encouragement to do more and better – your instructions are appreciated and will be delivered back in kind.

And finally, to all my friends, for making it all easier and more worthwhile.

Índice de Conteúdos

1	Introduction.....	7
1.1	Motivation for the Project.....	7
1.2	Interventional-Systems and iONE	7
1.3	Objectives – the iONE continuous improvement.....	8
1.4	Dissertation structure	10
2	State of the Art – Product Development and iONE	11
2.1	Medical Equipment Development.....	11
2.2	iONE – Product Description	14
2.3	iONE Development – Current Stage and inputs.....	19
3	Initial Situation, Problematic, Challenges and Tools.....	20
3.1	Initial improvement opportunities.....	20
3.2	Challenges, opportunities, and tools	22
4	System Analysis and Potential Improvements	25
4.1	System Cost Analysis.....	25
4.2	System Performance Analysis	32
4.3	Twin vs Single Pin EEF Adapter Analysis	46
5	System Cost Improvements	50
5.1	Clamping Plate and Blue Band components	50
5.2	NGE and SRB	52
5.3	External Gears	55
6	Leadscrew Nut and Linear Encoder	58
6.1	Linear Encoder Redesign.....	58
6.2	Leadscrew Nut Redesign	61
6.3	Linear Encoder and Leadscrew Redesign Testing.....	64
7	Linear Guides and System Assembly	74
7.1	Linear Guides Position and Assembly.....	74
7.2	Tolerance Analysis.....	75
7.3	Improvement Solution	79
8	Conclusions and Future Work.....	82
	References	84
	Appendix A – Datasheets.....	85
	Appendix B – Calculation results according to VDI 2736.....	90

Abbreviations

TP – Trajectory Platform

EEF – End-Effector

NGE – Needle Guide Extensions

LSN – Leadscrew Nut

p-LSN – Plastic Leadscrew Nut

b-LSN – Brass Leadscrew Nut

PNU – Power and Network Unit

SRB – Strain Relief Box

CU – Control Unit

PA – Positioning Arm

PIM – Plastic Injection Molding

OTS – Out the Shelf (standard)

FDM – Fused Deposition Modeling

SLS – Selective Laser Sintering

MFJ – Multi Jet Fusion

VC – Vacuum Casting

LG(s) – Linear Guide(s)

FEA – Finite Element Analysis

EOL – End of Life

V&V – Verification and Validation

Figures List

Figure 1 – Interventional-System’s logo [Interventional-Systems, 2020] 7

Figure 2 – Stealth Autoguide™ (left) [Medtronic, 2020] and Micromate™ (right) [Interventional-Systems, 2020] 8

Figure 3 – The PDCA process [Unknown, 2020] 9

Figure 4 – Structured Approach to Product Development [Pereira, 2019] 11

Figure 5 – Direct Approach to Product Development [Pereira, 2019] 12

Figure 6 – Design Waterfall – [U.S. Food & Drug Administration, 1997] 13

Figure 7 – iONE sub-systems 14

Figure 8 – Trajectory Platform interface (left) to the Positioning Arm (right) 15

Figure 9 – TP modular construction, full system (left) and one open module (right) 16

Figure 10 – TP Drive Chain example 16

Figure 11 – TP overall mechanical chain 17

Figure 12 – The NGE Interface to the EEF 18

Figure 13 – The system’s universal End-Effector, mounted (right) and independent (left) 18

Figure 14 – Linear encoders for ANG module 20

Figure 15 – Drive Chain A1 to Carriage A1 interface 21

Figure 16 – Leadscrew and linear guides 21

Figure 17 – Example of characterization graphics for drive chain backlash 22

Figure 18 – Examples of characterization outputs 23

Figure 19 – Trajectory Platform general dimensions 24

Figure 20 – iONE system costs 25

Figure 21 – iONE system unique part count 25

Figure 22 – The TP areas considered in the cost analysis 26

Figure 23 – TP areas cost (left) and number of parts (right) 27

Figure 24 – TP sub-areas cost (left) and number of parts (right) 27

Figure 25 – TP part types cost and number of parts 27

Figure 26 – Examples of TP holder parts 28

Figure 27 – TP screw distribution 28

Figure 28 – Insulation parts in PA™ connection 29

Figure 29 – Electronics sub-area w/+w/o the PCBs 29

Figure 30 – Overall structure area, housing (top) and blue tape (bottom) sub-areas 30

Figure 31 – Bearing block related components 30

Figure 32 – External gears main components 30

Figure 33 – The NGE assembly sub-area 31

Figure 34 – SRB housing components 31

Figure 35 – TP x and y axis and deviations illustrated for a HOME position TP 33

Figure 36 – Performance study; EEF transmitted forces to the TP	34
Figure 37 – Visual representation of Position Error	35
Figure 38 – Example of drive chain backlash characterization	35
Figure 39 – Reliance Gear Backlash calculations	36
Figure 40 – LSN backlash characterization	36
Figure 41 – Linear guide deviation equations [NSK, 2020]	37
Figure 42 – Worst-Case vs Actual Case	38
Figure 43 – NGE-EEF interface and spring play compensation calculations	38
Figure 44 – Example of the impact of NGE-EEF interface play in instrument deviation	38
Figure 45 – EEF adapter twin and deviation modes due to internal plays	39
Figure 46 – 2nd deviation mode impact without width restriction	40
Figure 47 – 2 nd deviation mode impact with width restriction	40
Figure 48 – EEF FEA analysis displacement results	40
Figure 49 – Linear guide deviation equations [NSK, 2020]	41
Figure 50 – Linear Guide upwards rigidity (left) and resultant instrument deviation (right) ..	41
Figure 51 – Simplified screw deviation calculation (left) and impact at instrument (right)	42
Figure 52 – EEF universal adapter single (left) and twin (right)	46
Figure 53 – Simulation contact sets (left) and standard mesh (right)	48
Figure 54 – EEF “solid body” geometry	49
Figure 55 – Clamping Plate and BB components general dimensions	50
Figure 56 – Online configurator quote results for additive manufacturing cost-optimization.	51
Figure 57 – NGE assembly area cost allocation	52
Figure 58 – NGE accessorial parts	52
Figure 59 – Quote results scaled for a total of 60 systems	53
Figure 60 – External Gears setup for the drive chain	55
Figure 61 – Drive chain position within a TP module	56
Figure 62 – Plastic Gears Assembly	57
Figure 63 – Example of the “denting effect”	58
Figure 64 – Washer for extra pressure between wiper and foil potentiometer	59
Figure 65 – Initial leaf spring wiper design – A1 (left) and A2 (right)	59
Figure 66 – Custom wiper design and parts	60
Figure 67 – Tolerance analysis – carriage A2 and foil potentiometer	60
Figure 68 – OTS wiper temporary/prototyping structural solution	61
Figure 69 – OTS wiper final structural solution	61
Figure 70 – Leadscrew Nut over definition scheme	62
Figure 71 – Leadscrew Nut potential redesigns	62
Figure 72 – p-LSN front view	62

Figure 73 – Translating Nut assembly.....	63
Figure 74 – Spherical Joint Nut assembly	63
Figure 75 – Testing system construction.....	64
Figure 76 – Test results for controlled foil potentiometer forces	65
Figure 77 – Test results for 168hrs at 50°C/95% relative humidity	65
Figure 78 – p-LSN system subject to stationary HOME position for 168hrs at 40°C/80% rel. humidity.....	66
Figure 79 – p-LSN characterization at 10°C	67
Figure 80 – Example of burn-in impact in motor current; pre-conditioning (left) and post-conditioning (right).....	68
Figure 81 – Drive chain backlash when installed with the p-LSN.....	68
Figure 82 – Test setup to evaluate the LSN backlash.....	69
Figure 83 – Reworked p-LSN design	69
Figure 84 – Reworked p-LSN motor currents at room temperature (top) and 10°C (bottom) .	72
Figure 85 – Characterization at 6°C with current B-LSN.....	73
Figure 86 – Baseplate-A1 linear guide assembly	74
Figure 87 – A1-A2 linear guide assembly.....	74
Figure 88 – Baseplate-A1 linear guide assembly – side section view.....	74
Figure 89 – A1-A2 linear guide assembly front view	75
Figure 90 – TP technical drawings LG mounting surfaces relevant tolerances	76
Figure 91 – Impact of mounting deviations on linear guide performance [NSK, 2020].....	78
Figure 92 – Illustration on the influence of flatness on the linear guides [MiSUMi, 2014]	79
Figure 93 – Recommended assembly procedure w/o reference edges, pins or vises – from Figure 100, appendix A.....	80
Figure 94 – Concept for Baseplate-A1 mounting jig	81
Figure 95 – Concept for A1-A2 mounting jig	81
Figure 96 – TP Maxon Gearbox GP10A 218416 datasheet extract	85
Figure 97 – Datasheet for the foil potentiometer.....	86
Figure 98 – Datasheet for the OTS wiper.....	87
Figure 99 – Datasheet for SPD/SI 0.4 modulus acetal gears.....	88
Figure 100 – Linear Guides Datasheet extract - installation	89

Tables List

Table 1 – Summary of Performance Calculations	44
Table 2 – Summary of each component contribution to drive chain backlash	44
Table 3 – Simulation results for “single pin” and “twin pin” geometries	48
Table 4 – FEA results for additional EEF study objectives	49
Table 5 – Additive Manufacturing Final Selection	51
Table 6 – Summarized results from VDI 2736 calculations	57
Table 7 – Summarized potentiometer results for April tests	70
Table 8 – Summarized reworked p-LSN backlash results for April tests	71
Table 9 – Linear Guide mounting surface maximum manufacturing errors	76
Table 10 – Comparison between required and actual LG mounting surfaces	77
Table 11 – Calculations according to VDI 2736	90

1 Introduction

1.1 Motivation for the Project

While nearing product launch for a 2nd generation, patented, SMART robotic platform for image guided therapies (targeting minimally invasive, micro-invasive and/or non-invasive interventional healthcare), iSYS Medizintechnik GmbH – Figure 1 – is also elaborating and starting a continuous improvement roadmap for the product.

Having received feedback from production activities and system hardware tests, the company has identified a few suboptimal areas on the hardware and is interested in a deeper study on the mechanical construct of the device and on the identification of a list of future improvements. Additionally, any immediate improvement for the suboptimal areas would also be of interest to the company.

Making use of the remote work capabilities supported by the company, namely the digitalization of all the work carried by the development and production teams, the analysis and improvement project could be done at a distance from the company's physical offices while maintaining close contact, via online calls, with the relevant peers.

1.2 Interventional-Systems and iONE

Interventional-System, or iSYS Medizintechnik GmbH, based in Austria (Bergwerksweg 21, 6370 Kitzbühel) is an “emerging player in the innovation and clinical integration of SMART Robotic Solutions for image guided therapies” [Interventional-Systems, 2020].



Figure 1 – Interventional-System's logo [Interventional-Systems, 2020]

Having released the iSYS1[®], first-generation, robotic platform for fluoroscopy-based image guided interventions back in 2010 and, in the meantime, worked on the development of the iSYS1 NAVI+ for CT-guided interventions and iFix (a patient stabilization method), it is approaching the market release of a second-generation robotic platform system with the internal designation of iONE and known as Micromate[™].

The iONE device, or Micromate[™], is a positioning and guidance system intended for the spatial positioning and orientation of instrument holders or tool guides to be used to hold and guide standard instruments, based on a pre-operative, operative (real time) plan and feedback from an image-guided navigation system or trajectory planning station with two-dimensional, three-dimensional imaging software and real time imaging.

The system intends to innovate on robotic-assisted minimally invasive procedures by providing a cheap, precise, modular/adaptable design that should allow for a small footprint in the operating room, easy access from the physician to the patient and quick deployment combined with fast surgery and dismounting times.

The iONE is also a culmination of development years in partnership with Medtronic™ in the making and certification of a neurosurgical/cranial robotic guidance platform: Stealth Autoguide™ – the Medtronic system is market-released and already at use at a pediatric health system in the US, the Phoenix Children’s Hospital, and is also a direct descendant from iSYS1. Both systems can be seen in Figure 2.



Figure 2 – Stealth Autoguide™ (left) [Medtronic, 2020] and Micromate™ (right) [Interventional-Systems, 2020]

The iONE intends to broaden the range of uses of Stealth Autoguide™ to other areas of healthcare interventional procedures to, and according to the company’s vision, ensure a higher quality standard to millions of patients worldwide. The product intends to merge micro-robotics with the company’s SMART philosophy – Safe, Multipurpose, Affordable, Robust and Trend Setting – for medical devices, while pursuing the highest-level goals of reducing the risk of complications during therapeutic procedures and opening up new opportunities for diagnostic and treatment methods [Interventional-Systems, 2020].

Achieving an affordable, innovative, and precise system is a continuous improvement process for Interventional-Systems meaning that there are always open opportunities for work. Having the new system design temporarily frozen while nearing market entry means, for the company, an opportunity to plan for future optimizations – it is within this context that the current project is inserted.

1.3 Objectives - the iONE continuous improvement

The continuous improvement effort, commonly referred to by the Japanese term of Kaizen (meaning change for good), is the constant pursuit of better. Usually consisting on a collective of small projects managed according to the philosophy of the PDCA cycle, the goal is to pursue quality through numerous projects with accumulating impact [Nóvoa & Faria, 2019]. The PDCA cycle is schematized in Figure 3 and consist in 4 phases:

- Plan – Plan the improvement actions;
- Do – Execute the actions according to what was planned;
- Check – Assess the obtained results;
- Act – Correct and replan;

The work carried (and as planned to be carried for this project), when related to the iONE system, was mostly targeted to address the “Plan” phase of the PDCA cycle, with the intention to take actions regarding the better understanding of the capabilities of the platform and the uncovering of potential improvement aspects. Despite this, and for certain topics, actions were taken not only to plan for changes but to achieve them through the proposal and testing of improvement solutions.

Therefore, it can be said that the project was mostly aimed at planning improvements, when contextualized in the grand scheme of the product development effort, but, had the ultimate objective of doing, checking and acting on actual cost/performance changes.

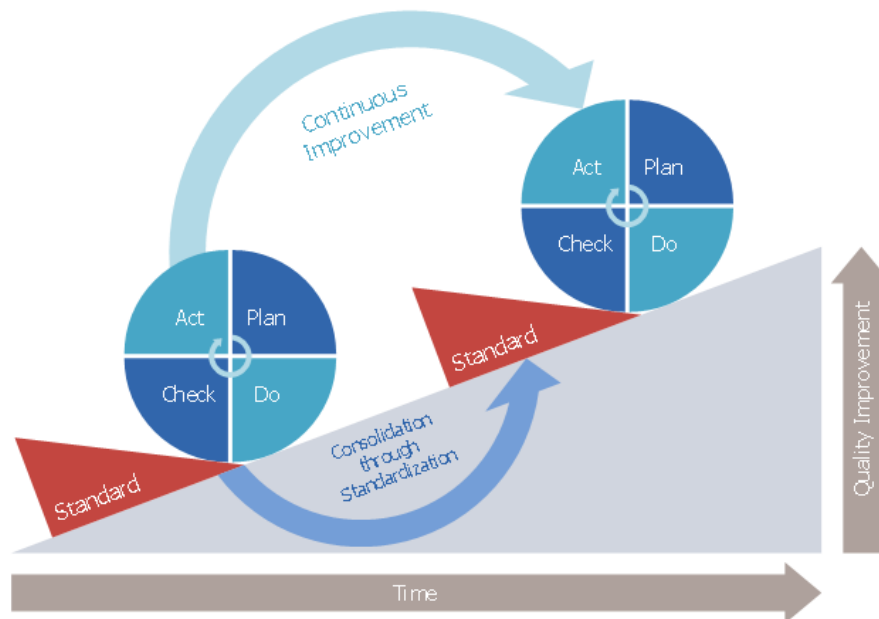


Figure 3 – The PDCA process [Unknown, 2020]

The project’s initial goals, as stated in the dissertation protocol were:

1. Design analysis of a robotic medical device for percutaneous and minimally invasive applications;
2. Identification of possible improvements;
3. Implementation of engineering practices to improve reliability and manufacturability;
4. Testing and characterization of the equipment and proposed changes.

During the pursuit of these previously mentioned objectives, however, a greater understanding of the system was achieved, and new possibilities risen. While still working within the initial objective of the project a more detailed list of the project’s objectives regarding the iONE system can be detailed as:

1. Analysis on the overall equipment cost;
2. Analysis on the manufacturing process selection (cost-effectiveness);
3. Analysis of the equipment mechanical positioning and position retention capacity;
4. Identification of the main contributing factors to equipment mechanical performance;
5. Estimation of device performance and contributing factors;
6. Identification of root-causes for major assembly difficulties;
7. Proposal of design changes for system improvement;
8. Test of proposed design changes;

Being a project performed in the context of a dissertation for a master’s in mechanical engineering it must be said that the project was mostly aimed at the mechanical aspects of the platform and that the electrical/electrical and software constructional aspects, although of extreme importance to the system, were not in scope – however, the impact of the mechanical construction in the electrical component performance was considered. Analyzing mechanical aspects of the system was planned to include activities such as: FEA, norm-based project calculations, accelerated lifetime testing, material resistance analysis and standard component evaluation.

1.4 Dissertation structure

The present document offers an overview of the activities performed within the context of the previously mentioned project, from contextualizing the reader within the general development stage, challenges and goals of the product to sharing details on its functionalities, architecture and potential points of improvement. In between, actions taken during the project will be discussed, main considerations will be presented, the thought process will be detailed, and the results/conclusions will be shared. To accomplish this, the dissertation will be divided into five major parts:

The first part's objective is to introduce the reader within typical product development concepts, with a special focus on medical device development, as well as to introduce the product's mechanical architecture, functionalities, and internal workings.

The second part is aimed at presenting the equipment's situation at the beginning of the project as well as the tools made available by the company for the system's analysis and improvement process. A final mention to the project challenges and outputs is also present.

The third part's objective is to provide a summary of the executed system analysis, both regarding cost and performance – the first considering potential cost reduction opportunities, and the latter considering accuracy during position and position retention. The rationale and main conclusions will be provided.

The fourth, most extensive, and final part, details the optimization effort, with several, justified, improvement proposals. Whenever possible the improvements were implemented in the system and feedback on the change is present, in other cases the implementation was not possible to achieve within this project's time frame and thus the improvement proposals were left as concepts.

2 State of the Art - Product Development and iONE

In this chapter, a brief introduction to product development precedes a description of the XY medical positioning platform. Regarding product development, the present work will be framed within the typical development cycle of a product so as to be better understand the challenges at the start of this work; regarding the platform description, the whole system (iONE) will be detailed along with its objectives, value proposition and requirements – this should allow a better understanding of the system and its most important functionalities.

2.1 Medical Equipment Development

Product development, and in particular medical product development, is important to be studied given the increasing control that has been taking place on the design of medical products. A concrete example of this control is REGULATION (EU) 2017/745 OF THE EUROPEAN PARLIAMENT AND OF THE COUNCIL, which obliges medical device manufacturers to follow a set of good practices, and document these practices, during product design as well as to have technical information readily available during, and for a set amount of time after, product commercialization – this has profound impact on the flexibility of the equipment’s design and on the possibilities for design changes as design decisions are made.

Product development theory, and implementation, is thus a very important area of study and for that reason it is included in this work. However, as the available information is quite vast, only a brief mention to the most important topics of product development is present in this document. The presented topics have been chosen to introduce the reader to product development and to inform on the several project phases and relevant documentation needs that are part of it – this is aimed at providing the reader with the ability to better understand the decisions taken during the project, in case of no previous experience in this field of work.

In broad terms a product can be defined as something commercialized by a company, targeting its customers, and typically intended to make a profit; and product development can be defined as a set of multidisciplinary activities that origin from a product idea or market opportunity that end with the launch of full-scale product production [Pereira, 2019].

These activities are particularly important if considering that product development is the most relevant phase to determine a product’s final quality and success – as is mentioned in [Speer, Ultimate Guide to ISO 13485 Quality Management System (QMS) for Medical Devices, 2018] and that they account for the most significant portion of time burdens for the company and for the most significant portion of product sell costs [Pereira, 2019].

Product development activities are usually guided by a certain workflow that is dependent on the company/institution they occur, nonetheless [Pereira, 2019] mentions two very common general approaches to product development that are, in one way or another, used independent from where the activities take place: Structured Approach and Direct Approach (“Ad Hoc”) – these are schematized in Figure 4 and Figure 5, respectively. It can be considered that the iONE system has followed a structured approach to product development and, at the time of this project, finds itself in between the last two stages: “Product Testing” and “Product Support”.



Figure 4 – Structured Approach to Product Development [Pereira, 2019]

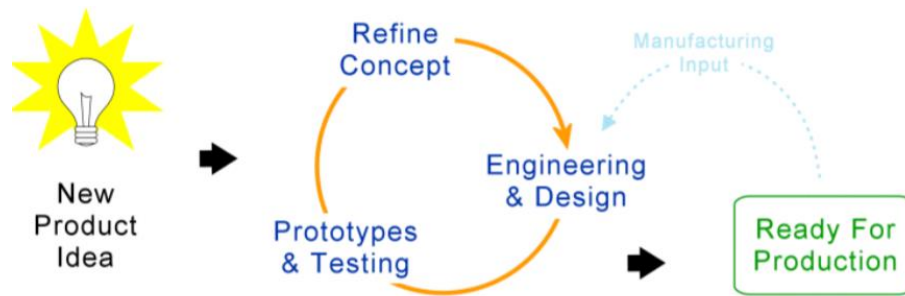


Figure 5 – Direct Approach to Product Development [Pereira, 2019]

The work detailed in this document must then be understood as part of an ongoing structured product development activity that is nearing completion. Still, despite most of the development effort occurring in a structured manner, most of the work that is dedicated to product optimization is occurring in parallel and follows more of a direct approach when it comes to concept generation and idea testing. It is, therefore, important to understand how this direct approach, taking place during optimization, can coexist with structured activities; we will begin with a look at the structured approach.

The structured approach to product development that guides the work activities for iONE is a requirement for medical devices as detailed in the European Medical Device Regulation (MDR), or, in particular, in EN ISO 13485:2016 “Medical Devices – Quality management systems – Requirements for regulatory purposes”, which is the harmonized standard that defines how an organization can ensure that the product realization complies with the applicable regulations. The impact of this norm in product development is linked to defined, very concrete, steps that should be followed during development and design activities – these steps are also, in some way, harmonized with the US FDA design controls 21 CFR Part 820.30 (thus, a controlled development process is not exclusive to the European Union), and include the following stages as summarized by [Speer, The ultimate guide to Design Controls for Medical Device Companies, 2018]:

- Design and Development Planning
- Design and Development Inputs
- Design and Development Outputs
- Design and Development Reviews
- Design and Development Verification
- Design and Development Validation
- Design and Development Transfer
- Control of Design and Development Changes
- Design and Development Files

These above-mentioned stages in product development are much like those present in the “Structured Approach” detailed in Figure 5 but are more representative of the many project iterations that are required during the development effort. This iterative development process is commonly represented in a waterfall scheme, such as the one detailed in Figure 6, where product definition activities show at the top, represented through user needs and design inputs, and the final equipment shows at the bottom, linked to these product definitions through verification and validation (V&V) activities.

The development cycle, according to the regulation and relevant norms, officially begins with the creation of a development plan, and can be considered as “ending” upon the completion of the Design History File – the Design History File is a specific term detailed in FDA design controls 21 CFR Part 820.30 that details a record where all design activities are clearly and precisely and documented in an organized manner for easy consulting by the development team members and auditors, and serves as proof of compliance with the international regulation.

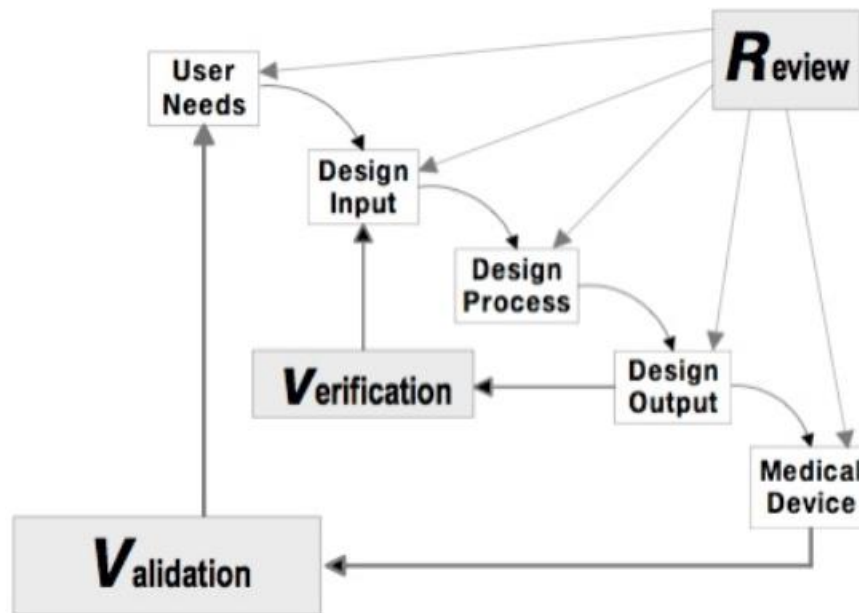


Figure 6 – Design Waterfall – [U.S. Food & Drug Administration, 1997]

Between the beginning and the end of product development all stages must be documented, starting with the user needs – these are the primordial requirements for the design and in sum express how the product will interact and benefit the customer. Building on top of these user needs are the design inputs, which include component/sub-system/system requirements; these requirements will condition the product concepts, architecture, and overall final form and will be considered throughout the entire design process and following V&V with the objective of ensuring proper performance and safety of the equipment (they do not consider business needs).

As a result of the design process a set of physical or software-based solutions (or combination of these) will be compiled – these are referred to as design output. While no specific process is required, per existing regulation, to exist during the design process (hence why optimization activities carried in this project followed the “Ad Hoc” approach) it is common for a brainstorm session to take place, followed by the creation of product concepts, product architecture and prototypes.

The design outputs will then be subject to a verification process to ensure that initially put forth design inputs are met, or, as [Speer, *The ultimate guide to Design Controls for Medical Device Companies*, 2018] puts it: “that the product is done right”. The design process and the feedback provided by the verification (which can include a broad range of activities such as design output inspection or prototype testing) lead to a cyclic development and refining of the soon to be medical device. At any point during this iterative cycling, design reviews can take place to ensure the activities are progressing according to plan and objectives are being met.

Eventually, the device will have met the necessarily/applicable design inputs/requirements. It is at this point that the device must be validated – this means that it must be proved that the device fulfills the initially put forth user needs or, in other words, that the design product is “the right product” [Speer, *The ultimate guide to Design Controls for Medical Device Companies*, 2018]. Typically, validation activities are performed by end-users following some sort of planned testing structure created by the equipment manufacturer.

The importance of these verifications and validation activities is that they provide feedback to the developing team and help steer product development in the correct path before and after the design and development transfer. Also, because international regulation, like the European Medical Device Regulation, forces the manufacturer to obey to certain general safety and performance requirements (GSPRs), the V&V activities will function as an extra guarantee that that the medical device follows all the necessary quality standards.

As mentioned, the next step after V&V activities is Design Transfer (it should be noted that transfer must begin prior to the completion of V&V), beginning with the transfer to production of the initial design specifications to build the first prototypes and continuing iteratively until production is validated. After this stage it is especially important to track any further design changes, as they may impact the system's reported functionality, performance, safety, usability, etc.; for this reason, there is particular mention in regulation to the need to have design change controls implemented in official design processes – this development phase is partially correspondent to the Product support stage detailed in Figure 4.

All the design work will be compiled in a special technical document referred to as Design History File – the conclusion of this document marks the “end” end of product development. Despite this, the standards require that post-market surveillance activities proceed for the market duration of the product and allow for the possibility to do further changes to the product.

With iONE launching in the market at March 10th 2020, the current project has to account for all this development baggage and must account for the impact of changes on function, usability, safety and on the “hidden cost” of technical documentation.

2.2 iONE - Product Description

Before delving into iONE's design inputs and verified performance it is perhaps easier to understand the product while looking at the design outputs – the present chapter will then introduce the iONE system and the main components and sub-systems that will be the focus of next chapters' analysis.

The system is modular and composed by the sub-systems shown in Figure 7. The total system weight is around 18kg; however, the user only needs to manipulate up to 3kg, which are mostly centered around the Positioning Arm and the Trajectory Platform (TP). The TP is a XY Positioning Platform and will be the focus of this work. Another sub-system, the end-effector, that ensures connection to the medical instruments will be detailed later.

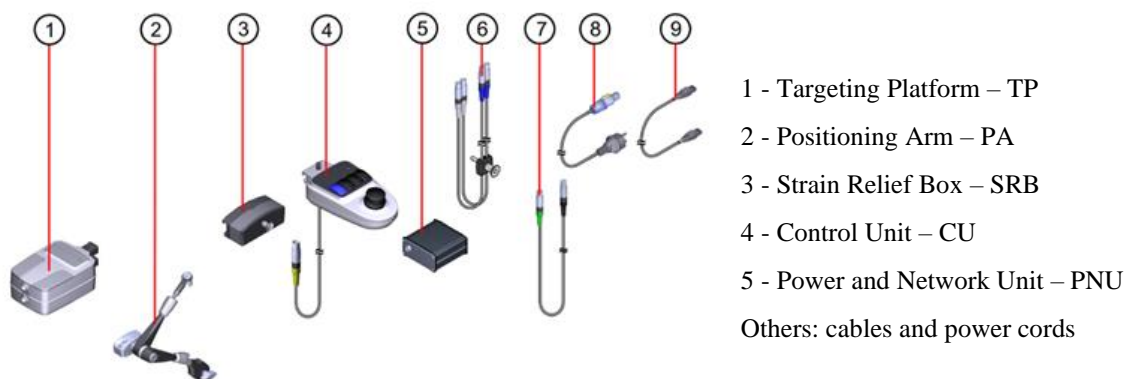


Figure 7 – iONE sub-systems

To better understand how the system provides value to its customers and, consequently, to understand the key aspects of the later analysis and necessary improvements it is important to understand the typical workflow for the physician that will operate the equipment, which consists of 8 essential steps:

1. Patient positioning;
2. Attachment of the table adapter (Positioning Arm adapters);
3. Sterile covering the patient;
4. Gross positioning the robot (Positioning Arm);
5. 2D/3D image acquisition;
6. Automatic, precision alignment to the target point (Trajectory Platform + EEF);
7. Instrument guidance to the target point (Trajectory Platform + EEF);
8. Medic control over the incision of the medical instrument (for most applications).

The core functions behind the system are thus:

- Gross-Positioning;
- Precise Positioning;
- Instrument holding.

The first step in positioning is referred to as gross-positioning and is accomplished by the user while interacting with the Positioning Arm, which is directly connected to the TP by the bottom starburst interfaces – see Figure 8. This mechanical arm allows for 7 degrees of freedom (DOF), a minimum of 300mm of range of motion and a quick reposition within less than 15 seconds (average of 5-10 seconds). The user is responsible for achieving the correct position, based on entry point and trajectory, within a deviation of $\pm 20\text{mm}$ and $\pm 15^\circ$.

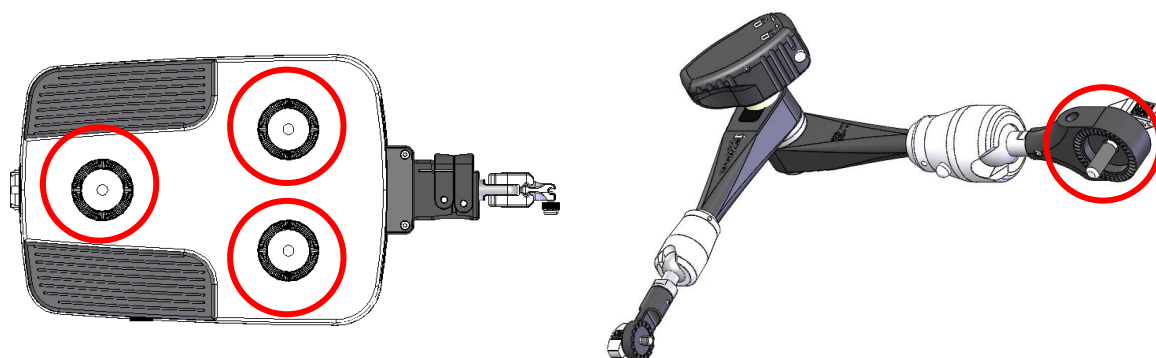


Figure 8 – Trajectory Platform interface (left) to the Positioning Arm (right)

The second and third steps are left to the TP, which must accurately achieve the precise entry point and trajectory with the medical instrument at its tip and then allow for a rigid holding of the instrument for the physician to operate it without concern for trajectory deviations.

The system's ability to achieve a precise position with the held medical instrument and the ability to be rigid and/or near play free are thus crucial to the equipment's performance and to the value that it can provide to the customer.

Because the user can have confidence in the precise medical instrument position and instrument guidance the overall loads for the system are very much reduced. Additionally, all loads acting on the system are only applied after movement is complete, meaning there is no real requirement for the system's dynamic performance, with the exception to the need to detect collisions – this is done via control of the motor current which, when in excess, triggers a break function (a 40N load corresponds to around 100mA being supplied to the electrical motors).

Trajectory Platform – The main system/sub-system

To accomplish the two crucial workflow steps (precise position and instrument guidance) the Trajectory Platform, the main system, translates the commands that are received from the Control Unit into mechanical motion. The mechanical motion is achieved by the movement of two modules: the upper module, that angulate the surgical instruments carried by the end-effectors, and the lower module, that performs translation. The two halves allow 2x2 degrees of freedom (DOF) and a range of motion of $\pm 20\text{mm}$ (lateral and longitudinal directions) and up to 15° angulation (for pitch and yaw angles).

The two modules that make up the Trajectory Platform are identical and called the POS and ANG modules (lower and upper module, respectively) – The system can be seen in further detail in Figure 9, where a full system is compared to an open module (where the housing elements have been removed to reveal interior details).

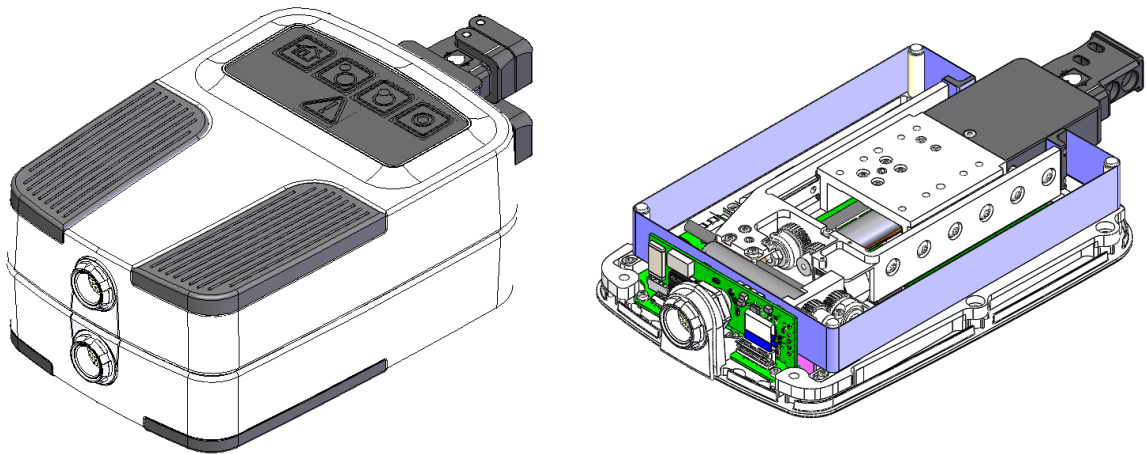


Figure 9 – TP modular construction, full system (left) and one open module (right)

Each module is then comprised of two carriages: carriage A1 and carriage A2, responsible for the x-axis and y-axis movements, respectively. It should be noted that carriage A1 sits on top of a baseplate and carriage A2 sits on top of carriage A1. Another important constructional aspect is that the link between the POS and ANG modules is achieved by a rigid connection of POS' carriage A2 to ANG module's baseplate.

Regarding carriage A1, it is responsible for the x-axis movement of itself and carriage A2 and is powered by drive chain A1. Carriage A1 is also connected to the blue tape, which is a fabric meant to safeguard the system from the intake of excessive dust, particles, and water during time spent not covered with a drape – which is a small interval between storage in a specific case and setup close to the patient.

Drive Chain A1, seen in detail in Figure 10, is built on top of a static structure referred to as the “Bearing Block”. Carriage A1 also contains a drive chain built into itself (this powers carriage A2's independent y-axis movement).

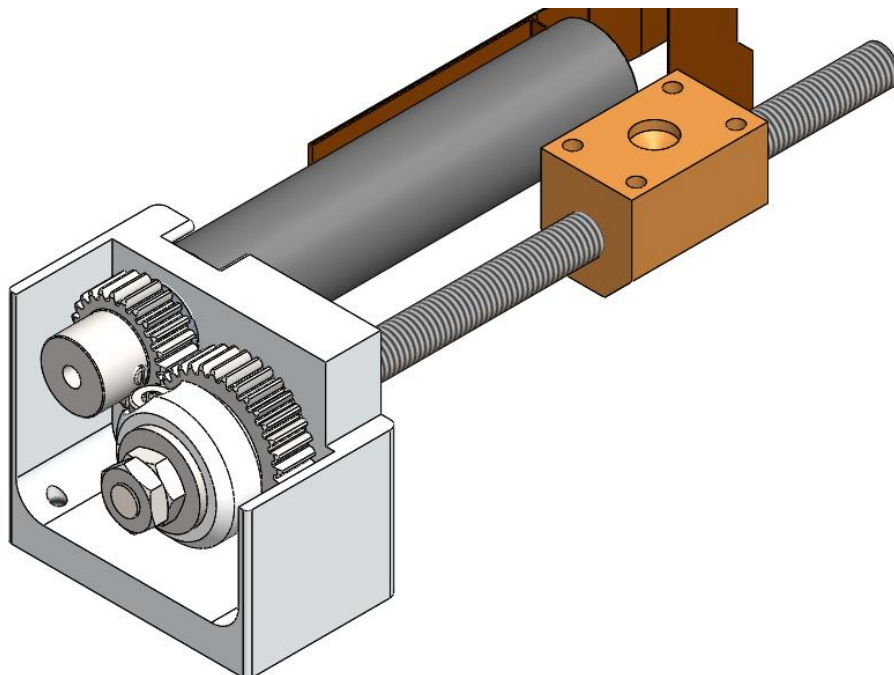


Figure 10 – TP Drive Chain example

Carriage A2 is, in turn, connected to the Needle Guide Extension (NGE), which will ensure a connection with an external sub-system responsible for the medical instrument holding, the previously mentioned EEF.

The system's overall movement chain can be seen in more detail in Figure 11, where special focus is given to the most basic unit of movement for the system – the drive chain. The figure details the drive chain that powers carriage A1 (which is similar to A2's drive chains) and clearly shows the presence of an electrical motor, a pair of gears (referred to as the "external gears") and a spindle plus nut configuration (referred to as the "leadscrew"). This drive chain converts the rotary motion of the electrical motor into linear motion of the carriages. It should be noted that each carriage slides on two miniature linear guides.

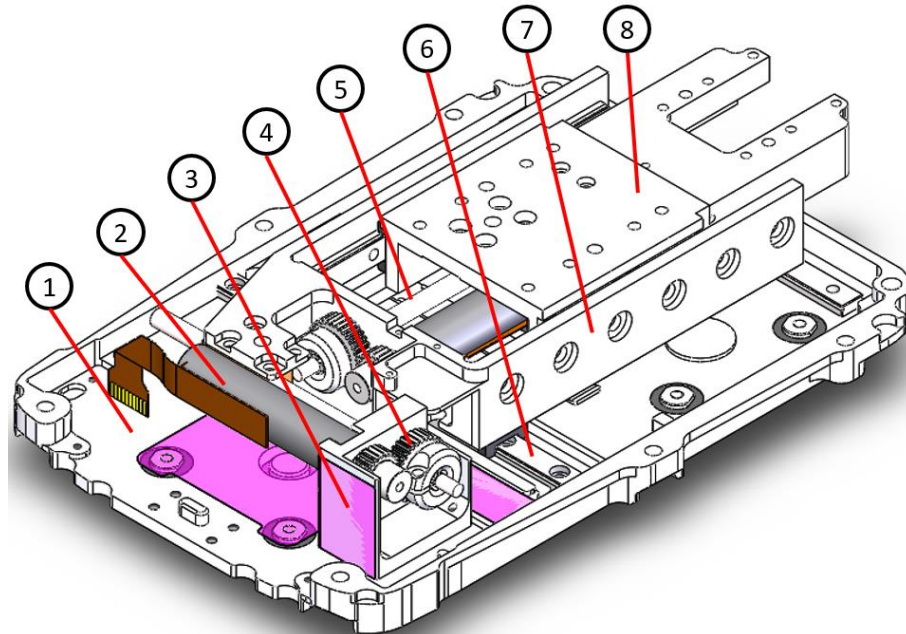


Figure 11 – TP overall mechanical chain

The full list of components that make up the overall movement chain is:

1. Baseplate – “Floor” structure for each module;
2. Electrical Motor – Activators for each of the module’s axis;
3. Bearing Block – Structure for carriage A1’s drive chain;
4. External Gears – Transmitters for the rotary motion;
5. Leadscrew – Converters for rotary-linear motion;
6. Linear Guides – Sliders for the Baseplate-A1-A2 relative movements;
7. Carriage A1 – Structure for the x-axis movement;
8. Carriage A2 – Structure for the y-axis movement;

Then, an additional structural component is attached to carriage A2: the needle guide extension, or NGE, is responsible for guaranteeing the output of the movement that is generated in the Trajectory Platform. To accomplish this, it interfaces with the EEF through a “snap” shaft-hole connection with the aid of two pins – see Figure 12.

This interface is intended to be dismountable to allow for the connection with several, geometrically different, EEFs thus ensuring that a new medical instrument will not require a redesign of the TP but instead the design of a specific EEF, if not able to connect to the previously existing structures.

This interface is crucial for the TP and should be kept in mind as it will be object of a detailed analysis in future chapters. It represents a challenge for the system as it must allow a suitable fit of the EEF, locking it both axially as well as radially, while allowing for concentric rotation.

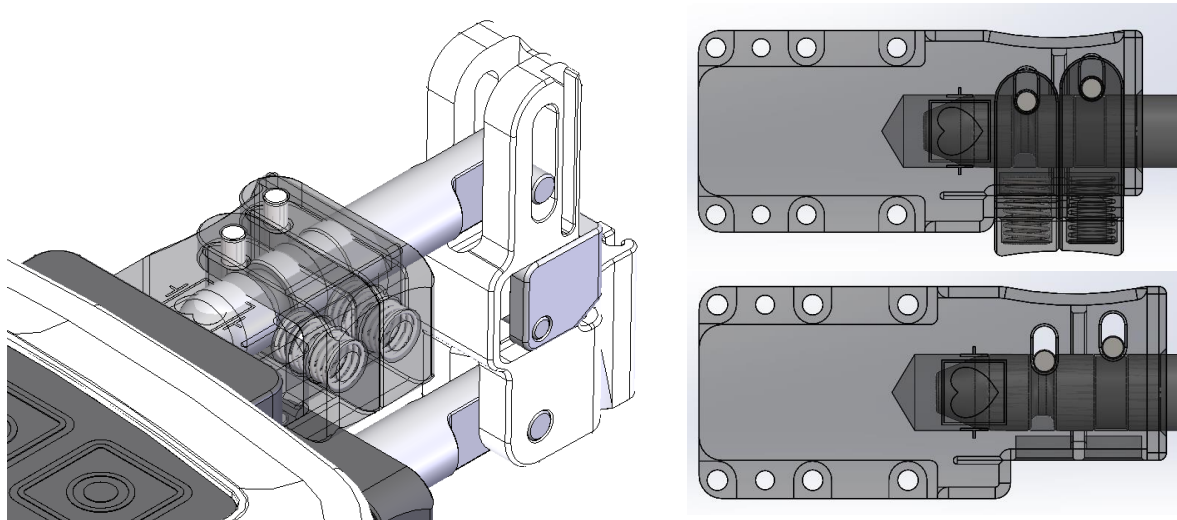


Figure 12 – The NGE Interface to the EEF

End-Effector – Interface to the medical instrument

The connection between the Trajectory Platform and the medical instrument is guaranteed by the EEF sub-system that, despite not belonging to the iONE system, is under the scope of the next chapters’ analysis for its impact on the overall accuracy. A universal EEF is detailed in Figure 13 also mounted with a Needle Guide (used to hold needle-type medical instruments).

The End-Effector is responsible for translating the POS and ANG movements into translation and rotation of the medical instrument. It consists in a rigid body with two articulations at the POS and ANG level – these interfaces connect to the guiding joints that enter directly inside the NGE as previously seen in Figure 12.

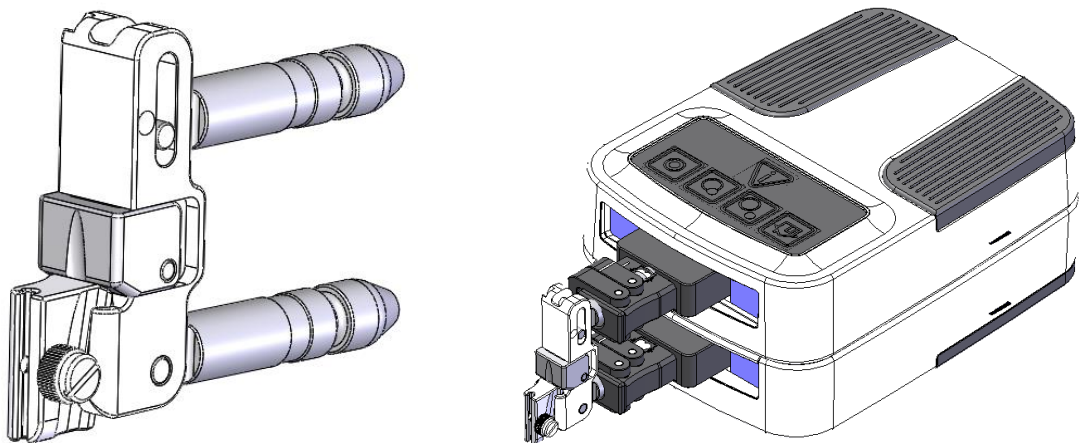


Figure 13 – The system’s universal End-Effector, mounted (right) and independent (left)

The EEF is also responsible for bearing a marker with spheres for position detection (not shown in the figures). This is important to understand as it a feature that ensures the system can accurately determine the medical instrument position at any time and in close-loop, meaning it can compensate for internal plays and slight manufacturing deviations when required to achieve a determined position during live-imaging.

When live-imaging is not being used then it is the user’s responsibility to align the medical instrument using a joystick or by inputting a determined position via software. In the first case the user will guarantee a sort of “closed-loop” position control, however, it is the open-loop application (no external equipment position control, i.e. the alignment is performed based on a pre-operative path definition – this is state of the art for free-hand instrument insertion) that is the worst-case and that requires the most attention from the mechanical project activities, as the system’s play/hysteresis will play a vital role in the position error of the medical instrument.

2.3 iONE Development - Current Stage and inputs

The equipment is, as mentioned, market-ready and fully developed with the first batch of 20 units expected to leave production directly to customers around early June 2020. The equipment is, however, still in a “early-access” stage; it is therefore possible for the product to be optimized, at this time, without the full impact that will occur from next year onwards.

The design inputs that constrain the previously mentioned outputs are clearly detailed in the design history file, and it is possible to verify a list of hardware and software requirements of which the most important for this work are:

- The system must be able to move up until a 40N load is applied in any axis;
- The motor current, upon reaching 100mA, should trigger a system shutdown, and it should be coincident to the maximum 40N load;
- The drive chain must be self-locking;
- The total system height must not exceed 90mm;
- The system should be capable of a range of motion of 40x40mm and $\pm 30^\circ$;
- The system should safeguard the ingress of liquids;
- The system should require no preventive maintenance;
- The system should be capable of operating on 10-30°C | 30-70% relative humidity;
- The system should sustain conditions of 0-40°C | 20-80% relative humidity;
- The NGE and EEF must be produced in non-conductive, radiolucent materials;
- The system should have a mean Euclidean 3D error of less than 1.2mm and an upper bound confidence 3D Euclidean error of less than 2.0mm for a target point at 100mm.

Most of these requirements should be revisited at the relevant section, later in this document. However, in broad terms and considering the above-mentioned requirements, some general comments can already be made on the system:

The range of temperature and humidity specified for the device is not a big constraint and should allow for the confident use of plastics and/or other materials with low maximum operating temperature requirements without worrying about creep (and other temperature-related effects) or moisture problems.

Electrical safety and usability requirements impose material restrictions, as already mentioned with the NGE and EEF. Other requirements are possibly present for other sub-systems, meaning that this project should take into account the relation of existing materials with international regulations.

When considering the mechanical design, as no preventive maintenance should be required for the equipment, it is necessary to evaluate the solution for its ability to function for extended periods of time – currently the expected lifetime for the system are 7 years.

Mechanical resistance, while necessary to evaluate, will most likely not represent a big challenge given that the expected maximum loads are rather small – system shuts down after 40N triggering a collision warning. Rather, equipment rigidity is quite likely to be the main challenge, given the tight accuracy requirements for the equipment at a 100mm target – this is further problematic considering the distance between modules is 32.55mm.

For this optimization project the current system construction can be considered as a reference, given that performance is validated – except for 3D Euclidean Error, which is a requirement that will be evaluated in this project. If future design changes are compared to the current system and prove to be beneficial in achieving a better performance, or reducing cost, then they are justified and should be considered as successful improvements.

3 Initial Situation, Problematic, Challenges and Tools

Having situated iONE development within the overall development process and having understood the basic concepts of the system, main functionalities and the value proposition to the customers it is now important to clarify the main objectives of this work and how the project was planned to handle them.

The objective of this work was, put simply, to better understand the hardware of system and to improve on it. This understanding can come in varied ways: system plays, system rigidity, tolerance allocation, root-causes for assembly problems, cost allocation, new potential materials/production processes/suppliers and design alternatives. Full freedom to pursue work in any of these fields was given and thus the work wasn't constrained in any sense, though some suboptimal areas were already previously identified and proposed as possible working topics.

3.1 Initial improvement opportunities

Right at the beginning of the project two areas were already identified as potential improvement points, these were the leadscrew nut and the foil potentiometer. These are two independent and essential sub-systems of the TP.

Foil Potentiometer

The foil potentiometer is part of the TP's linear encoder which is responsible for identifying the system carriages' position during the start of the system as well as providing data that is cross-checked with the rotary encoder data, present in the electrical motors, to detect system breakdowns and performance deterioration.

The linear encoder is composed of a foil potentiometer and a magnetic band linear incremental encoder that together allow the system to determine the initial carriage position with an absolute precision of $10\mu\text{m}$, and from system start until shutdown allow for the detection of a position change with a $1\mu\text{m}$ sensitivity. One linear encoder (foil potentiometer and magnetic band configuration) is used in each of the system's moving axis as shown in Figure 14 for the ANG module.

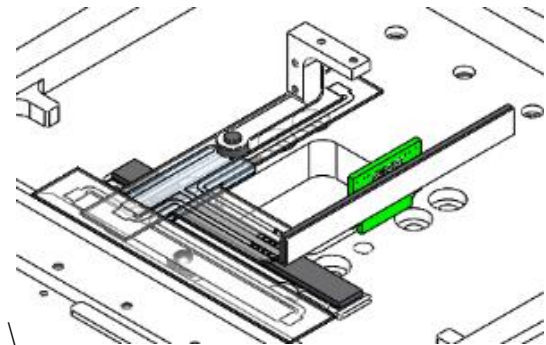


Figure 14 –Linear encoders for ANG module

It is essential that the foil potentiometer can provide an absolute position accuracy better than 1mm at the system start to prevent any major malfunction of the system – like over travelling, and consequently collision of the carriages with the system's mechanical limits.

Testing of the foil potentiometer performance was indicating major loss of precision surrounding the system's HOME position (this effect was referred to as the “denting effect”) when the carriages were at the center of the TP (the position from which they are allowed to move $\pm 20\text{mm}$ in any XY direction) when the system was subject to storage in 50°C for a period of around one week. In addition, it was found that some axes would verify discontinuities on the linear encoder's signals during the full range of motion of the device.

The root cause for this problem was necessary to be determined and a solution was imperative, as this problem could indicate an equipment failure during its lifetime use, especially when subject to challenging environmental conditions during operation. In addition, the system posed assembly difficulties, with the bent structures that support the foil potentiometer wipers frequently not adapting to the system's tolerance stack – this was detected due to interference between components during system assembly.

Leadscrew

The leadscrew, as detailed during system description, is part of the TP's basic drive chain and is the responsible component for translating the motor's rotary motion into carriage linear motion. This component is comprised of an M4 spindle and a brass nut that is rigidly connected to the moveable carriage using one M4 set screw and four regular M2 screws – see Figure 15.

The nut is designed to have a nominal gap to the carriage surface of 1mm, thus allowing the adjustment of the position of the nut's thread relative to the spindle to accommodate manufacturing tolerances.

The adjustment of the nut position is done manually during assembly via tightening of the four screws. These allow for free vertical translation of the nut as well as a very small y-axis rotations and almost negligible translations in the other axes.

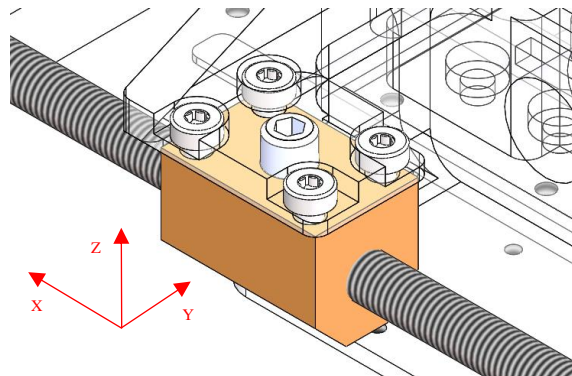


Figure 15 – Drive Chain A1 to Carriage A1 interface

Due to the mechanical construction of the module (see Figure 16) it is imperative for the leadscrew to be properly aligned with the linear guides, which rigidly define the allowed travelling axis. The leadscrew nut, in its current state, represents a mechanical over definition and does not allow for full compensation of the manufacturing tolerances, as it does not provide adjustment possibilities for y-axis deviations nor z-axis angular deviations of the spindle relative to the linear guides.

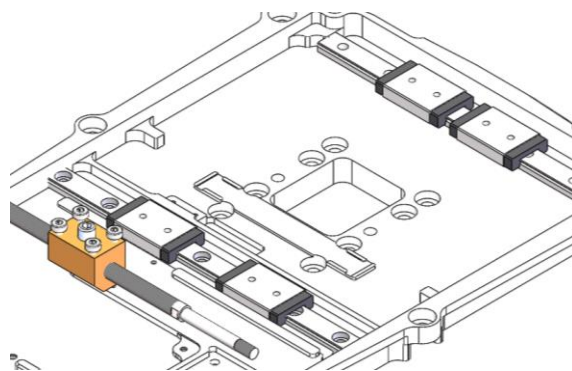


Figure 16 – Leadscrew and linear guides

This mechanical over definition directly reflects into problems such as assembly difficulties, with many mounting iterations being required to precisely fit the components in a precise relative position, and additional loads for the electrical motors, as the misalignments should be translating directly into increased friction (meaning false collisions might be detected).

Even though the system is mountable in its current design, the nut's connection to the carriages was considered as a key point for system optimization. Therefore, a design change was being considered for these components at the beginning of the project and the study would be included within the scope of this work.

Linear Guides

Due to assembly problems and general comments from external assembly/project partners, there was a general feeling of doubt surrounding the linear guides used in the TP. In addition to the leadscrew nut adjustment to the carriage, the linear guides themselves were posing troubles and requiring many iterations during assembly to achieve the necessary alignment.

It was being detected that motor currents would spike at the slightest deviation of the linear guides and that small screw adjustments of the carriages to the linear guides' rails or moving blocks could jam the system. In addition, their general handling was difficult and doubts surrounding the need for four moving blocks and/or two rails were raised.

Another raised doubt surrounded the possibility of using different types of guiding elements or changing the way they were being fix to the module's carriages and baseplate. These topics would be included within the scope of this work.

System Backlash and Drive Chain

As detailed previously, the system’s main goal is to achieve and hold a precise position for a held medical instrument. In open-loop scenarios this ability is entirely dependent on the ability of the drive chain to achieve precise positions. The graphical results shown in Figure 17 are an example of typical data output from a fresh (non-worn) TP characterization regarding drive chain backlash from which the maximum error between intended and actual carriage position can be deducted for all axes (more details on characterization in section 3.2). As it can be seen, the drive chain shows some backlash when moving their axes in positive vs negative direction, which is a natural phenomenon that, while not being possible to fully eliminate, must be kept within acceptable values. The maximum values for these rotary encoder vs linear encoder deviations, however, are not fully understood and the only existing criteria has been put up informally as: “the maximum deviation should be within $\pm 30\mu\text{m}$ for non-conditioned systems”.

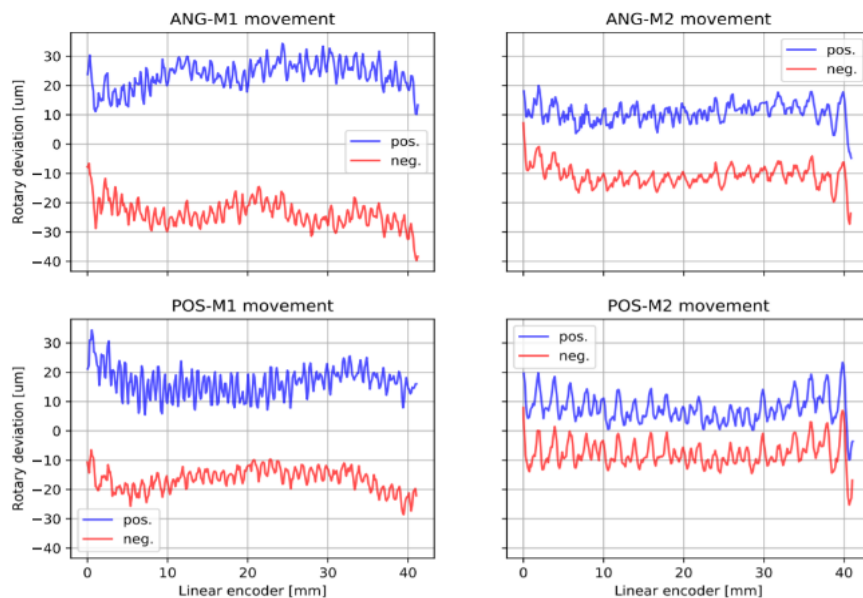


Figure 17 – Example of characterization graphics for drive chain backlash

A potential study topic for this work would, therefore, be the analysis of these deviations, the understanding of their root-causes, their evolution with product lifetime use, their impact on overall system accuracy and the definition of acceptable limits.

3.2 Challenges, opportunities, and tools

Training and Tools

For the activities that are to be carried in this work a set of tools and development documents were made available. The development documents contained, amongst other things, 3D CAD data on the entire system (in the form of .SLDPRT, .SLDDRW and .SLDASM), datasheets of the components, past system test data and production information (current suppliers, assembly build instructions, part quotes, etc.).

Additionally, the tools available for the system study and optimization effort were, amongst other, the system characterization scripts, the possibility of accessing a climate chamber for temperature/humidity dependent tests and the development team’s availability to carry with testing activities that, due to remote work, would not be possible to be done hands-on.

The system data, being digital, was readily made available for immediate analysis, while an opportunity for hands-on experience with the system was proposed. The hands-on experience involved a first contact with the system, the partial assembly of a TP, a first contact with the system’s production testing scripts, an introduction to the in-house and partner testing possibilities and the introduction of the several contact persons for the different project needs.

Characterization Capabilities

Due to the electronic architecture of the system and the software development efforts a set of production testing tools were already available to help with the optimization work. The most significant testing tool available is the possibility of self-diagnosis of the TP through a characterization script. The script makes use of the system’s internal sensors to obtain numerical data and generate graphical outputs of the system’s, and each individual axis’, performance.

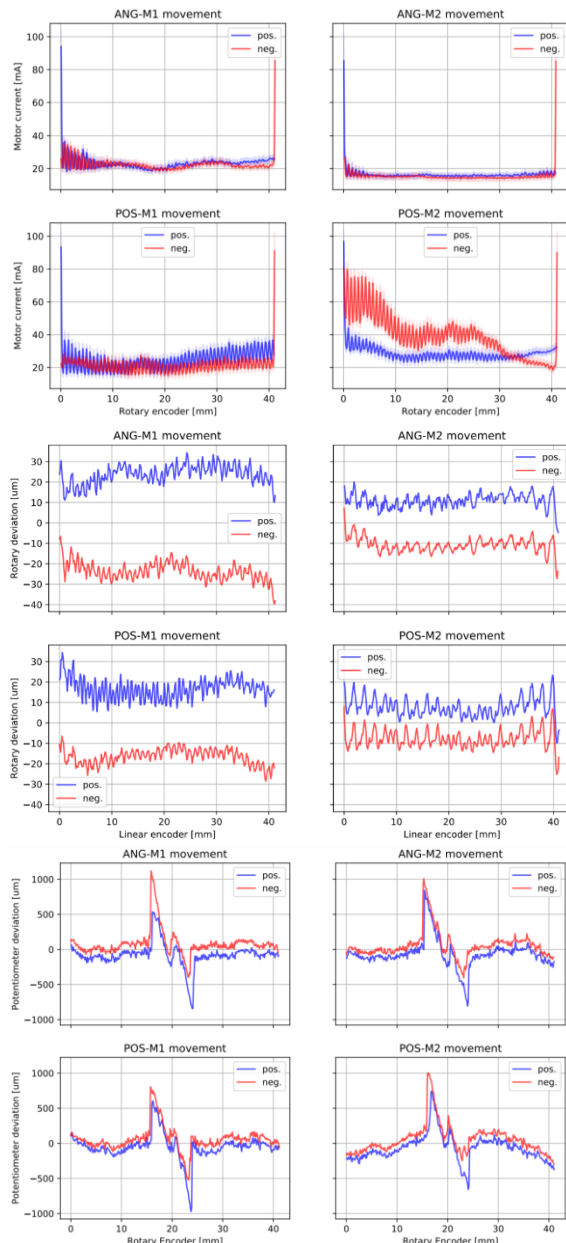


Figure 18 – Examples of characterization outputs (not all from the same system)

The graphics in Figure 18 are a small example of the full data that can be provided by the internal sensors via use of the characterization scripts and are the most relevant outputs for the type of activities that will be performed during this work.

The upper most graphic details the motor current at the different axial positions of the carriages for movements during a no-load condition. This is especially important during production to determine misalignments, as the motor current can spike at some positions as is possible to observe for the POS-M2 movement (movement of carriage A2 for the POS module) – typically a value under 40mA is desired for no-load cycling at the beginning of life and at room conditions.

The intermediate graphic details the rotary encoder deviation to the linear encoder. The linear encoder is directly connected to the carriages’ position while the rotary encoder is at the electrical motors and is the one used for controlling the open-loop movements. Therefore, this graphic is detailing the deviation between the supposed system position (measured at the rotary encoder) and the actual system position (measured by the linear encoder).

The bottom graphic is an example of the deviation between the foil potentiometer and rotary encoder, which can be used to evaluate the quality of the foil potentiometer signals and is showing the previously mentioned “denting effect” for a wearied and thermally stressed system.

These outputs will be used with frequency throughout this project’s testing activities as they provide reliable data on the status of the equipment.

Product Challenges

When considering the need for further development and changes to the product it is important to consider the main challenges associated, which can be as varied as: size, planned annual output, material restrictions, certification restrictions, etc.

Miniature Size

One of the system's key functional points is its overall miniature size, intended to allow the positioning of the TP inside an imaging equipment, such as a fluoroscopy C-arm, computerized tomography or Cone-Beam CT machine, at the same time as the patient. For general dimensions of the equipment, please see Figure 19.

This is also one of the most challenging aspects for the development and optimization of the iONE, as it is difficult to find standard parts, to thicken geometrical features (typical when high rigidity is desired), to ensure proper precise measurements of the system's deviations and to design the overall internal assembly structure.

Another challenge is the ability to produce and test design changes due to the required tight manufacturing tolerances coupled with the small, custom geometry, parts – this results in big lead times and sometimes high costs. Additionally, and as the system is aimed at being manufactured in small scale for the first year(s) there are also limitations in the production methods that can be used in a cost-effective manner; most of the system's components are produced by CNC machining for this reason – possible alternative manufacturing methods will later be discussed for some components.



Figure 19 – Trajectory Platform general dimensions

Component and Sub-System Requirements

Despite the fact that the system has undergone verification and validation activities that are a testament to its (mechanical, electrical and software) ability to achieve the necessary accuracy performance, it is still a challenge to identify its ability to retain position and what the main contributing factors to position accuracy and position retention are.

Understanding the mechanical capabilities of the system, in its current state, and for the several sub-systems should allow a better understanding of the main factors contributing to the performance in this main function. Additionally, it should allow for the definition of present and future design requirements – if the current capability is estimated, it can be put forth as a design requirement (design input) for future design changes; an example would be:

If the system is currently mechanically capable of achieving a 3D Euclidean error inferior to 1.5mm then a requirement can be put forth that the system should be mechanically capable of achieving a 3D Euclidean error inferior to 1.5mm, meaning that future design changes will be verified against this requirement and accepted/rejected based on their ability to achieve the required accuracy. Additionally, understanding the several components influence in performance should allow for this requirement being decomposed into sub-system requirements such as maximum drive chain hysteresis, maximum interface plays, etc.

4 System Analysis and Potential Improvements

As mentioned in previous chapters, a system analysis was necessary to, on one hand better understand the system, and on the other hand identify improvement areas. In this chapter some of these analyses will be presented, along with their intention and main findings. The data is often translated into Pareto charts to see on one side the relative cost between sub-systems/components (left vertical axis) and also cumulative impact (right vertical axis); the absolute cost values have been omitted purposefully given the sensibility of the data.

4.1 System Cost Analysis

The first big activity performed on the system was a cost analysis. Identifying the several parts that make up the system, their quoted price, suppliers, and production processes was a sure way to better understand the assembly and potential for price reduction.

iONE – Full System

The relative cost and number of unique parts relative weight between systems is detailed in Figure 20 and Figure 21. As it is possible to observe, the Trajectory Platform represents a substantial contribution to the equipment’s overall cost and number of parts, around 50% for each; hence the need to prioritize this system.

Other systems, while representing a substantial amount of influence, have a much simpler architecture compared to the TP with only a few major components adding to relevant costs. Many components for the CU, PNU and SRB are small standard parts, such as connectors, buttons, or seals, that are required for usability, electronics or safety and are thus not possible to change.

A special mention goes to the Positioning Arm where most of the costs are due to externally supplied, custom, core component

and on the complex geometry of connecting interfaces that are also not possible to change at this moment (design completely locked). Additionally, the medical grade cables are required for the system due to electrical safety, and are, therefore, not something that can be tackled without a major rework of the design (superficial plans exist but only for future generations).

Having understood the key influence of the TP in the whole iONE system costs, the remainder of the cost analysis focus on this platform; however, there are some final mentions to other system’s components that could perhaps represent a cost reduction opportunity.

TP – Trajectory Platform

The TP is composed of 96 unique parts and thus it would be necessary to devise a course of action for the cost analysis. As the main intention is understanding potential improvements, it would be necessary not to address the individual components but rather the sub-systems that make up the core system of iONE.

With this goal in mind a series of low-to-high level of designations was created, totaling 3 major levels, designated: Assembly Area, Assembly Sub-Area and Part Type - the first two levels were defined to be directly related while the third one is independent from the other two.

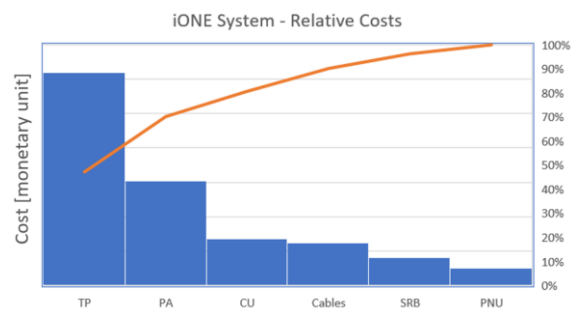


Figure 20 – iONE system costs

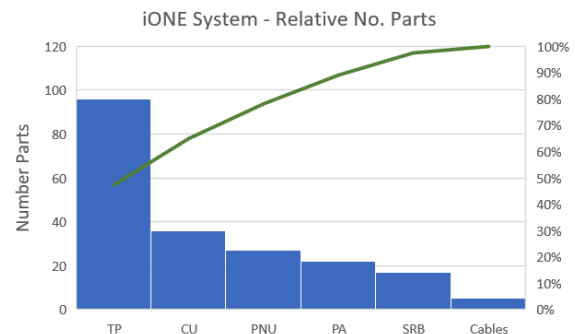


Figure 21 – iONE system unique part count

Assembly Area + Assembly Sub-Area

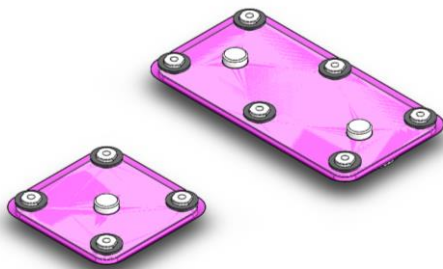
- Electronics
 - PCBs
 - Linear Encoder
- NGE
 - Buttons
 - Structure
- Overall Structure
 - Housing
 - Blue Tape
 - Baseplate
- Mechanical Chain
 - Motor
 - Bearing Block
 - Leadscrew
 - Carriage
 - Linear Guides
- PA connection
 - Ring Plate

Part Types present in each Area/Sub-Area

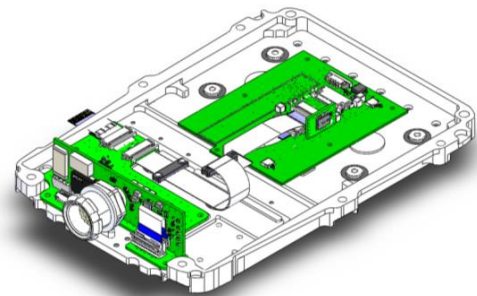
- PCB
- Connector
- Holder
- Magnetic Strip
- Housing
- Display
- Blue Tape
- Baseplate
- Motor
- Bearing Block
- Gear
- Leadscrew
- Carriage
- Linear Guide
- Ring Plate
- Dismountables (screws, pins, nuts...)
- ...

The several areas are visually represented in Figure 22.

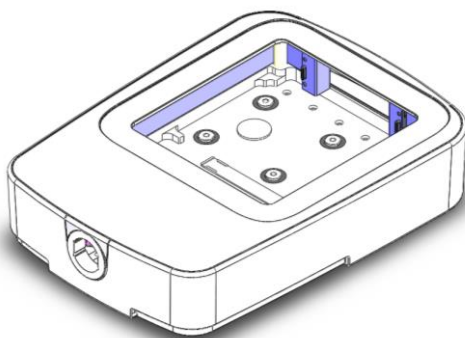
PA Connection



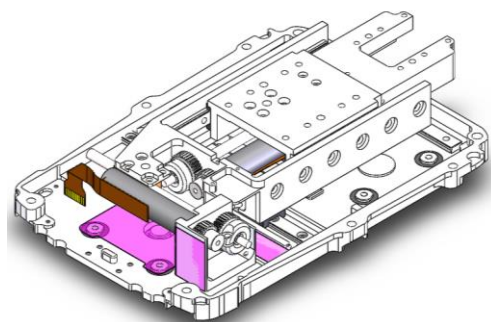
Electronics



Overall Structure



Mechanical Chain



NGE

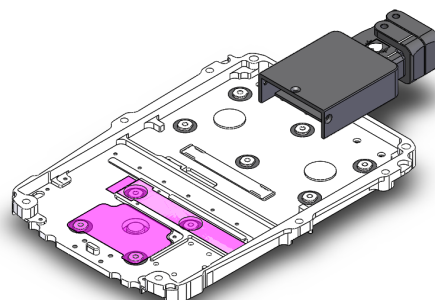


Figure 22 – The TP areas considered in the cost analysis

General Analysis

These designations are intended to allow an easier perception of the system areas and of the type of components that impact the system costs the most. They also allow for the creation of easily readable Pareto charts that visually identify the more important optimization aspects – two aspects are considered: cost and number of parts.

Observing Figure 23 it is very clear that the mechanical chain of the TP is the most costly part of the system – this is directly linked to the also large number of parts that make up that system. At first sight this would seem like the the best area to tackle for cost reduction.

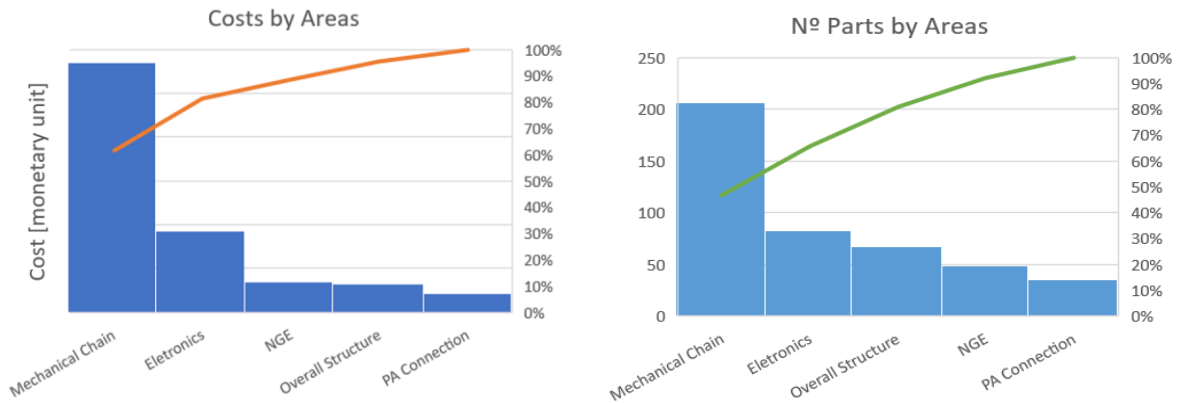


Figure 23 – TP areas cost (left) and number of parts (right)

However, when considering Figure 24 it is evident that the most contributing components to that high cost are also not possible to change: The PCBs are electrical and thus out of scope, the motors have large electrical dependencies and the leadscrew, despite being a custom component, is not possible to order as a standard part due to the miniature size requirement.

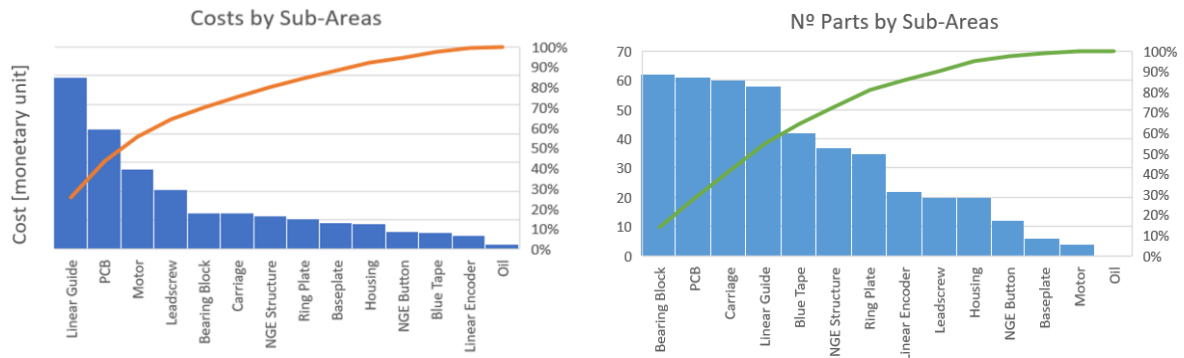


Figure 24 – TP sub-areas cost (left) and number of parts (right)

It is thus important to consider part-types in this analysis, which are detailed in Figure 25. The first entry that comes up after the already mentioned unchangeable parts are the “Holder” parts. Representing around 25% of the system cost and being the second largest part type in the system, these custom parts are in the system to act as structures for other components – these are the most promising cost optimization points.

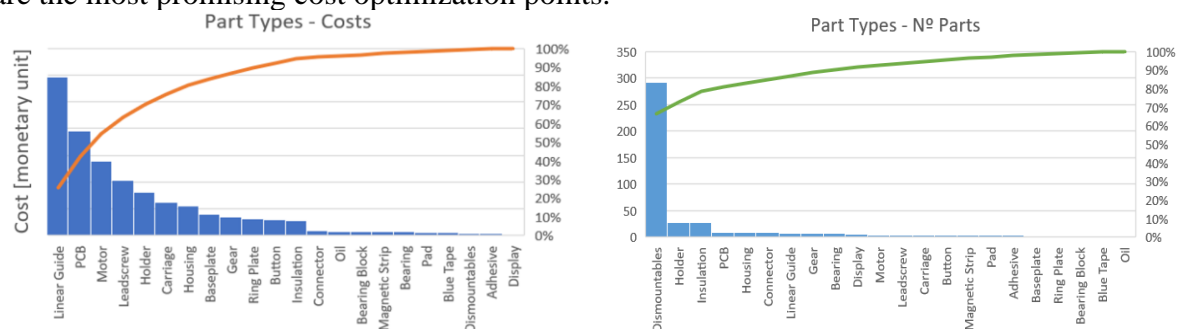


Figure 25 – TP part types cost and number of parts

The holder parts, some of which are shown in Figure 26, also have a few traits in common: they are all very small, custom, and mostly machined parts. The system could thus benefit from either an integration of these parts into other parts or a manufacturing process change.

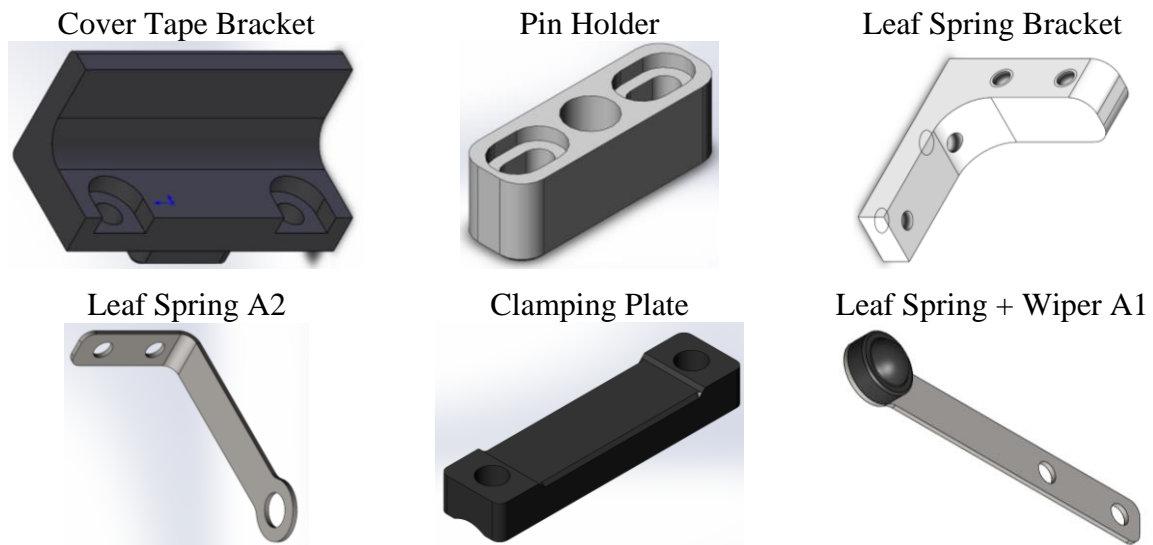


Figure 26 – Examples of TP holder parts

Also considering Figure 25, it is possible to understand that most total parts for the TP are dismantlable standard components (or fasteners), from which about 80% are screws. A more in-depth look at their distribution in every sub-area can be found in Figure 27.

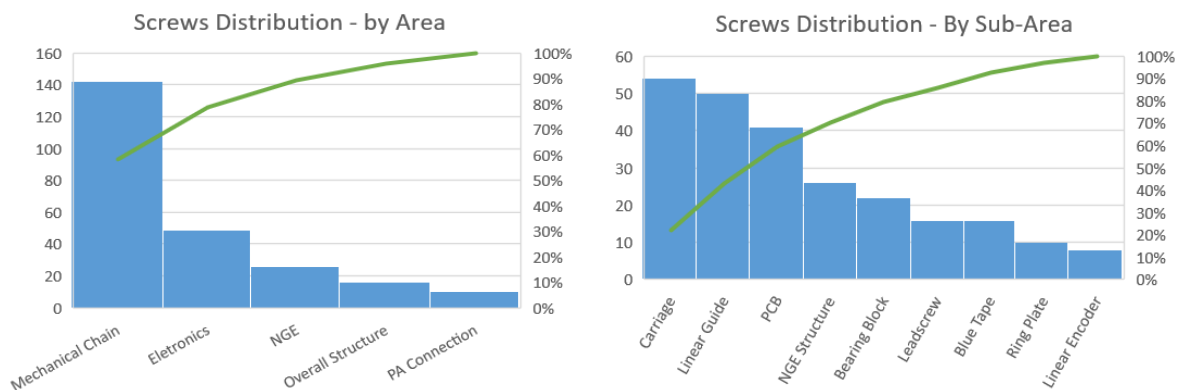


Figure 27 – TP screw distribution

The impact of fasteners on the total assembly time, due to their large number, is very significant, and, despite not representing an overall significant purchasing cost, accounts for a significant portion of the total assembly cost. The assembly cost is, in turn, estimated to be responsible for around 10% of the total system cost (plus administrative costs). Therefore, a reduction on the number of fasteners would seem like another possible point for improvement.

Although screw reduction could provide beneficial to system assembly, not all fasteners impact the system assembly time equally. Analysis on the assembly process and hands-on experience has permitted to conclude that a significant amount of assembly time, around two thirds, is spent correcting system misalignments between the leadscrew and the linear guides which, when occurring, lead to system jamming.

Only a reduction on the total amount of fasteners in these sub-areas (total of 70 components) could provide satisfactory assembly cost benefits. However, there might be easier alternatives, such as preventing misalignments in the first place; for this reason, no special attention was given to the total number of screws in the system.

Assembly Sub-Area Comments and Improvements

PA connection – This area of the TP is responsible to ensure a connection with the gross-positioning arm, which in turn is connected to the exterior. Because of this, and given electrical safety requirements, it is important that there is sufficient insulation at this interface. With the current design, this is achieved with a combination of insulation foils and custom insulating washers and T-nuts – parts can be seen in Figure 28.

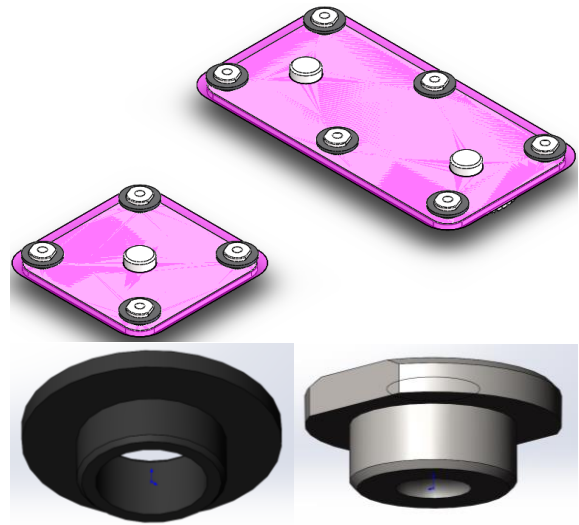


Figure 28 – Insulation parts in PA connection

Upon analyzing the sub-area and identifying the space restrictions and component-to-component interaction it was considered that a rework of the insulation components would not be possible, and would represent a considerable effort while providing only a small benefit to cost optimization.

However, if the connection were to be reworked in the future, to include a quick-connection/quick-release mechanism (considered to be a big step forward in the system usability), instead of the current handle tightening mechanism then it could prove very beneficial to alter the design of the insulation elements to eliminate the custom components and replace them by a simpler feature such as a foil or pad – cheaper, more easily assembled and equally well performing.

Electronics – This area of the TP – shown in detail at Figure 29 – is better analyzed without the influence of the PCBs (which are not in scope). Not considering these components, it is possible to find a considerable amount of the previously mentioned “Holder” parts, especially when examining the linear encoder. Additionally, the clamping plates used for holding the flexible cables that make connection between the PCBs, were also detected as having a significant impact on system costs, which is surprising given their simple geometry and miniature size.

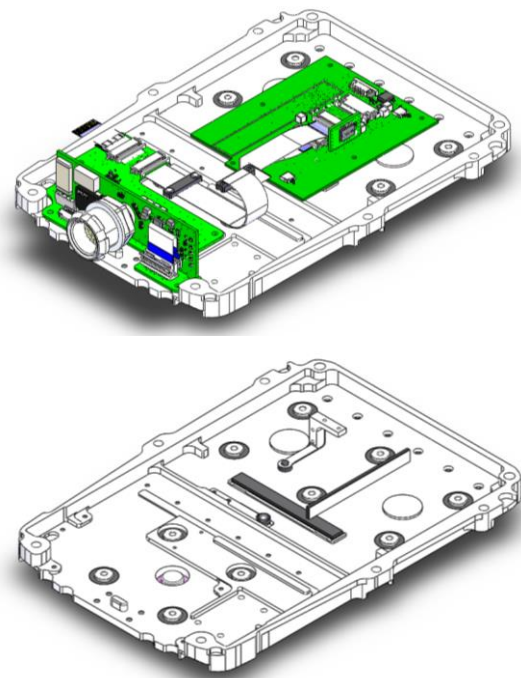


Figure 29 – Electronics sub-area w/+w/o the PCBs

As the linear encoder system is already targeted for change, meaning potential redesign, it would be important to consider the possibility of reducing the number of holder parts that make up its structure by incorporating them within other major components.

Overall Structure – When considering the overall structure of the TP – Figure 30 – it is important to make the distinction between two major sub-assembly areas: the “blue tape” and the “housing”. This is important given the different finality, functionalities, and selected manufacturing processes.

The housing of the TP is obtained by plastic injection molding (PIM), meaning a substantial investment has already taken place on these component’s tooling, the sub-area is thus beyond any kind of change as it would represent a huge cost for the company.

The blue tape sub-area, however, is not subject to those constraints and represents 10% of the total system part numbers, meaning improvements are most likely possible. This is especially true if we consider the blue tape’s main objective, which is the prevention of excessive dust and liquid to the system’s interior – only partially accomplished – and the fact that this element induces increased friction for the system given the tension on the four pins.

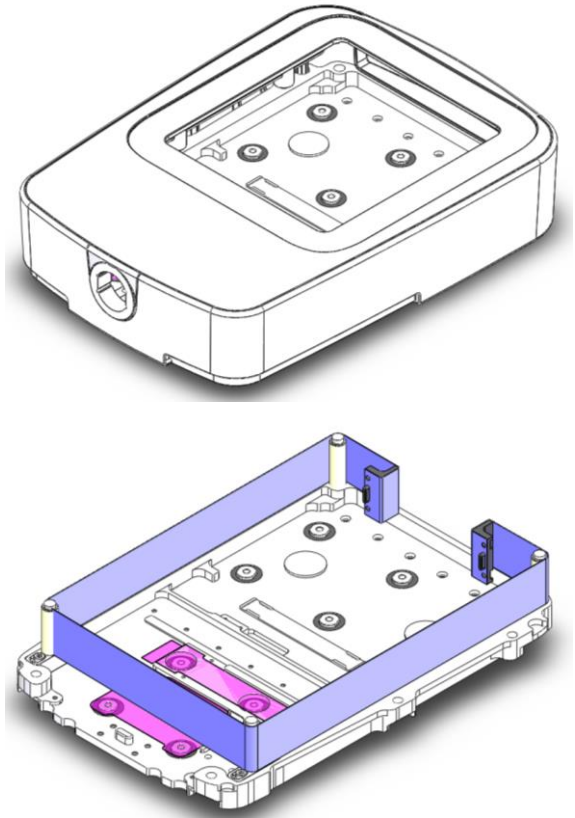


Figure 30 – Overall structure area, housing (top) and blue tape (bottom) sub-areas

A blue tape rework could be a potential improvement step for the system, if either a part number reduction or a tightening of the sealing capacity is achieved. Despite this, even if it is not possible to change the blue tape system, or at least not in the short-term, an immediate step that can be taken for cost-optimization is optimization of the “holder” parts (cover tape bracket and pin holder – previously shown in Figure 26).

Mechanical Chain – Some topics were already previously mentioned, like the linear guides and the leadscrew, but a few further comments can still be made on the mechanical chain, mainly considering the components that ensure the link between the electric motors and the leadscrew, these being the gears and structural elements (see Figure 31 and 32).

The bearing block and all its related components, present also in carriage A1, represent around 5.5% of the total system costs and about 7% of the total parts.

A possible point for improvement in this area of the TP is related with the gears and associated components. The current gears are part of a high precision (AGMA Q14) stainless steel pair, which could probably be changed to a plastic pair to reduce costs, noise, and ensure self-lubrication with minimal impact on drive chain backlash.

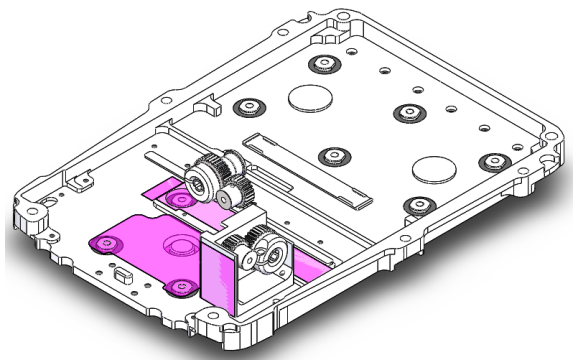


Figure 31 – Bearing block related components

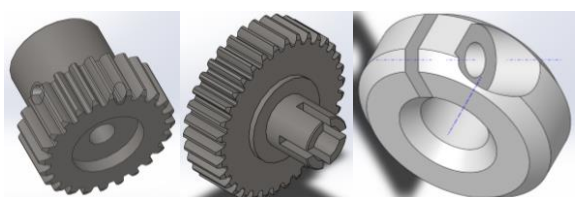


Figure 32 – External gears main components

A more detailed analysis of the bearing block, external gears and leadscrew will be presented later as these parts are all interdependent due to the drive chain design.

NGE – The TP connection with the EEF is shown in Figure 33. While not particularly complex it does account for a substantial impact on system costs, at around 7,4%.

Due to equipment safety requirements these parts must be non-conductive and are thus manufactured by CNC machining of PEEK, with a particular high cost for the two buttons at each module's interface (alone representing 2.5% of the total system costs). The material selection for these parts, as well as the manufacturing processes could be studied for a cost optimization.

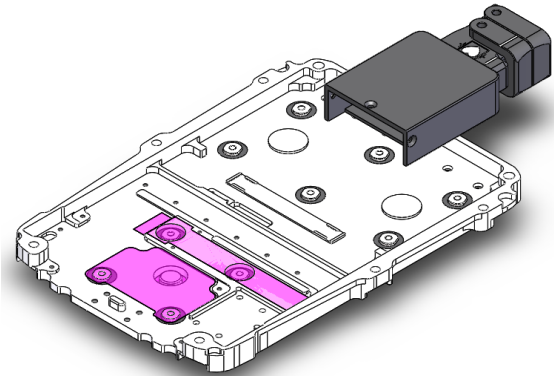


Figure 33 – The NGE assembly sub-area

SRB – Strain Relief Box

A small, yet special attention, was given to the SRB, a small sub-system for the iONE system responsible for cable safety, but with a non-negligible cost impact on the overall system.

The housing for this system – parts shown in Figure 34 – is currently obtained by CNC machining of PEEK, yet no special (or substantial) load solicitation is expected to occur on these parts, meaning there should be room for cost-optimization. The components material and manufacturing process selection was thus selected for further analysis.

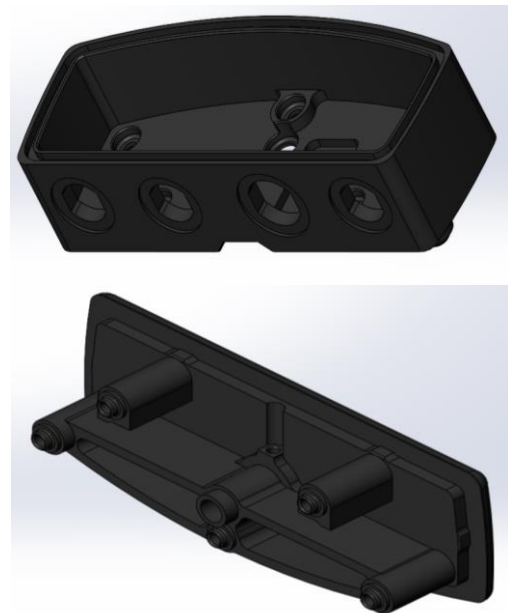


Figure 34 – SRB housing components

It was later found that these housing parts are validated through heavy testing and costly certification, which means a redesign or process change would require a lot of administrative work and cost (re-certification at an external laboratory), which would lead to a null cost improvement; the change was discarded. The part was, nonetheless, evaluated for a different material and manufacturing process with the intention of gathering additional information for future design decisions.

4.2 System Performance Analysis

Completed the cost analysis, a mechanical performance analysis was conducted. This analysis focused on the mechanical capacity of the system to achieve accurate medical device positioning and, above all, to guarantee rigid position hold, of said device, during use (needle-based and/or drill-base procedures) – a better understanding of maximum target errors, and main influencing sub-systems/components/interfaces was sought.

The information presented next intends to capture the considerations, rationale and conclusions that derived from said performance analysis, which involved the Trajectory Platform (TP) and the EEF Universal Adapter Twin.

The analysis was conducted following considerations on the use of the equipment and was supported, whenever possible, by past testing evidence, part inspection and some basic Finite Element Analysis. This analysis resulted in a model that intends to:

- Provide understanding on the component-to-component interactions of the system;
- Provide understanding on the overall system play and rigidity;
- Identify the sub-systems most affecting the overall performance;
- Serve as basis for the identification of major optimization areas for the system;
- Serve as basis for a future mechanical characterization of the system

Background for the Analysis

There is limited data regarding iONE's mechanical design decisions, calculations, performance, manufacturing tolerance's stack and the influence of individual components/sub-systems in the overall system performance as of the time of this analysis. Therefore, there is a need to understand the mechanical capacity of the system in its primary tasks of accurate positioning and position retention of medical instruments, such as needles, drills (for minimally invasive surgeries) and endoscopes.

The focus of this analysis is the Trajectory Platform. Understanding which components are critical to the system play and rigidity is important to determine next performance optimization steps, and also to understand if previously defined component/sub-system-level requirements for the system are valid, so they can be formalized. As an example, a major point of internal discussion is the acceptable level of backlash that is permitted on the drive chains; this backlash is measured by means of the system's characterization python scripts, and is thus an easily accessible indicator of the system's performance which is employed thoroughly during system testing and manufacturing checks – the present analysis intends to allow for the understanding of the impact that the measured backlash has on the overall system performance and what might be a maximum value for this parameter, amongst other things.

Regarding the EEF Universal Adapter Twin, it will be considered as a whole, meaning it will be important to understand its impact on overall performance compared to the TP, not which of its components are most influencing performance – this will be done in section 4.3.

Deviations and Error Calculation

The iONE has the crucial task to position the medical instrument accurately aligned with the entry/contact point and entry/contact angle, making use of 2 axis movement, and then hold that position for the physician to carry on with medical instrument maneuvering on the third axis. This is important to understand how deviations can occur on the system, what their impact is on the instrument reaching the target and how they will be calculated in this analysis.

A first simplification for this analysis is the position where the system will be studied. This analysis will consider the TP in HOME position, as it is easier to decompose loads and deviations in the several x, y, and z axes. It will be considered that the user controls the z-axis and that x-axis and y-axis position/position retention is to be guaranteed by the TP.

As the user is responsible for z-axis control, deviations of the system in this axis will not be considered. While it is true that not all z-axis deviation is resultant from user inputs, as vertical loads will undoubtedly cause elastic deformation of the TP in the z-axis, this deviation will have a small impact into x-axis and y-axis deviation due to the either vertical or up to 15° angulation (software cap) that the instrument may assume; therefore, and because the user always controls the instrument z-axis position via real time imaging, he will control the instrument position/insertion via small increments and control the impact of elastic deviation at every increment – the system must then ensure other deviations (X and Y axis, shown in Figure 35), which the user is not actively controlling, are as small as possible.

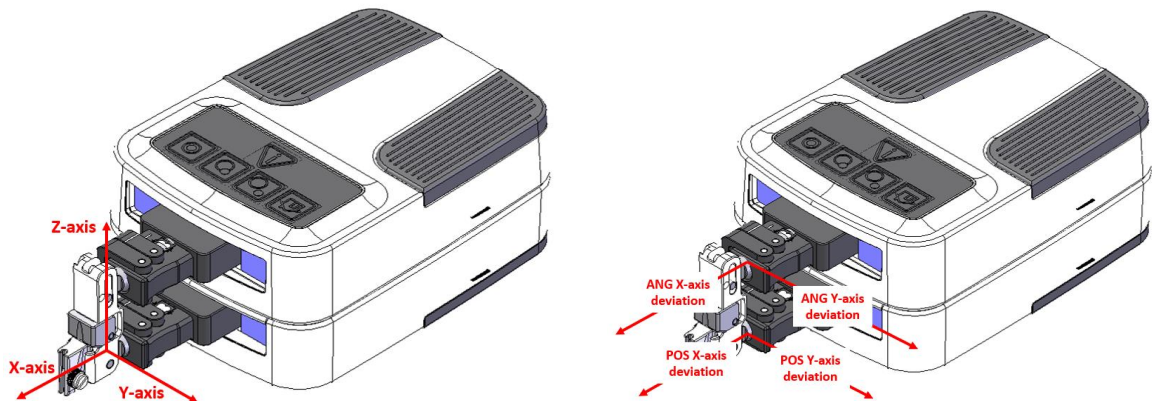


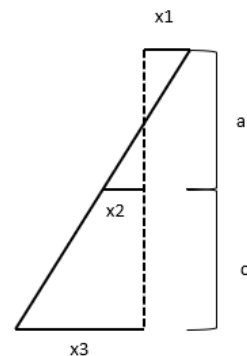
Figure 35 – TP x and y axis and deviations illustrated for a HOME position TP

The X-axis and Y-axis deviations of the medical instrument will be analyzed for their root-cause in the TP and EEF, and will always be considered for their impact at a target 100mm deep – this is because of the system requirement already mentioned in section 2.3:

- The system should have a mean Euclidean 3D error of less than 1.2mm and an upper bound confidence 3D Euclidean error of less than 2.0mm for a target point at 100mm. (as a statistical study will not be employed, a maximum 2.0mm of 3D Euclidean Error will be considered)

The calculated mechanical deviation will be a 2D Euclidean Error, given that only x-axis and y-axis will be considered, however, as mentioned, this is the important error for the system mechanics. Also, a 0.5mm constant 3D Euclidean Error will be added to the 2D calculated mechanical error to account for small z-axis deviations and for imaging errors – this value has been put forth by Product Management given no-load accuracy studies done in the past – thus we can add the 2D mechanical error to the 0.5mm of 3D error to understand how the system performs in relation to the mentioned specification. The 2D mechanical Euclidean error can be estimated based on how far the POS and ANG are deviated from their intended position. Let:

- **x1** – be the ANG deviation;
- **x2** – be the POS deviation;
- **a** – be the distance between ANG and POS (measured between each module’s NGE bore centers);
- **c** – be the distance to the target point measured from the POS module (considered from POS’ NGE bore center);
- **X|Y Deviation** – Any deviation to a module due to play or elastic deformation in x-axis or y-axis;
- **POS|ANG Deviation** – POS or ANG’s total deviation due to play or elastic deformation.



$$2D \text{ euclidean error} = \left(1 + \frac{c}{a}\right) * (\text{POS Deviation} + \text{ANG Deviation}) - \text{POS Deviation}$$

$$(\text{POS|ANG} \text{ deviation}) = \sqrt{(\text{X Deviation})^2 + (\text{Y Deviation})^2}$$

For the POS/ANG deviation several factors will contribute:

- Initial positioning error based on open-loop user commands (influenced by system backlash)
- X and Y plays on the system
- X and Y rigidity of the system when the user applies loads to the medical instruments

For this analysis it will also be important to consider that the sandwich structure of the TP means that a deviation on one module will induce a deviation on the other module, as they are stacked vertically by a rigid connection.

Use loads – Impact on rigidity

The expected loads for the iONE are needle-type loads and drill-type loads – as an accurate positioning platform the system will result in a controlled, direct, and accurate movement of the medical instrument, leaving to the user the sole need to control the vertical position of said medical instrument – the exerted forces are thus very controlled and very soft. However, due to the miniature size of the device these forces may have a considerable impact on the maximum 3D Euclidean error.

In needle procedures the user will apply almost residual forces to the needle, mostly in the vertical direction and most likely directly above the ANG module. The forces for needle procedures have not been quantified but the agreed value with Product Management is of around 0.5N vertical force, of which a small amount can be done off-axis. For drilling procedures, however, the vertical forces have been usability tested and are expected to be always inferior to 10N – these forces, however, may not be applied entirely within the drill axis and thus it was agreed that a 2.5N of force, applied normal to the drill axis at an upwards vertical distance of 32.5mm (equal to the distance between NGE bores center) from the ANG module, would be representative of the maximum force + leverage that would result from an actual use case. Considering a similar situation for needle loads, the EEF will transmit forces to the Trajectory Platform as illustrated in Figure 36.

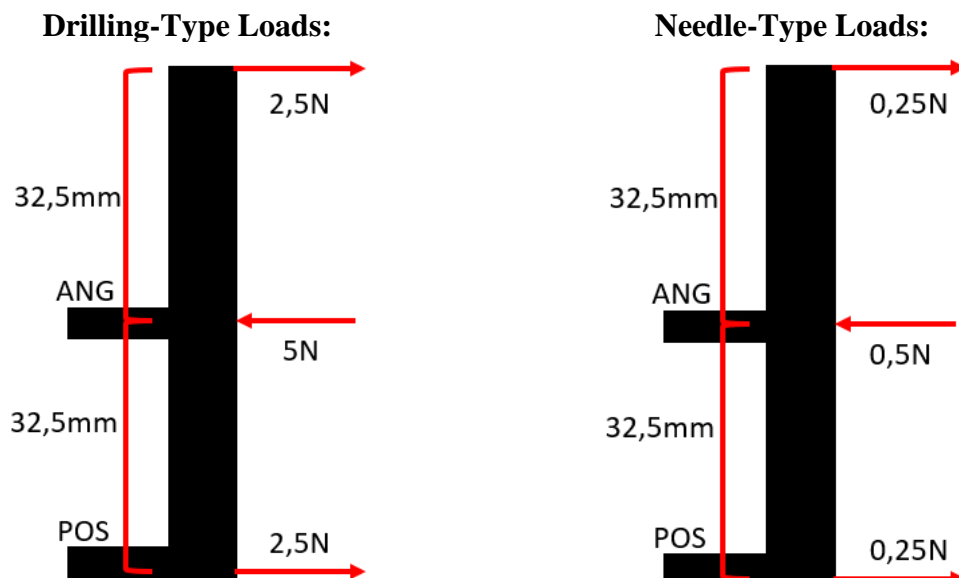


Figure 36 – Performance study; EEF transmitted forces to the TP

Due to the sandwich construction of the iONE each module (POS and ANG) can be considered in separate and the rigidity results for one module can be used directly on the other module (with a correction factor of 2 due to the difference between the absorbed loads between POS and ANG). The following analysis will be performed for the ANG module, which will be subject to, in worst-case conditions, a 5N y-axis load. The EEF will be studied in separate.

Deviations Analysis

Positioning Error

The positioning error is the first parameter that will influence the system’s deviation. The system will, in close-loop, achieve a position (this operation has an associated error, accounted for in the previously mentioned 0.5mm 3D Euclidean Error) from which the user can manually input the system to deviate for an extra needle placement or an extra drilling procedure. This user input will result in an error in positioning that is associated to drive chain backlash.

Figure 37 should work as a visual representation on the impact from the system’s drive chains backlash on the maximum position error. When the rotary encoder reaches the intended position the actual carriage position will be lagging. As the backlash is not always symmetrical the worst-case condition is not necessarily half of the backlash but instead the maximum deviation between the intended position and the carriage position.

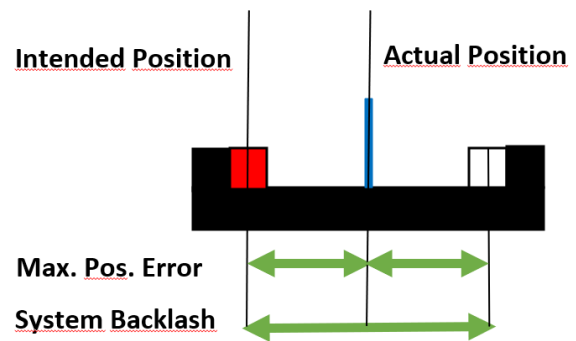


Figure 37 – Visual representation of Position Error

The movement command that is inputted by the user will be controlled from the rotary encoder present on the electrical motor (since the transmission ratio is known), which means that play in the motor gearbox, external gears, spindle axial play + deformation and leadscrew nut (LSN) axial play will contribute to the measured deviation – this value at the beginning of the TP life is around 30µm, measured by the characterization scripts seen in Figure 38.

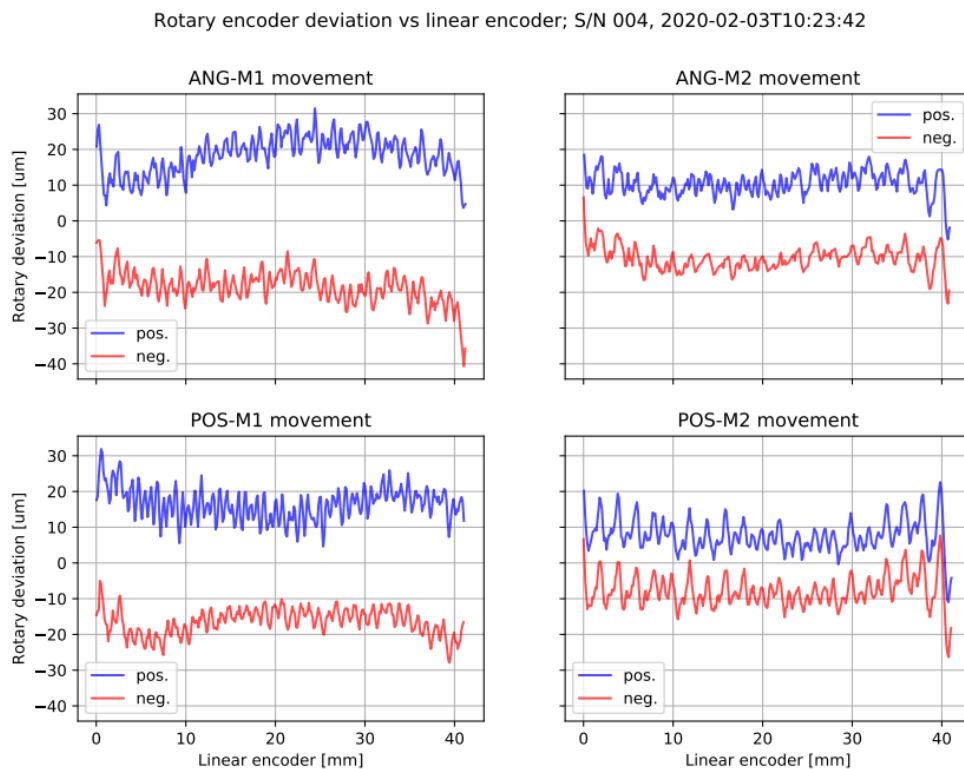


Figure 38 – Example of drive chain backlash characterization

This backlash is being influenced by the several drive chain components and it is important to understand their individual impact to identify what the key areas of optimization are. The calculated values for the several drive chain components are:

1. Motor Gearbox

According to Maxon’s datasheet (Figure 96 at appendix A) for maxon GP10A218416, the motor gearbox average angular backlash is of 1.8°. Considering the drive chain transmission ratios (34/24 for the external gears and the 0.7mm pitch for the spindle) and that the maximum motor gearbox backlash is worst-case 3° the impact on the total backlash would be of **4.2µm**.

2. External Gears

The external gears are Reliance’s P04S1B2F4A-24 and C04S1B3F4A-34. Their operating backlash should be summed to the inter-axial tolerance – see Figure 39.

BACKLASH FOR STANDARD GEARS

The table below refers to the allowable backlash within the range of Spur, Bevel, and Worm gear pairs with a designated centre distance. The allowable backlash is necessary to absorb the deviations of noise and oscillation in order to maintain smooth operation.

Gear Type	Condition	Module (m)	Backlash (mm)
Spur Gear	Brass/ Ground	< 0.9	0.02 - 0.06
	Brass	0.9 to 0.75	0.04 x m - 0.10 x m
	Ground	0.9 to 1.0	0.04 x m - 0.08 x m
Bevel Gear pair	Stainless steel or Brass	< 0.9	0.02 - 0.08
		0.9 to 1.5	0.05 - 0.12
Worm Gear pair Centres < 50 mm	Worm - Stainless steel	≤ 1.0	0.08 - 0.20
	Worm wheel - Brass		

Note. These figures apply to the standard gear range only.
To convert Circumferential Backlash to Angular Backlash see page T4-15

$$B = 2 \tan \phi \cdot \Delta C \quad \text{where} \quad \begin{aligned} B &= \text{Circumferential backlash} \\ \phi &= \text{Pressure angle (Tan } 20^\circ = 0.36397) \\ \Delta C &= \text{Distance between theoretical nominal} \\ &\quad \text{and actual centre distance} \end{aligned}$$

Note: Maximum Angular Backlash = $\frac{\text{Maximum Circumferential Backlash} \times 57.3 \times 60}{\text{Pitch Circle Radius}}$
(minutes of arc)

Figure 39 – Reliance Gear Backlash calculations

Considering 0.4 module gears with the worst-case of 0.06 mm of backlash, this will be converted into 1.4µm of total drive chain backlash. Adding the bearing block inter-axial distance tolerance of ±0.02mm (in both axial of the plane) it would result in an additional 0.5µm of backlash. The total backlash from the external gears would then be **1.9µm**.

3. Spindle

The drive chain’s spindle influence in the total backlash is difficult to quantify, as it is influenced by the bearings axial play as well as from the spindle’s elastic deformation, the first one not being quantifiable as no data is available. For the elastic deformation, however, it can be calculated based on the expected 5N; for this load, and considering steel’s Young Modulus of 200GPa, and a 4mm diameter spindle, the drive chain backlash would be affected by **4µm**.

4. Leadscrew Nut

No datasheet is available for the LSN, however, its axial backlash was tested in the setup shown in Figure 40, and the results were averaging **5µm**.



Figure 40 – LSN backlash characterization

5. Carriage Tilt

Due to the friction of the system, and the fact that the linear encoder used to determine the system backlash is present in carriage A1, this carriage will slightly tilt between direction changes thus adding to those 60µm of system backlash. Past system tests show friction values, for test conditions similar to use conditions, of around 3N – employing linear guide rigidity calculations from the NSK manual [NSK, 2020], as shown in Figure 41, and considering the worst-case 5N, carriage tilt should influence sensor readings at most by **3.5µm**.

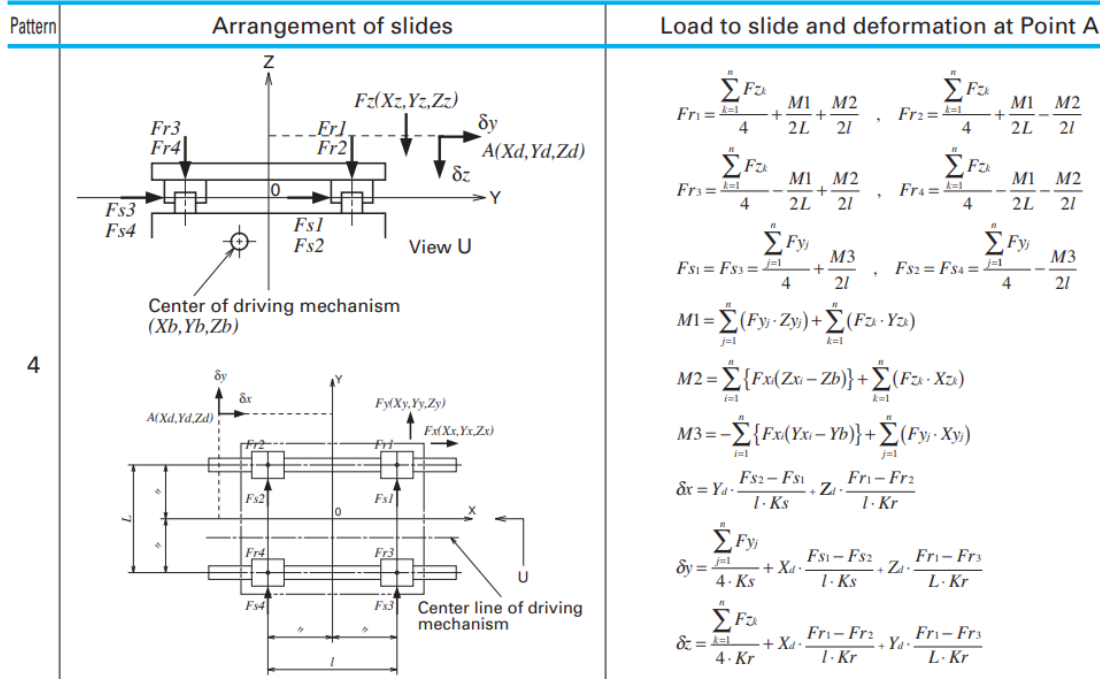


Figure 41 – Linear guide deviation equations [NSK, 2020]

6. Total Error

Adding up all the above-mentioned backlashes: 3.5+5+4+1.9+4.2 = **18.6µm**, the obtained value is quite far from the measured **60µm** of backlash. That difference is most likely due to the not calculated spindle axial play (should be adding at least 40µm of backlash in worst-case chains). A test on the drive chain is thus essential to provide data that may justify this rationale and thus to better understand the key optimization areas.

System Play

The system play will be the next factor degrading the accuracy performance of the equipment and it affects the position retention of the medical instruments. Even though the system’s own weight coupled with some of its circular fit features will contribute to minimizing the system play, in this analysis the full system play, derived from maximum worst-case system tolerances, will be considered. The position retention is influenced by the following plays:

1. Drive Chain to Carriages – LSN and Spindle;
2. NGE to EEF – gap between the EEF guiding joints and the NGE bore;
3. EEF internal Play – gaps between the pins and the EEF slots.

These components will be studied in more depth for their influence in play.

1. Drive Chain

When the system has achieved final position the position retention for carriage A1 y-axis is given by the LSN and Spindle present in drive chain A1, while the position retention for carriage A2 x-axis is given by the LSN and Spindle present in carriage A1. All other axis, for each carriage, are retained using the linear guides – the linear guides play is of $1\mu\text{m}$, per the manufacturer’s datasheet so these components will not be considered for play deviation.

The LSN and the spindle are two components influencing the positioning precision of the system, as they added to the system’s backlash as measured by the characterization scripts. Because of this they were already considered in the positioning error and should not be added again; their play, not being responsible for the whole system backlash would actually allow the system to get closer to the intended position (visually represented at Figure 42); not considering the LSN and spindle play outside of drive chain backlash is thus worst-case.

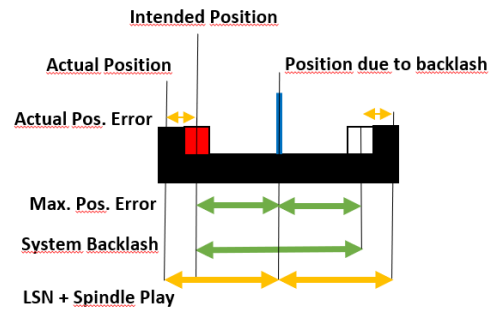


Figure 42 – Worst-Case vs Actual Case

2. NGE to EEF

As the linear guides are low clearance ($1\mu\text{m}$ of play), no other TP component can be considered to influence the system play, except for the interface between the NGE and the EEF.

The EEF guiding joint fits with play inside the NGE bore, and two springs ensure a “snap” connection. If we consider the typical system loads, even the lowest load of 0.5N (typical for a needle intervention) is much more than the spring can withstand while minimizing play, thus this interface’s play is influencing the final system precision (calculations at Figure 43).

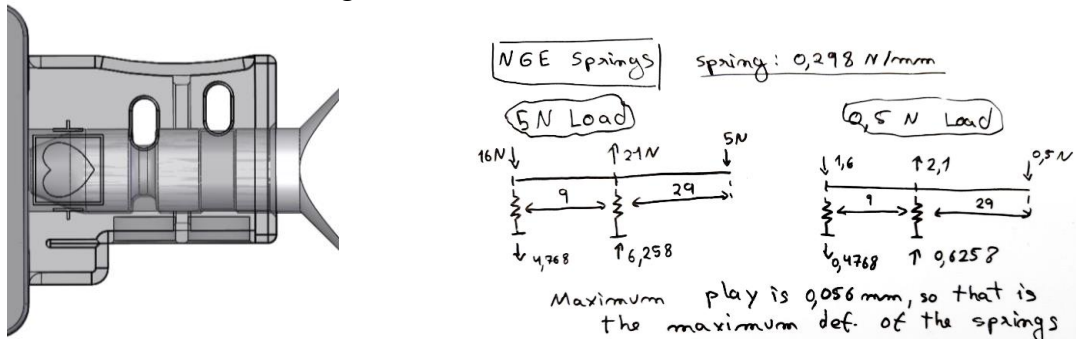


Figure 43 – NGE-EEF interface and spring play compensation calculations

The distance between the furthest support point to the medical instrument is around 30mm , while the length of contact between the EEF guiding joint and the NGE is around 20mm . If we evaluate the play between the two components and consider Figure 44:

- NGE bore diameter: $\phi 10\text{ mm } -0/+0.015$
- EEF guiding joint diameter: $\phi 10\text{ g9 } (-0.041/+0.005)$

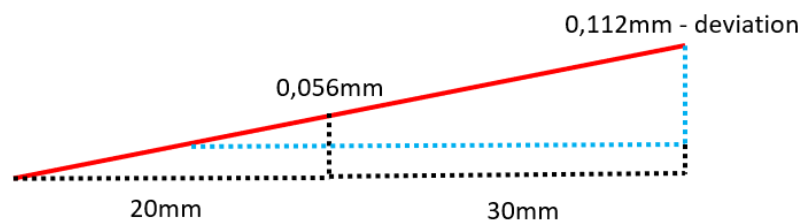


Figure 44 – Example of the impact of NGE-EEF interface play in instrument deviation

The maximum deviation due to this play is thus **0.112mm**.

3. EEF Internal Play

The EEF universal adapter twin construction is itself another source of play for the system as there are several internal moving and attachable components. The construction can be seen in Figure 45 along with the expected deviation modes. It is important to understand that the 1st and 2nd deviation modes are not independent and thus only one deviation mode will be considered in this analysis. The worst-case deviation mode will be considered.

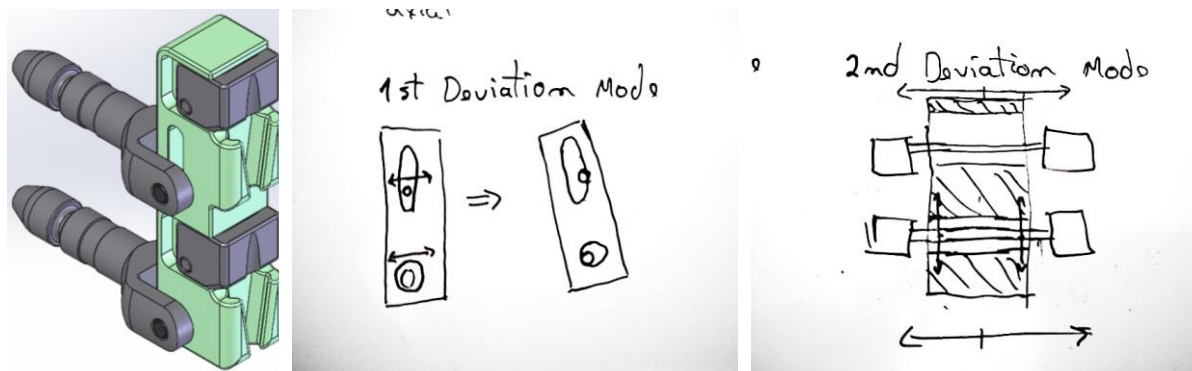


Figure 45 – EEF adapter twin and deviation modes due to internal plays

1st Deviation Mode

As seen in Figure 45 the 1st deviation mode is a rotational deviation of the EEF body due to the play between the pins and the respective recesses where they are attached. This should be added to the EEF body width play to the fork-like geometry of the guiding joint (2nd mode translation deviation):

- EEF body width: 16.2 mm +0/-0.03
- Guiding joint fork width: 16.22 mm +0.03/-0

The deviation caused by width play has a maximum value of 0.08mm, which will directly impact the medical instrument position with a translation (direct influence on maximum 3D Euclidean error) – however, only half of this value will be considered as the central position is the intended position, leaving 0.04mm of play to each side. Considering now the rotation:

- POS pin
 - Pin diameter: ϕ 4 mm \pm 0.05
 - Hole diameter: ϕ 4 mm +0.012/-0
- ANG pin
 - Pin Diameter: ϕ 4 mm \pm 0.05
 - Hole Diameter: ϕ 4 mm N7 (+0.02/+0.05)

A POS module maximum deviation of 0.062mm and an ANG max. deviation of 0.1mm must be considered – however, the EEF own weight will have centered the joints which means the user should only be able to deviate each pin inside the hole by about half the max. play. Considering this we end up with a max. 3D Euclidean Error, per the trigonometric model shown in “Deviations and Error Calculation”, of 0.3mm to which we add the 0.04mm of “width play” for a total error of **0.34mm**.

2nd Deviation Mode

The 2nd deviation mode is another rotational deviation, that is not independent from the 1st deviation mode due to sharing the same interfaces/joints. If we consider that the POS module maximum deviation of 0.062mm can result in a sideways rotation of the EEF, which has a length of contact with the pin of about 16.2mm, this would result in a maximum 3D Euclidean Error of 0.383mm – see Figure 46.

Despite this, the calculation did not consider that the top of the EEF body would be blocked by the fork guiding joint – this feature allows a maximum 3D Euclidean Error of 0.123mm, as shown in Figure 47 – which is **inferior to 1st deviation mode and thus not considered**.

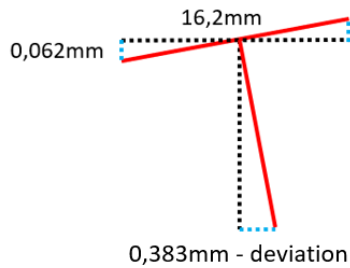


Figure 46 – 2nd deviation mode impact without width restriction

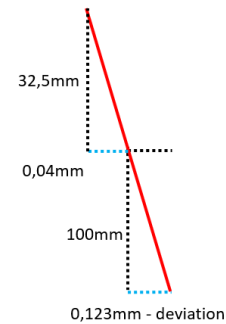


Figure 47 – 2nd deviation mode impact with width restriction

System Rigidity

1. Structural Components

The EEF, NGE, Carriage A1 and Carriage A2 were considered in a Solidworks FEA to assess their impact on overall deviation of the medical instrument for a drill load. The results:

- NGE elastic deformation: 6.5µm
- Carriage A2 elastic deformation: 1.5µm
- Carriage A1 elastic deformation: 3µm

The EEF will be further detailed:

Needle Loads

X-axis deviation - 15 µm
Y-axis deviation - 81 µm
Euclidean Error - 82 µm

Drill Loads

X-axis deviation - 98 µm
Y-axis deviation - 81 µm
Euclidean Error - 127 µm

This analysis considered the configuration shown in Figure 48. The long cylinder had the top tip at a 32.5mm vertical distance from the ANG module to have the loads applied at the intended position and the bottom tip was 100 mm below the POS module (thus reflecting Euclidean error at a target 100mm deep) – this part was considered rigid.

The needle guide, which ensures the connection between the EEF body and the needle and was considered in PA6 for needle loads and rigid for drill loads (as the interface should be another).

The EEF body, pins and joints were considered in TECAPEEK (actual material in current EEF – part still in development) and positioned so all play was eliminated before loading.

Further information on the FEA model used for these results can be consulted in section 4.3. The results shown above make use of the most refined mesh possible and a rigid interface between the disposable needle guide adapter and the EEF body.

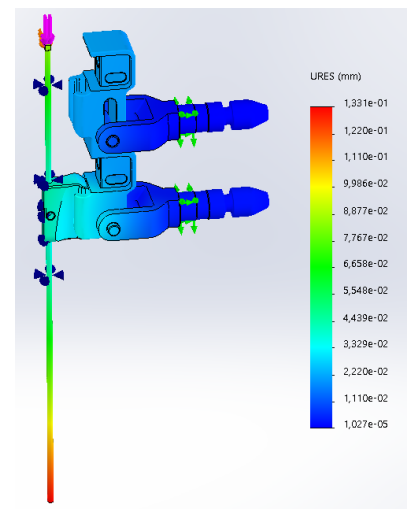


Figure 48 – EEF FEA analysis displacement results

2. Linear Guides

Baseplate – Carriage A1 linear guides

No information is available on the linear guides rigidity. However, considering the equations from NSK linear guide manual [NSK, 2020] shown in Figure 49 for the Baseplate-Carriage A1 linear guides, and a rigidity of 10N/μm (proposed value for this study, based on NSK miniature linear guides) the calculated deviation at the medical instrument is **20μm**. Considered values:

- L = 81.7 mm
- l = 24 mm
- Ks = Kr = 10N/μm
- Driving Point
 - Xb = -7 mm
 - Yb = -70.85 mm
 - Zb = 15 mm
- Load Point = Deviation Point
 - Xy = 13 mm
 - Yy = 74.85 mm
 - Zy = 14 mm
 - Fy = 5 N
 - Fz = 10N

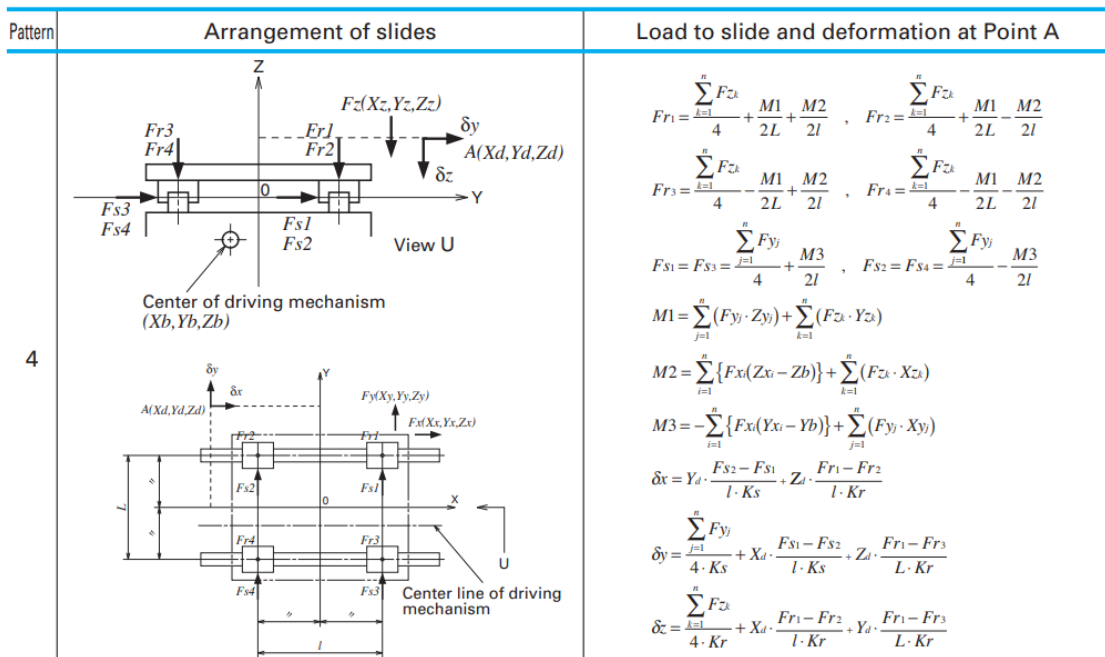


Figure 49 – Linear guide deviation equations [NSK, 2020]

Carriage A1 – Carriage A2

The linear guide configuration for the carriage A1-carriage A2 interface has all the moving blocks turned into the interior of carriage A1, meaning all of them will be subject to an upwards compression/extension force. The rigidity and consequent deviation are detailed in Figure 50.

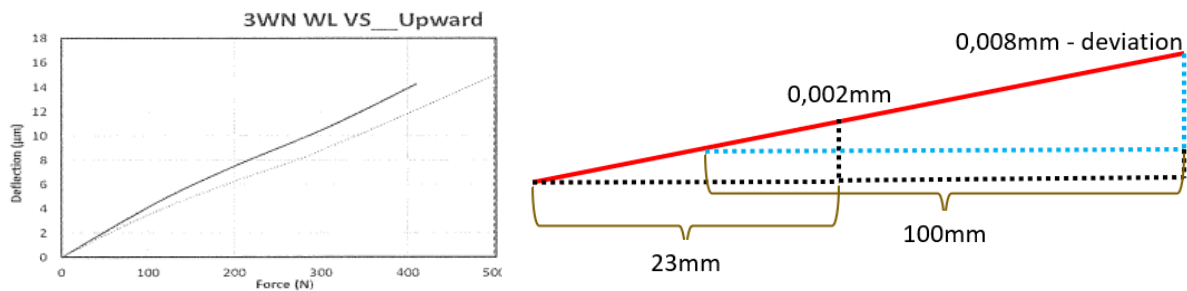


Figure 50 – Linear Guide upwards rigidity (left) and resultant instrument deviation (right)

For a 5N load around $1\mu\text{m}$ of deviation can be expected (linear guide play, as rigid deviation is negligible), which means that the maximum needle deviation will be around $8\mu\text{m}$ - Figure 50. However, one should consider that the fit between carriage A1, the linear guides and carriage A2 is nominally designed to be with 0 play/interference, but a total of $\pm 40\mu\text{m}$ of manufacturing tolerances are possible, which means that a loose fit can be the case. Because no play compensation method exists other than the 8 M2 screws that connect carriage A2 to the linear guides, these will be subject to the 5N (+ rotational momentum) and will elastically deform.

Screws will not resist to compression forces so the load should be distributed to only 4 of 8 total screws. This means the screws will be subject to approximately 1.25 N from the force and 5.5 N from the momentum (load applied 100mm away from the center of the linear guides) – considering their rigidity of 200GPa they would be deforming up to $10\mu\text{m}$ (total carriage deviation in 23mm of $20\mu\text{m}$).

Despite the play being able to go up to $40\mu\text{m}$ that is not expected since the production is validated and controlled, and article inspection indicates the manufacturer achieves quite tighter tolerances – thus, it will be considered that the carriage will likely hit the linear guide blocks during deformation and thus a compromise value for the trigonometric calculation will be used: for this analysis a $20\mu\text{m}$ deviation will be considered in 43mm – this is the contact length between carriage A2 and the linear guides blocks. The maximum deviation to the medical instrument, following this rationale is of about **$46.5\mu\text{m}$** – see Figure 51.

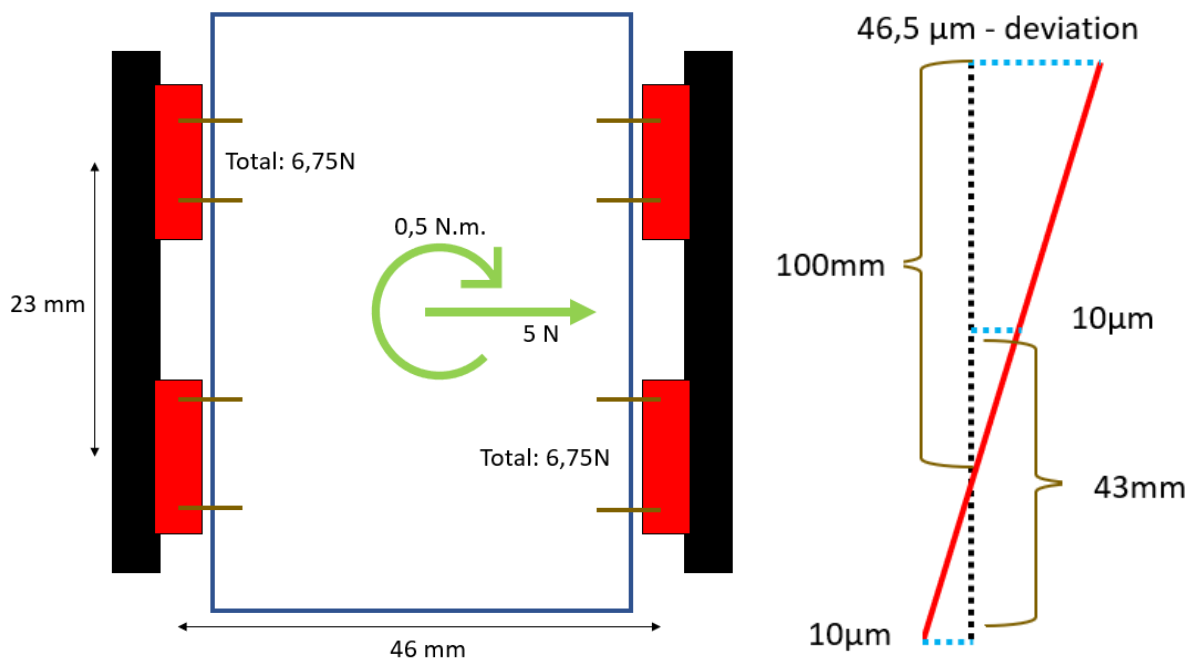


Figure 51 – Simplified screw deviation calculation (left) and impact at instrument (right)

Linear Guide Calculations Validity

The linear guides calculations account for some considerations and simplifications that might result in dubious results. There is no better way to confirm these results than with a test where the different components influence on overall performance is evaluated, however one can have a feeling for the general accuracy of the calculations by comparing them to past tests.

These past tests (informal tests, on “pre-development” versions of the system) have shown a y-axis deviation of the NGE, for a 5N load, in the order of 0.07–0.1 mm – comparing this with the calculated $(28+8+46.5+11\mu\text{m})$ 0.0935mm is an indication that the final result from the calculations is not disconnected from the actual system performance.

Conclusions

Drill-Type Loads

Having completed the analysis, it is possible to summarize the several deviation parcels for the ANG module, as it is the one subject to the 5N. The results:

- Positioning error due to drive chain backlash – **0.03mm** (x-axis + y-axis, separate and independent)
- NGE to EEF interface play – **0.112mm** (y-axis)
- EEF internal play – **0.05mm** (x-axis)
- Components rigidity – **0.021mm** (y-axis)
- Linear Guides rigidity – **0.0755mm** (y-axis)

For the POS module:

- Positioning error due to drive chain backlash – **0.03mm** (x-axis + y-axis, separate and independent)
- NGE to EEF interface play – **0.112mm** (y-axis)
- EEF internal play – **0.031mm** (x-axis)
- Components rigidity – **0.0105mm** (y-axis)
- Linear Guides rigidity – **0.03775mm** (y-axis)

Joining x-axis and y-axis deviation we have the following total deviations:

- POS module – **0.200mm**
- ANG module – **0.242mm**

Because the ANG module is installed directly on top of the POS module, and because the POS module will deviate to one side (dragging the ANG) and the ANG to the opposite side the POS deviation must be subtracted to the ANG's to be able to directly use the derived trigonometric mode present in "Deviations Mode":

- POS deviation – **0.200mm**
- ANG deviation – **0.042mm**
- Maximum 3D Euclidean Error at 100mm – **0.792mm**

To these, a direct error must be added due to:

- EEF width play impact – **0.04mm**
- EEF rigid deviation impact – **0.127mm**
- Image registration equipment – **0.5mm**
- **Final Max. 3D Euclidean Error – 1.46mm**

The TP + EEF universal twin adapter is thus theoretically capable of fulfilling the requirement of maximum 3D Euclidean error inferior to 2.0mm even in the presence of adversary conditions such as a misguided user load input during a drilling procedure.

Needle-Type Loads

The same rationale can be applied to needle-type loads – in this case the plays will still influence the system the same, but the rigid deviation will be cut by 10 fold (since the considered loads are 10 times inferior) – an exception is made to the EEF rigidity, the calculated deviations have been shown before.

Additionally, it is important to consider the disposable, MJF printed, needle guide. This component, by itself, can introduce as much as 0.4mm of 3D Euclidean Error according to an analysis carried independently from this project's activities. The total worst-case deviation is then **1.54mm of maximum 3D Euclidean Error.**

Summary of Calculations

Table 1 will group the several components for their influence in the system deviation, for both POS and ANG modules, and also provide data on the expected improvement gained from completely eliminating the influence from that system on the instrument deviation. The “POS Dev” and “ANG Dev” are deviation values based on the expected position of the module in case of no play and infinite rigidity and considering the POS-ANG vertical stack interaction.

Table 1 – Summary of Performance Calculations

Sub-System	Drilling procedure [μm]			Needle Procedure [μm]		
	POS Dev	ANG Dev	% Improv.	POS Dev	ANG Dev	% Improv.
Drive Chain	30	0	14%	30	0	20%
NGE-EEF	112	0	37%	112	0	47%
EEF	31	19	4%	31	19	13%
Overall Rigidity	11	11	8%	1	1	1%
Linear Guides	38	38	28%	8	8	5%
Total	3D Euclidean Error = 0.87 mm			3D Euclidean Error = 0.6 mm		
Camera Error	0.5 mm					
EEF Rigidity	0.127 mm			0.039 mm		
Needle Guide	-			0.4 mm		
System	3D Euclidean Error = 1.46 mm			3D Euclidean Error = 1.54 mm		

Note: It must be considered that the position deviation is a non-linear function of the several deviations (thus the sum of the percentage improvement contribution of each sub-system does not amount to 100%)

The percentage contribution of each component to the Drive Chain is shown in Table 2.

Table 2 – Summary of each component contribution to drive chain backlash

Component / Sub-System	Deviation at POS [μm]	% Contribution
Drive Chain	30	-
Motor Gearbox	2	7%
External Gears	1	3%
Spindle Elastic Deviation	2	7%
Spindle Play	(Estimated) 21	69%
LSN Play	3	8%
Carriage Tilt	2	6%

Maximum System Backlash

As mentioned previously, heavy discussion as taken place on what is a valid criteria for the admissible system backlash – this is because currently the criteria is set at $\pm 30\mu\text{m}$ of maximum allowable deviation between rotary encoder and linear encoder (intended position vs actual position of the system), which is only fulfilled at the early life of the device and does not allow much margin for system changes.

Regarding this topic it is important to understand that heavy usage of the system has showed that the main deterioration of the system occurs at the level of the drive chain backlash, not being detected any other relevant deterioration in position accuracy or position retention. Thus, the maximum allowable difference between the position measured by the rotary encoder and the linear encoder, given this worst-case analysis and the need to achieve a maximum of 2.0mm 3D Euclidean Error, would be of **138 μm** – very unlikely to be the case even at EOL.

Next Steps and Improvement Opportunities

This analysis was subject to several considerations and simplifications, reason why the results might not fully represent the actual 3D Euclidean Error of the system, however, it should allow for a better understanding on the relative impact of every sub-system on overall equipment performance, which was its main goal anyway. To validate this analysis and to accurately understand actual system performance, a static characterization is necessary – however, such an analysis was not possible to be concluded in the timeline of the writing of this dissertation, though work is in preparation.

Regarding mechanical improvement opportunities, the NGE-EEF interface was found to have substantial impact in the overall performance of the system and a rework could provide very beneficial to the system. Such an optimization was not explored in the context of this project but given this data an alternative concept is being procured in parallel by another project.

The company also decided to implement, based on this analysis, a higher threshold for the allowed rotary vs linear encoder deviation. A $60\mu\text{m}$ threshold was defined to ensure that no product is restricted from entering the market (previous criteria was too strict) while ensuring high performance is still achieved (hence why the threshold was defined quite far from the maximum possible $138\mu\text{m}$).

4.3 Twin vs Single Pin EEF Adapter Analysis

The Trajectory Platform’s medical instrument interface equipment, the EEF, is a functional piece of equipment essential to equipment performance, as detailed in section 4.2. In this section, a further analysis of the EEF will be conducted, including a Finite Element Analysis (FEA) to its structure (some of the results were already used in the previous section).

This activity was carried to support ongoing development activities taking place at Interventional-Systems concerning the development of a new geometry for the EEF universal adapter. This adapter may be used for all kind of medical instrument holding, being important to ensure proper rigidity to lessen unintended deviations when considering the need to position the medical instrument accurately at deep targets inside the human body.

While special geometries may be used for specific medical instrument holding, and special medical procedures, the universal adapter functions as a jack of all trades and must be prepared to hold either heavy, up to 2.5Kg (usually static operated instruments such as endoscopes), or negligible weight instruments such as needles. To ensure the connection with varied kinds of medical instruments a disposable adapter is attached to the EEF; this piece usually contains a round recess for the instrument alignment and a screw to lock the instrument movement during system positioning/repositioning.

Two currently available geometries for this universal adapter can be seen in Figure 52, varying mostly in the guiding joints geometry, one consisting in a “single” pin and the other in a “twin” pin (fork guiding joint), both will be considered in the FEA that will be detailed next.

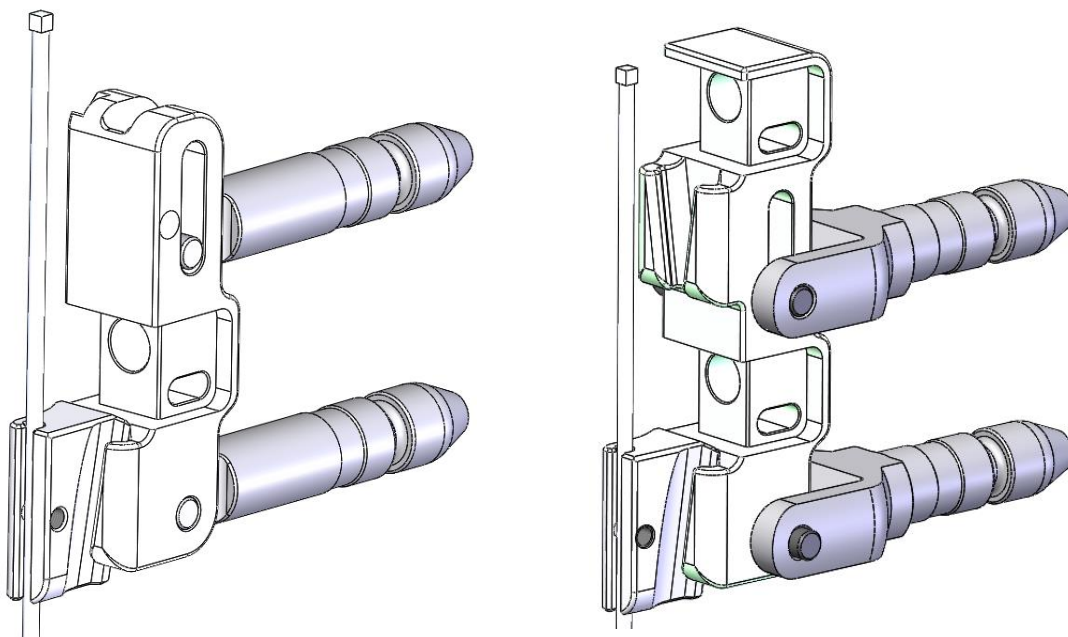


Figure 52 – EEF universal adapter single (left) and twin (right)

The main objective of this activity would be understanding how relevant the difference between the “single” and the “twin” guiding joint is. The “single pin” structure is preferable given that all of the side surfaces of the EEF are free from moving parts and thus that more surface is available for including extra features; this is particularly important given the plan to incorporate spheres for image tracking of the EEF position directly into the EEF body structure.

Other secondary objectives in this analysis were set as the simulation work progressed and involved the understanding of the impact of the main EEF structure, of the rotational pivot pins and of the disposable adapter (in terms of structural geometry, interface geometry and material) in the EEF’s performance at static position retention.

Analysis Considerations

Making use of the 3D CAD models and Solidworks® Simulation add-in, it was possible to conduct a static study to determine the performance of both EEF geometries and fulfill other secondary objectives.

The considered loads for this study were the loads considered for the TP performance study, as detailed in section 4.2 – these include the needle-type loads, 0.5N vertical load and 0.25N transversal force, and drill-type loads, 5N vertical load and 2.5N transversal force, applied at the top of a medical instrument at exactly 32.55mm. Additionally, a 25N (2.5kg) vertical force was also considered to simulate heavy instrument holding.

For the EEF guiding joints a fixed hinge fixture was considered at the surface which contacts with the furthestmost NGE pin, to simulate the allowable rotation of the guiding joints inside the NGE and restrict their axial movement (which is accomplished by the back NGE pin).

The disposable adapter was mated into both of the EEFs lower connection interfaces and a $\phi 2$ mm cylindrical body (that simulates a needle) was installed at its bore – this is shown in Figure 52. The needle has a small cube designed at the top to ensure proper load orientation can be applied at the correct 32.55mm distance of the ANG module, and its total height is such that the bottom tip is hanging 100mm below the EEF – because of this, the needle's tip displacement can be used to understand the Euclidean error at a 100mm deep target that results from the EEF rigid response to static loading.

All EEF components were considered in their designated material during the simulation adjustment phase, varying latter according to the secondary simulation objectives. The EEF main body, the guiding joints, and the rotation pins (that connect the guiding joints to the EEF body) were all considered in PEEK. The disposable adapter was considered in PA6 for needle-type loads and rigid for drill-type loads (as another, more rigid geometry is being developed for that function). The needle used to measure the resultant displacement was considered rigid.

Having defined the external boundary conditions and materials to be used throughout the several simulations a simulation adjustment phase ensued. The objective was that of refining the component-to-component contact/contact sets to ensure results could be obtained without simulation warnings or errors and that practical simulation run times could be achieved. No large displacements or rigidity matrix re-calculation options were enabled for all simulations (and no warnings were triggered).

To understand the validity of the results the external forces were evaluated during the first adjusting simulations, to ensure that in HOME position the ANG module pin would absorb near to no load (as it is free to move vertically in the EEF body slot).

Also during the simulation adjustment phase, the mesh type was varied and its size was progressively refined to understand the impact of these parameters in the final results – as needle tip displacement results varied only slightly from the standard mesh type and size to other types and refined sizes (deviations smaller than 10%), the standard mesh and mesh size were selected for all analysis (see Figure 53); this would also ensure directly comparable results between different simulation runs.

The contact sets (seen in Figure 53) were defined so that the needle had a rigid connection to the disposable adapter and that the disposable adapter itself would be rigidly connected to the EEF main body (this would later be changed to a no pierce contact to evaluate the interface impact on performance). The rotation pins were set with a no-piercing contact set to the EEF body contacting surfaces and with a global bonded contact to the guiding joints. The guiding joints were also defined with a no piercing contact set to the EEF body exterior (“twin pin”) and interior surfaces (“single pin”).

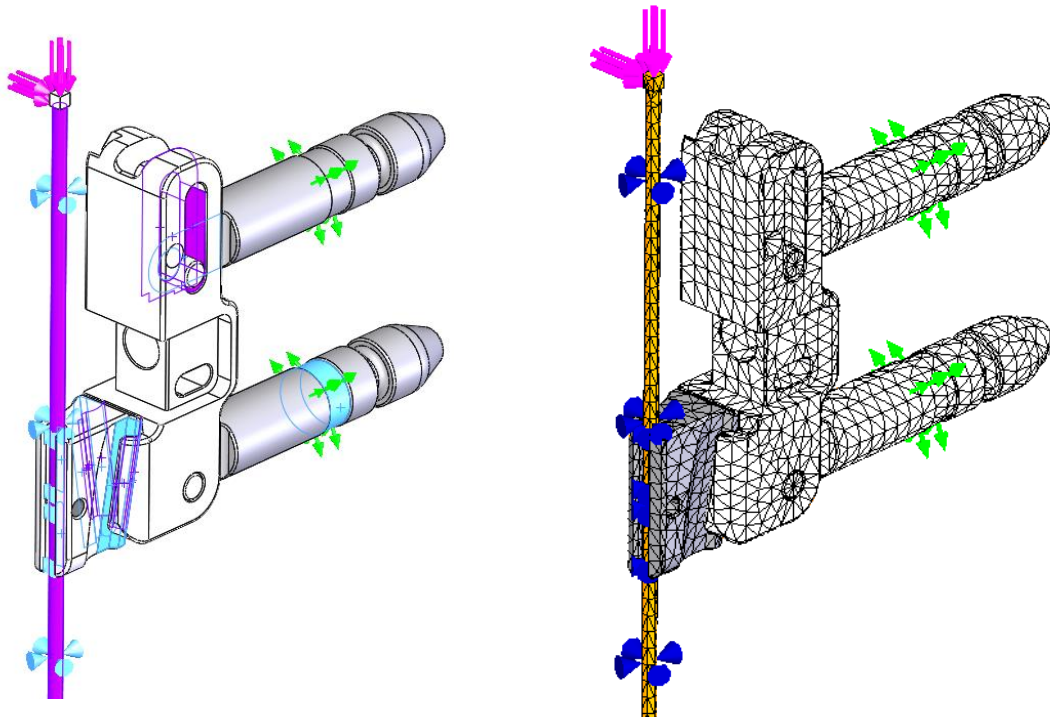


Figure 53 – Simulation contact sets (left) and standard mesh (right)

First simulations Results

As the simulation adjustment phase began showing satisfactory results (deformations evaluated for no piercing and overall twisting behavior of the joint pins and resultant forces evaluated for only slight vertical load absorption by ANG module) the parameters were frozen and repeated for several simulation loads and for both EEF “single” and “twin pin” geometries. The results are summarized in Table 3.

Table 3 – Simulation results for “single pin” and “twin pin” geometries

Load Type	EEF	URES	UX	UY	2D Error
Needle (rigid disposable adapter)	Single Pin	0.012	0.006	0.010	0.011
	Twin Pin	0.010	0.004	0.009	0.010
Needle	Single Pin	0.021	0.006	0.020	0.021
	Twin Pin	0.020	0.005	0.019	0.020
Drill	Single Pin	0.205	0.128	0.151	0.197
	Twin Pin	0.147	0.099	0.095	0.137
Endoscope	Single Pin	0.303	0.273	0.005	0.273
	Twin Pin	0.261	0.229	0.010	0.229
Note: Values in millimeter; 2D error is Euclidean XY deviation at the needle tip					

These results seem to indicate that no substantial difference exists between the “twin” and the “single pin” EEF geometries, considering Needle and Endoscope loads – maximum 2D Error results with a 19% difference in worst-case. Given that a “single pin” geometry is beneficial from a constructional aspect, the difference between 2D Error results is not enough to discard the “single pin” design.

For drill-type loads the 2D Error difference reached up to 40%. However, the EEF body might still be designed thicker to accommodate a more rigid “single pin” guiding joint – this should allow a compromise between functionality and rigidity. Either way, the 60µm difference only accounts for 3% of the 2mm maximum permissible error, so the “single pin” design is, in actual terms, a practical solution.

Additional Objectives

For the additional objectives of this analysis the “single pin” EEF geometry was considered as well as the same simulation parameters used up to this point for drill-type loads. The objective then became understanding the influence of certain components (and their geometries and materials) in the overall performance of the EEF.

A first study considered the benefits of changing the material and diameter of the rotational pivot pins. The pins were thus independently considered with a 5mm diameter (from previous 4mm) and in steel, from the previous PEEK pin simulation. The results are present in Table 4 and appear to indicate minimal performance increase with changes to this component.

Table 4 – FEA results for additional EEF study objectives

Pivot Pins Study				
Condition	PEEK (Standard)	Steel	ϕ 5mm PEEK	
URES [mm]	0.159	0.141	0.148	
Disposable Adapter Study				
Condition	Non-Rigid Adapter Body	Non-Rigid Adapter Interface	Non-Rigid Adapter Interface & Body	
URES [mm]	0.239	0.199	0.358	
EEF Solid Body Study				
Condition	PEEK (Standard)	Non-Rigid Adapter Interface	Non-Rigid Adapter Interface & Body	
URES [mm]	0.092	0.149	0.302	
EEF Solid Body Tilted Study				
Condition	Single Pin (Standard)	Single Pin w/ Solid Body	Twin Pin (Standard)	Twin Pin w/ Solid Body
URES [mm]	0.413	0.186	0.350	0.187

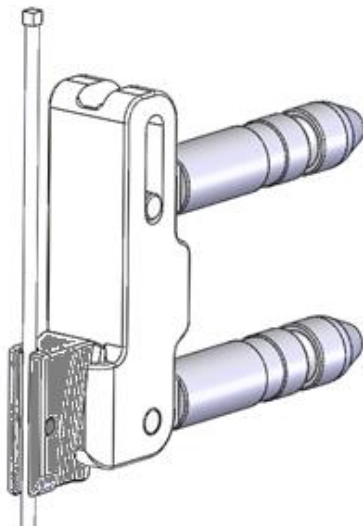


Figure 54 – EEF “solid body” geometry

A second study was carried to determine the influence of the disposable adapter. For this study, this guiding component was either considered as deformable, or its interface to the EEF body was considered as non-rigid (in some cases also both). The results shown in Table 4 seem to indicate that the disposable component may have a substantial impact in overall static performance. While for needle loads the geometry shouldn’t represent a big concern, for heavier instruments and/or higher load applications, the use of two adapters is recommended (see the two interfaces present in the “twin pin” geometry shown in Figure 52).

The final consideration was regarding the EEF main body structure, as the cutouts in the current geometries are surely impacting rigidity.

The EEF was redesigned without the cutouts as shown in Figure 54 and simulations were repeated. The results in Table 4 indicate that this might be the feature most impacting system performance, especially when considering the calculated deviations for endoscope vertical loads with the EEF tilted by 15°. It is recommended that the EEF main structure is kept as rigid as possible to minimize rigid deviations.

5 System Cost Improvements

Having detailed the cost analysis for the system and having mentioned several potential topics for cost-optimization in section 4.1, the next sections will focus on analyzing solutions. Whenever considering the need for quotes, the number of parts necessary to assemble 60 systems were considered as the reference number – expected annual sale volume at product launch. This is not the case, however, if the process in study is typically used for lower order quantities, which is the case of vacuum casting – in this case quotes were asked for 20 parts and the price was then scaled for 60 systems to allow for direct comparison with other processes.

5.1 Clamping Plate and Blue Band components

The clamping plate and the blue band components, cover tape bracket and pin holder, are very small parts – general dimensions can be seen in Figure 55 – with simple geometries. However, they represent a cost that is not in line with their size or complexity as they are ordered in small quantities. These components can thus be targeted for a manufacturing process change.

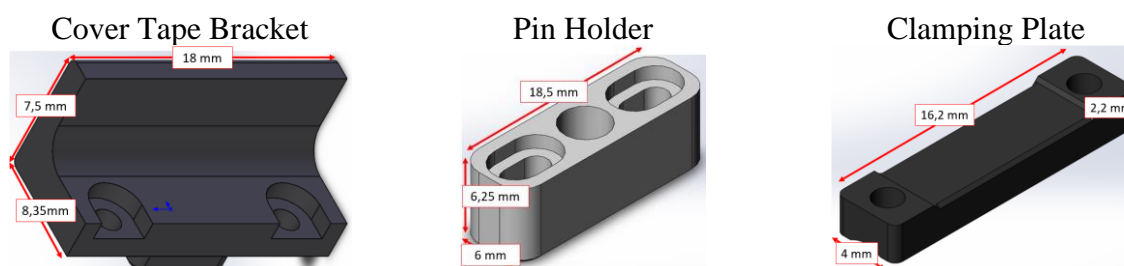


Figure 55 – Clamping Plate and BB components general dimensions

In the current design the pin holders are in aluminum and produced by CNC machining. Their only functionality is the support of the pins that serve as corners for the blue band/tape, making it possible to translate the holder(s) and fix it onto the baseplate with 2 screws in such a position that the fabric is stretched. This part could easily be produced, in small quantities, by additive manufacturing processes such as Fused Deposition Modeling (FDM), Selective Laser Sintering (SLS), HP's Multi Jet Fusion (MJF), etc., provided that the material is changed to a plastic such as PA12, ABS or similar. Metal additive manufacturing processes could also be considered, however, given the low temperatures (max. 40°C) and small (if even existing) loads stressing these components they were not considered given their much higher cost.

The cover tape bracket and the clamping plate, in the current design, are obtained by plastic machining and produced in PEEK. The material is not cost-effective for the application and, again, the parts could easily be obtained by additive manufacturing. Both these parts as well as the pin holder could thus be bundled together and quoted for additive manufacturing in a plastic such as PA12 and ABS.

Having additive manufacturing processes in mind the parts had to be slightly changed, to ensure they would still properly assemble within the TP. Consulting typical manufacturer's websites such as [Materialise, 2020] it was possible to understand that typical manufacturing tolerances ranged around $\pm 0.2\text{mm}$, meaning that all features intended to have these parts fitting with other components should have a clearance of around 0.2mm – this way it would be possible to ensure manual assembly with ease.

Having made the necessary changes, the parts were quoted in three different additive manufacturing companies situated near the physical assembly location. The companies provided general customers with an online configurator that allowed for a first cost-optimization analysis. Results, taken directly from the several companies' websites, are summarized in Figure 56.



Figure 56 – Online configurator quote results for additive manufacturing cost-optimization

Results for MJF and SLS quotes revealed particularly interesting, with both processes showing considerably reduced manufacturing costs compared to FDM, SLA and, above all, CNC machining. Each of the companies was then directly contacted to procure additional information on manufacturability, prices and other formalities required by Interventional-System’s supplier procurement process. The process can be summarized in 5 steps:



Following this procedure, it was possible to understand that the pieces were ready for manufacturing (inputs on manufacturing were positive) and that actual part cost could be further reduced through negotiation, especially for the Multi Jet Fusion (MJF) process.

Table 5 – Additive Manufacturing Final Selection

Final Decision – MJF process – PA12 – Company 2

Clamping Plate (Cost Reduction – machining)	Pin Holder (Cost Reduction – machining)	Cover Tape Bracket (Cost Reduction – machining)
0.50€ (-93%)	0.50€ (-96%)	0.50€ (-94%)

The costs seemed promising and a sample (12 parts of each) was ordered to assemble a total of three systems. The parts revealed to fit in the TP and are now supplied by company 2 as the cost-optimization benefit of this transition is substantial (see Table 5).

As mentioned in chapter 4.1, the blue band sub-system could benefit from an overall redesign to reduce the total number of parts and potentially improve dust and liquid ingress. This redesign was not possible to be tackled in the time frame of this project, and thus the only improvement for the sub-system is the cost reduction of the two “holder parts”: pin holder and cover tape bracket – other major improvements are open as a potential future improvement.

5.2 NGE and SRB

Considering the analysis of chapter 4.2, the NGE connection to the EEF is likely to be under-performing. Because of this a redesign proposal project was attributed to other members of the company. As a major redesign is not in scope of this project the objective of this analysis is the short-term cost-optimization of the already existing parts.

During cost analysis the components of the TP responsible for connection with external equipment, such as the EEF, have been grouped under the designation of “NGE assembly area”. This is because the NGE is the essential component of that assembly area, serving as the structural piece that rigidly connects to carriage A2 and offers a bore for the connection of the EEF guiding joints. As the main structural part of the assembly area, the NGE is a key component that must show adequate structural properties, such as rigidity, resistance, and thermal stability, reason why it is manufactured in PEEK. All other parts act as accessories to the NGE, to either act as cover parts or as interfaces to the user. A comparison between the cost allocation for the several NGE components is detailed in Figure 57.

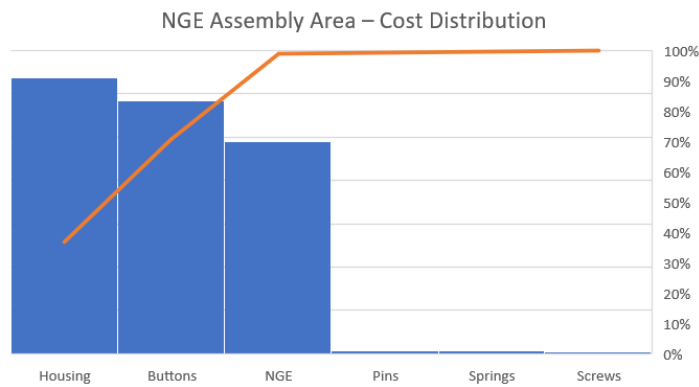


Figure 57 – NGE assembly area cost allocation

As it is possible to understand from the pareto chart in Figure 57, the housing and buttons account for a very significant portion of the total cost, at around 80%. The parts that make up the housing as well as the buttons are shown in Figure 58 along with their general dimensions.

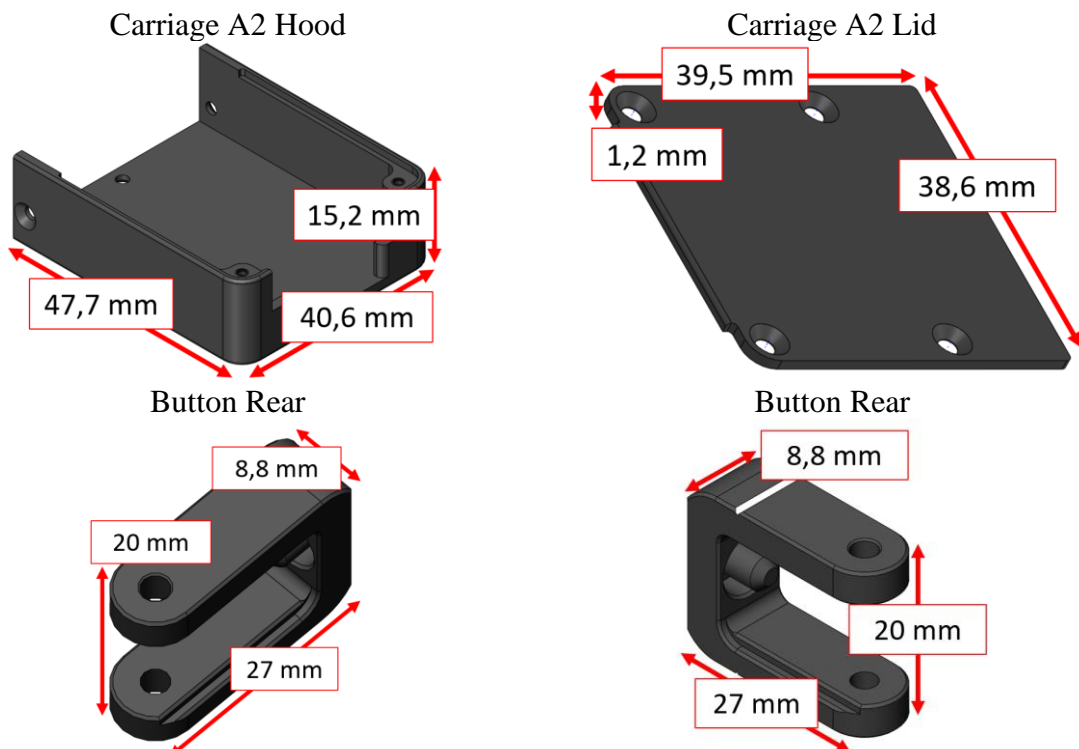


Figure 58 – NGE accessory parts

These parts, whose purpose is to complement the NGE, are having a rather significant impact on the “assembly area” costs, which can perhaps be explained by their material and manufacturing process choice. The parts are obtained by PEEK machining, which is not necessarily the most cost-effective material selection given the small loads (when even existing) and temperatures involved in the storage, shipping and use of the device.

While the parts are not too large to obtain by additive manufacturing, they are external parts and thus subject to strict aesthetical requirements, meaning that this process is not competitive due to the need for post-processing. Because of this, processes such as Plastic Injection Molding (PIM) and Vacuum Casting (VC) were selected for cost analysis.

Due to the short-term nature of this cost optimization activity the cost of tooling with a PIM process might be difficult to justify, so Vacuum Casting was considered as the main alternative process. However, as it would be interesting to compare the cost of VC to that of PIM for future decisions, some quotes were requested also for this process.

In addition to the NGE related parts, the SRB cover was also included in these quotes with the mere objective of compiling additional data to help with future development decision, as already explained in chapter 4.1.

For VC, and as PEEK is unnecessarily expensive for the application, all parts were quoted for ABS-like PU materials – the available materials varied with the company, but the main characteristics that guided material choice was: black color, Shore D > 80 and Max. Temperature >80°C. For PIM, the parts were quoted for PA6, given the same rationale.

To obtain these quotes, as well as manufacturability inputs, the same process as detailed in chapter 5.1 was followed, with five different possible suppliers being contacted (two for PIM and three for VC). One of the potential PIM suppliers did not respond, so PIM quotes are rather limited and might not be entirely representative of actual market prices.

The quotes, shown in Figure 59, revealed it is possible to obtain a cost reduction (around 50%), considering some of the best quotes, for the NGE related parts when considering both Vacuum Casting as well as Plastic Injection Molding as alternative manufacturing processes.

Quotes Results

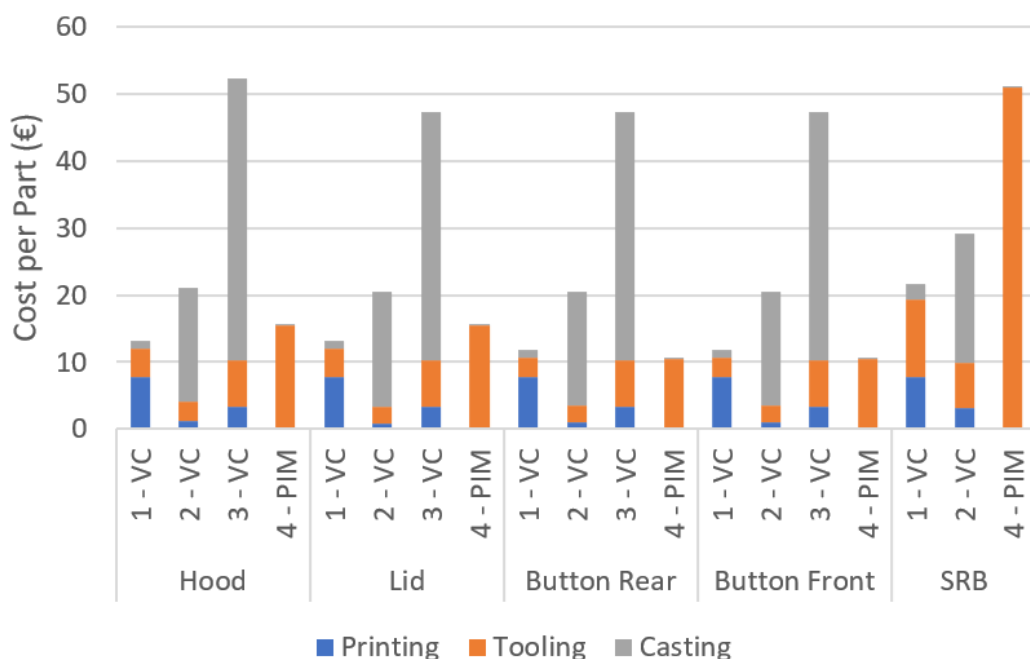


Figure 59 – Quote results scaled for a total of 60 systems

It is also interesting to observe that Vacuum Casting showed the most competitive prices for almost all parts with PIM providing only slightly better results for the buttons. However, it must be noted that Figure 59 represents cost per part when scaled for orders totaling 60 systems, or a total of 120 parts (given 2 parts of each exist in every TP), which means that as a short-term fix Vacuum casting might provide a much better alternative provided that the NGE-related parts are reworked before 60 systems are required to be delivered to customers.

Additionally, it must be noted that despite that quotes were delivered for all parts it was noted that the suppliers, when questioned, would mention that the buttons small size could result in surface defects if Vacuum Casting was employed – if that is the case, and it is not possible to obtain pristine surface condition by VC, than these two separate button could most likely be joined into a single piece for ease of manufacturing, or be obtained directly by PIM.

The NGE related quotes were inserted into the IT system and will be considered during next production round. The SRB quotes, especially with VC, can be used in the future when considering the design of somewhat complex, small production scale plastic parts – these are hardly competitive when obtained by PIM due to the tooling costs, which also restrict design changes, and machining of the complex geometries has proved to be unnecessarily expensive.

5.3 External Gears

Again, following the analysis carried out in chapter 4.1, it might be possible to also improve the system, cost-wise, by targeting the external gears. This part of the drive chain consists in a pair of miniature, 0.4 modulus, stainless steel spur gears. The pinion is rigidly connected to the motor shaft through the pressing of two screws, inserted in its hub, and has 24 teeth; the other gear is connected directly to the spindle of the leadscrew through the use of a gear clamp and has 34 teeth. The setup is shown in Figure 60.

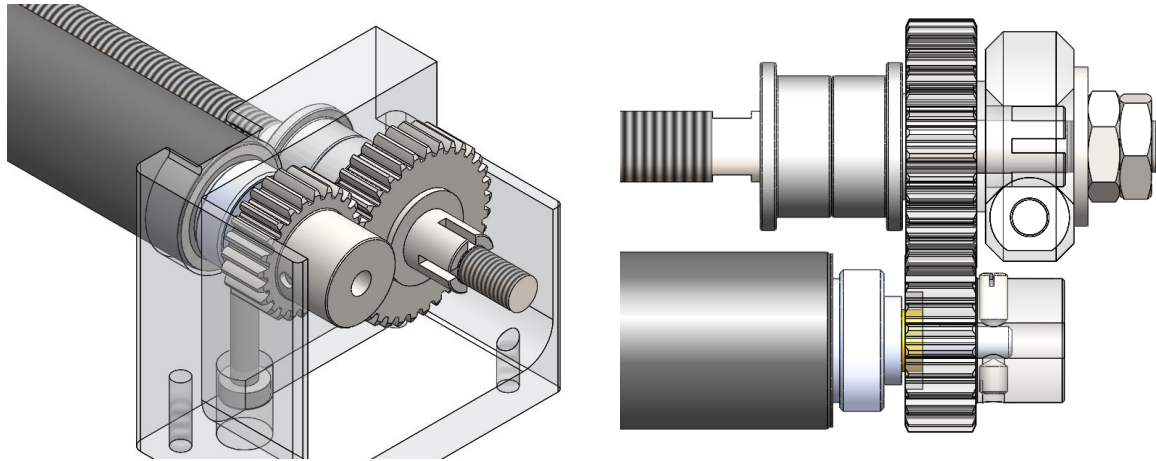


Figure 60 – External Gears setup for the drive chain

When thinking about a potential cost-optimization the use of plastic gears has potential. Considering that the transmitted binaries are rather small and that the rotational speed of the gears is neither too fast nor too slow, as will be detailed later, and that no special attention is given to the balancing of the gears during installation, without prejudice of the pair's performance, then the use of a plastic gear pair could provide several benefits such as:

- Reduced Cost
- Noise Reduction
- Self-Lubrication
- Less overall/eccentric mass

To understand what kind of plastic gears are available in the market several possible suppliers were contacted. The research revealed that most suppliers do not own a stock of plastic gears with this size (modulus) and teeth number – these are not commonly available standard products – and would ask for a minimum order quantity (MOQ) of around 5000 pieces.

This MOQ is not at all possible to satisfy having cost-optimization in mind, so it became necessary to choose other plastic gear sizes. Considering SDP/SI's online catalogue [SPD/SI, 2020], an Acetal pinion with 0.4 modulus and 24 teeth was readily available for purchase, however, no 34 teeth gear was available. Despite this, it would be possible to obtain 32 or 35 teeth acetal gears.

As can be seen in Figure 61, increasing gear sizes is problematic given the small clearance, of around 3mm, existing between the Bearing Block (which would have to be enlarged) and the PCB to its left; the same is true when considering a decrease in gear size, given the even smaller clearance between the electrical motor and the leadscrew nut of 0.96mm.

Considering the best option of a 35 teeth gear, the increase in diameter is 0.4mm, meaning it will fit the assembly – it will require, nonetheless, a change to the bearing block (width) and to the TP software (as the ratio between rotor rotation and carriage translation will change). While the part cost benefit will be evaluated within the scope of this project, the work hours required to change the software and V&V tests will not be considered, meaning the change might ultimately not be so beneficial to the company as stated in this document.

Having selected two standard acetal gears – datasheet can be consulted in Figure 99 at Appendix A – it is necessary to ensure they fulfill the required load bearing capacity. For this, and given the plastic materials, VDI 2736 was used.

Knowing that the electrical motors shutdown when a 40N external force is reached on any axis, this can be considered as the maximum load for the leadscrew. The relation between the axial load at the leadscrew and the binary load at the motor has been experimentally identified to be 36622 N/N.m., which in turn means a maximum of approximately 0.0011N.m at the electrical motor. The electrical motor is directly connected to a standard planetary gearbox with a reduction factor of 16, meaning the pinion is subject, at maximum, to approximately 0.014N.m.

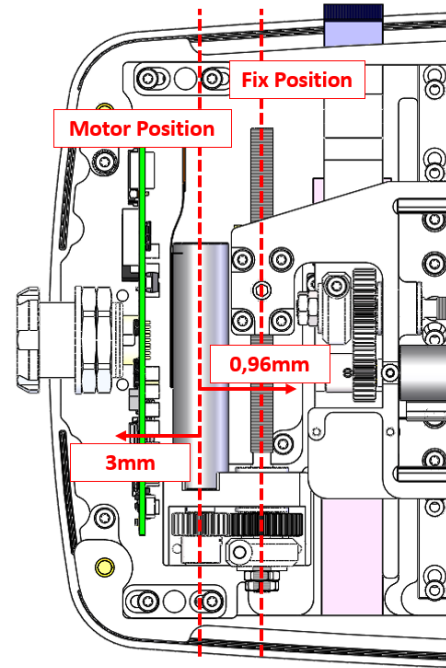


Figure 61 – Drive chain position within a TP module

The same rationale can be applied to the rotational speed given that the carriages travel at maximum velocity of around 7mm/s and that the full reduction factor of the drive chain is $514.7 \cdot 10^{-6}$ mm/s/rpm. The speed at the pinion is thus 850 rpm.

According to VDI 2736 it is important to guarantee that the tooth/flank temperature of the gear is within acceptable levels, that the tooth root is capable of carrying the required loads, that the frictional wear is acceptable as well as the deformation. For acetal/POM gears it is stated, in VDI2736, that it is not necessary to verify the tooth flank load-carrying capacity (the tooth root load carrying capacity is enough).

Following the VDI nomenclature:

- Tooth/Flank Temperature Calculation

$$g_{FuB} = g_0 + P \cdot \mu \cdot H_V \cdot \left(\frac{K_{g,FuB}}{b \cdot z \cdot (v_t \cdot m_n)^{0,75}} + \frac{R_{\gamma,G}}{A_G} \right) \cdot ED^{0,64} < 80^\circ C$$

- Tooth Root Load Carrying Capacity Calculation

$$\sigma_F = K_F \cdot Y_{Fa} \cdot Y_{Sa} \cdot Y_\epsilon \cdot Y_\beta \cdot \frac{F_t}{b \cdot m_n} \leq \sigma_{FP}$$

- Frictional Wear Capacity Calculation

$$W_m = \frac{T_d \cdot 2 \cdot \pi \cdot N_L \cdot H_V \cdot k_w}{b_w \cdot z \cdot l_{FI}} \leq W_{zul}$$

- Deformation Calculation

$$\lambda = \frac{7,5 \cdot F_t}{b \cdot \cos \beta} \cdot \left(\frac{1}{E1} + \frac{1}{E2} \right) \leq 0,07 \cdot m_n$$

Table 6 – Summarized results from VDI 2736 calculations

	Pinion	Gear	Min. Saf. Factor
Calc. (Max.) Temperature	30.04 - (80)	30.02 - (80) °C	N/A
Calc. (Max.) Tooth Root Load	0.011 - (47)	0.010 - (47)	4113
Calc. (Max.) Frictional Wear	0.0214 - (0.04)	0.0193 - (0.04)	1.87
Calc. (Max.) Deformation	$5.5 \cdot 10^{-6}$ - (0.028)	$4.9 \cdot 10^{-6}$ - (0.028)	5127
The considered/calculated values for each parcel can be found in Table 11 at Appendix B			

Considering the results summarized in Table 6 it is possible to conclude that the pair of acetal gears can be safely put to use in the TP without worrying for long time performance deterioration. To mount this pair of gears to the bearing block, however, would require some changes to the overall assembly design.

The motor gearbox shaft is $\phi 2$ mm and the spindle's is $\phi 3$ mm, while the standard gears internal bore diameter is $\phi 4$ mm. This could easily be overcome by using a small, standard, silicon tube press fitted inside the gear – this would allow for a first, near end positioning of the gear – coupled with the already existing set screws (which can be drilled during assembly directly onto both the gear and the flexible tube) – see Figure 62.

Making this change, considering the previous cost of the metal gears and clamp, would result in a **cost reduction for the sub-system of around 70%**.

Implementation wise, given that there are many time-consuming development steps required to make this change it has not been selected for development yet. Also, any bearing block rework is pending the conclusions of other activities such as the leadscrew, which will be detailed in the next chapter.

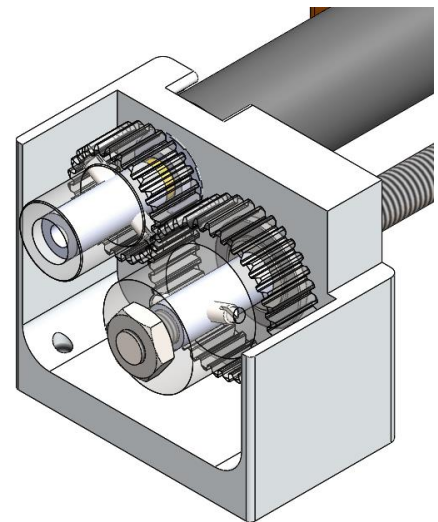


Figure 62 – Plastic Gears Assembly

6 Leadscrew Nut and Linear Encoder

The leadscrew and the linear encoder were already previously identified as potential improvement topics in chapter 3.1, and further analyzed for their impact in cost at chapter 4.1. In this chapter their performance and design will be discussed with more detail and improvements will be proposed and tested. This chapter continues the work from chapter 5 – System Cost Improvements in the sense that the solutions will be considered also for their manufacturability and overall impact on system costs.

6.1 Linear Encoder Redesign

The linear encoder, as mentioned before, contains the foil potentiometer and the magnetic band as well as several structural “holder” parts. It is important, when considering changes for a cost-optimization, to also consider the foil potentiometer problems as detail in chapter 3.1.

Any optimization solutions should consider both improving the cost, by either swapping custom parts to standard ones or integrating existing structural components into other major components, as well as provide some sort of technical solution to the “denting” effect.

Denting Effect and Foil Potentiometer Signals

The functionality of the foil potentiometer has been described in chapter 3.1. During system testing, and because of periodical system characterizations, it has been found that the foil potentiometer would, in some conditions and for some systems, fail to provide reliable position readings for certain areas of motion. The areas that surrounded the plunger during system storage (system is usually stored in the center position – HOME position) were showing major deviations, as can be seen in Figure 63.

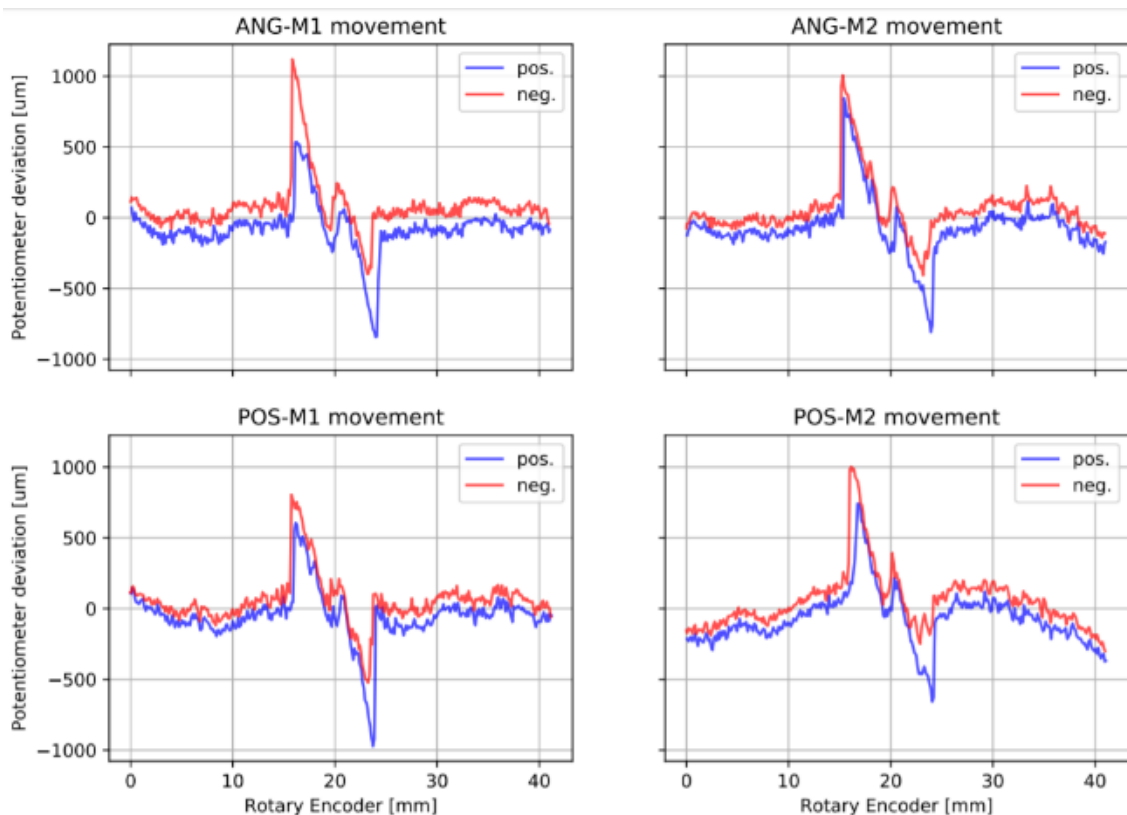


Figure 63 – Example of the “denting effect”

Another problem found during testing, although much less frequent, was signal reading failures at certain carriage positions.

Systems showing this behavior were subject to a small design change to include a washer meant to further deform the leaf springs that pressure the wiper against the foil potentiometer as detailed in Figure 64. The washer proved successful at ensuring proper signal readings, suggesting it was a matter of lack of pressure.

These observations suggest that the “denting effect”, as well as the signal reading failures, were being caused by uncontrolled forces acting on the foil potentiometer (more detailed analysis of the effect and potential root-causes can be found in chapter 6.3).

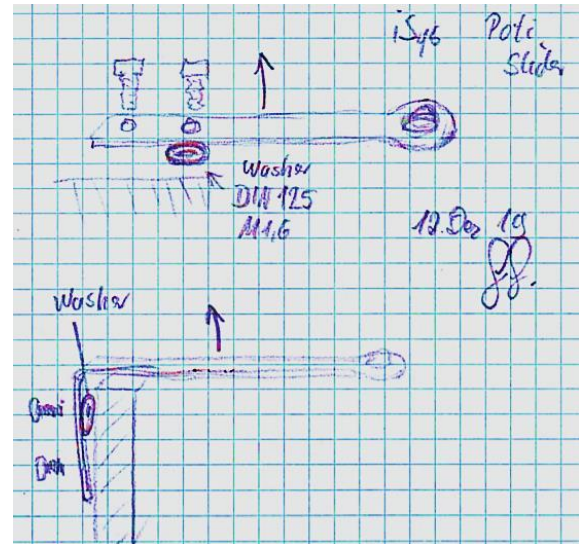


Figure 64 – Washer for extra pressure between wiper and foil potentiometer

Overall, the main problem with the current design of the linear encoder system is that its performance is conditioned by the overall manufacturing and assembly tolerance stack. In addition, it has been reported that the leaf springs themselves, which are bent during production at a supplier company, are often found to have an angle outside of the design specifications, leading to manual adjustments being required during assembly to ensure pressing of the foil potentiometer – the problematic design is shown in Figure 65.

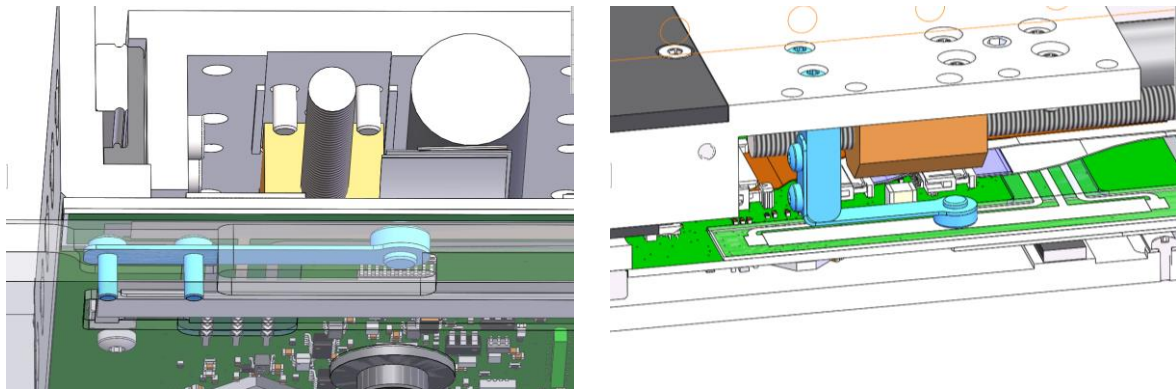


Figure 65 – Initial leaf spring wiper design – A1 (left) and A2 (right)

To ensure controlled forces acting on the foil potentiometer, the ability for the plunger/wiper to accommodate to overall manufacturing and assembly tolerances, to ease assembly and to reduce the use of “holder parts” two new designs were proposed.

New Design Proposals

The new designs were both based on the use of spring-loaded wipers (or plungers) – with this feature the selection of the correct spring, stiffness and length wise, would ensure that the wiper would be allowed to translate (due to spring deformation) to accommodate to the overall system’s tolerance stack and would also ensure proper pressure was transferred to the foil potentiometer at every position.

Custom Design Proposal – One of the design proposals came from an external supplier involved in testing the equipment and consisted in designing custom plastic injection molded (PIM) parts that would make up a miniature spring-loaded wiper – Figure 66.

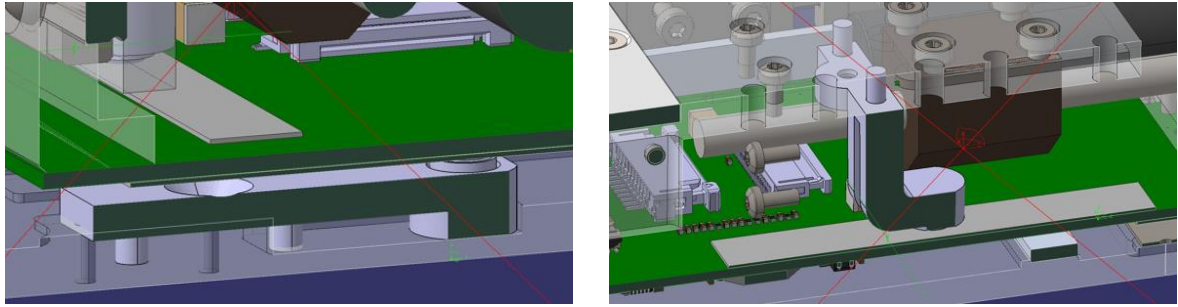


Figure 66 – Custom wiper design and parts

While providing advantages due to the freedom with which complex and miniature shapes could be obtained, the custom PIM parts would not help with reducing the number of “holder” parts in the system, and would lead to the need of investment in tooling, restricting future design changes and leading to higher cost in prototyping.

Standard Wiper Design Proposal – The other design proposal was co-developed as part of the objectives of this dissertation and included a similar spring-loaded design. The intention was, however, to make the most use possible of OTS (off-the-shelf) components. To choose the correct components a small system analysis was necessary, mainly the need to determine what forces were acceptable for the foil potentiometer and the necessary spring stroke length.

For the foil potentiometer the datasheet present in Figure 98 of Appendix A was consulted as well as the supplier, being understood that forces up to 5N were considered as admissible for ball wiper diameters larger than $\phi 2.7\text{mm}$.

For the spring stroke length an overall tolerance analysis was carried for the worst-case of carriage A1-A2 distance – detailed in Figure 67. The tolerance stack was found to be around $\pm 0.11\text{mm}$, not considering any other part that might be necessary to support the wiper.

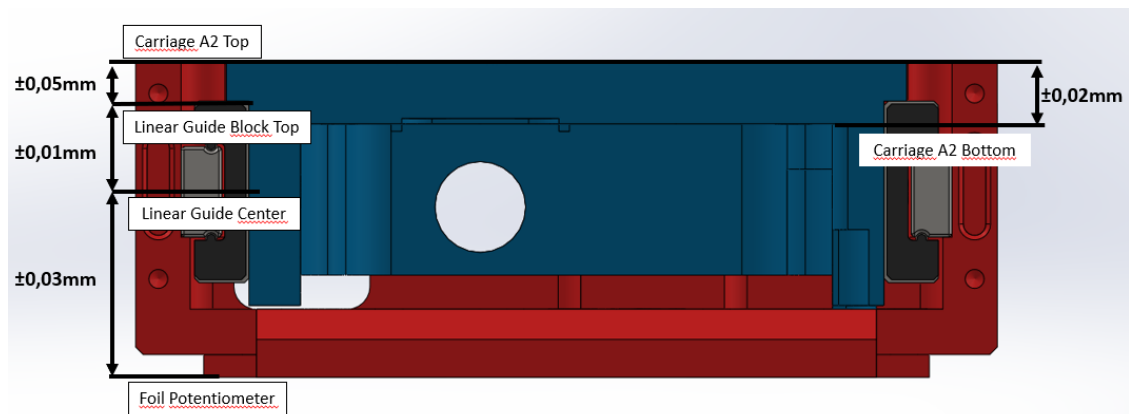


Figure 67 – Tolerance analysis – carriage A2 and foil potentiometer

Considering the need for maximum compactness a Kipp K0333.04 wiper was selected – datasheet can be consulted in Figure 98 of Appendix A – with the following characteristics:

- Full stroke length: 0.8mm
- Min/Max force: 3-7N
- Ball wiper: $\phi 3\text{mm}$ in POM

The wiper would need some supporting structure to allow contact with the foil potentiometer. For immediate prototyping and for refurbishing existing assembled systems some adapter parts were considered – detailed in Figure 68. With the prototyping adapter parts, the worst-case tolerance stack would be $\pm 0.16\text{mm}$, meaning the uncertainty of the force of the spring would be $\pm 0.8\text{N}$. The nominal distances were then selected for an average force of 4N, allowing a variation between 3.2-4.8N. Therefore, the prototype could provide the required, safe, forces and accommodate to the overall tolerances.

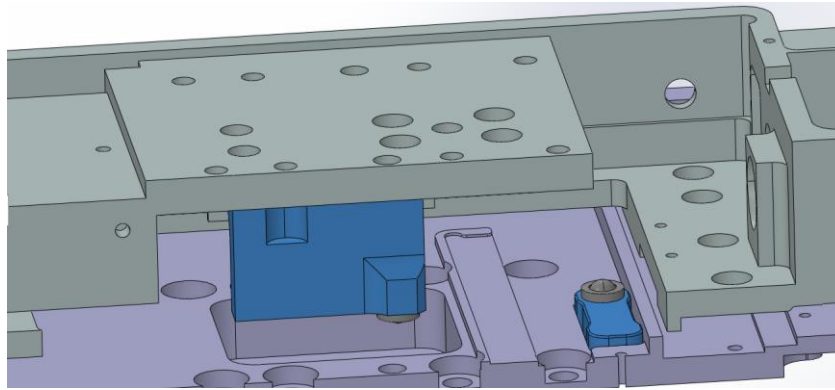


Figure 68 – OTS wiper temporary/prototyping structural solution

However, the intention would be to fully eliminate these “holder parts” in the future, to reduce the total number of parts in the system, improve assembly and reduce costs. To accomplish this, it was proposed that the wiper could be inserted directly into carriage A2’s structure and into the baseplate. The wiper is designed to be press fitted (slight press) into a $\phi 4\text{mm}$ hole, which was considered in the solution detailed in Figure 69.

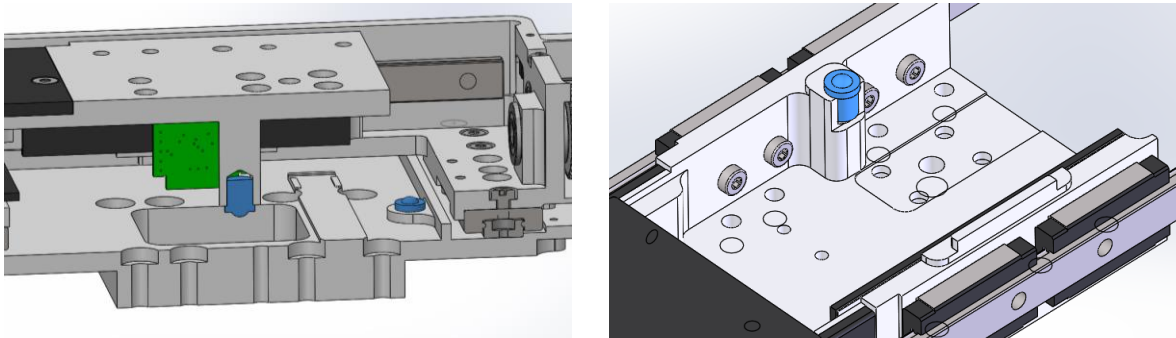


Figure 69 – OTS wiper final structural solution

This design would require only a small change to both carriage A2 and baseplate, and greatly reduce the total number of parts in the system. However, despite the final change being possible, its implementation will necessary stay pending until verification tests prove the OTS wiper performs adequately – testing will be detailed in section 6.3.

6.2 Leadscrew Nut Redesign

The leadscrew nut, as detailed previously, is the component responsible for the connection between the spindles and the carriages, ensuring the transmission of the spindle rotation directly into carriage linear movement during system fine positioning, and preventing any movement of the carriages during position retention.

This interface component, as design currently, is over-defining the assembly and creating substantial problems during system mounting, regularly conflicting with the linear guides. The case of carriage A1 will be detailed further as it is quite similar, and worst-case given the larger distances that accumulate manufacturing tolerance errors, when compared to carriage A2.

Figure 70 shows with some more detail the over definition between the nut and the linear guides. As the bearing block is screwed to the baseplate, and so are the linear guides, any manufacturing/assembly tolerance will deviate the spindle axis from the linear guides axes; also, the bearing block width and carriage A1 length, if not near nominal values will conflict given that the nut is attached to both.

While manufacturing tolerances are tight, meaning that assembly is possible for the system, this procedure is difficult, with several readjustment required for the screws that connect the nut to the carriage, so as to alleviate friction between the nut and the spindle. A redesign of the nut-carriage connection could alleviate these problems if it could ensure the elimination of the overall assembly over definition (shown in Figure 70), letting the nut accommodate to both the spindle and carriage.

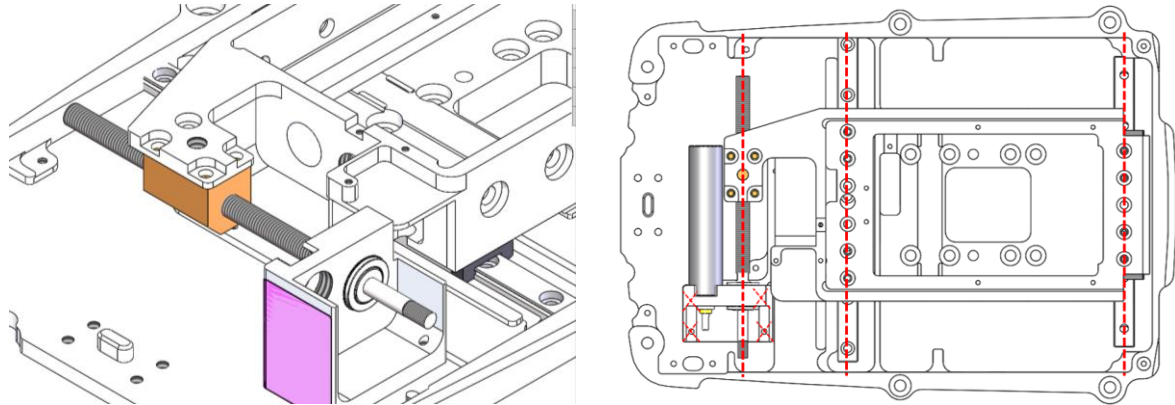


Figure 70 – Leadscrew Nut over definition scheme

To achieve this goal, and similarly to the linear encoder improvement activity, some redesigns were proposed, these can be consulted in Figure 71. The Plastic Leadscrew Nut (p-LSN) was proposed by a partner company and the Translating and Spherical Joint Nuts were developed in the scope of this project and made use of the current Brass Leadscrew Nut (b-LSN) design, with the intent of being possible to refurbish into existing systems for testing.

Plastic Leadscrew Nut

Translating Nut

Spherical Joint Nut

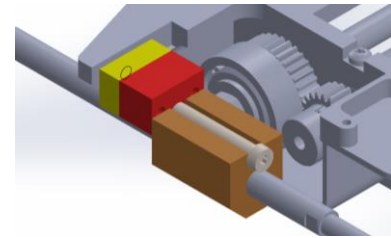
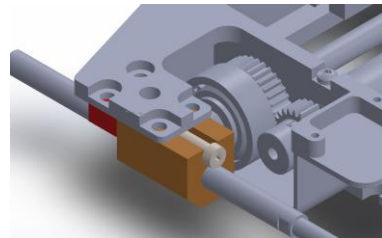
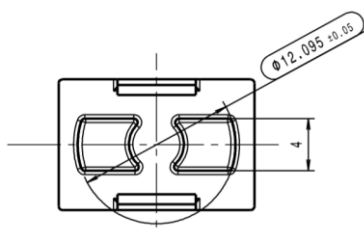


Figure 71 – Leadscrew Nut potential redesigns

Plastic Nut

The Plastic Nut (p-LSN) was proposed to be produced by PIM in a POM+PTFE copolymer and featured a reformed interface to connect with the carriages. The moving axis would be blocked by a slight press between the nut top bosses and a matching slot in the carriage, while all other movements would be free to adjust to the relative position of the components. The clamps designed to the side of this nut are merely intended to help guiding the nut during assembly and serve no functional purpose. The design can be seen in detail in Figure 72.

This design would result in the nut essentially becoming a pluggable component, which is quite positive assembly wise. However, this redesign would require a changing the carriages in which the nut is intended to fit, as these would have to be produced with a matching slot.

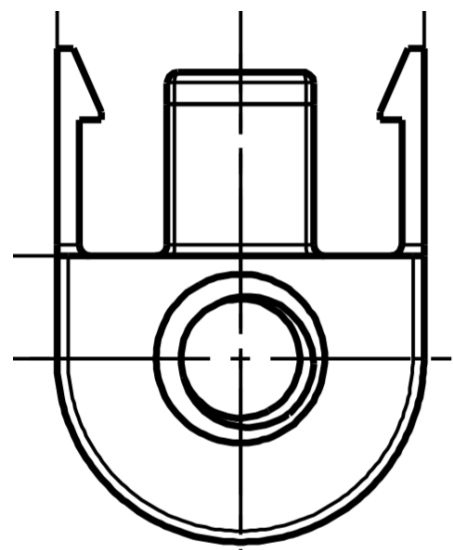


Figure 72 – p-LSN front view

Translating Nut

The intention with the Translating Nut design was to make use of the current brass nut and carriage design, at least for testing prototypes, and only rework the way the nut is attached to the carriage – see Figure 73.

By using an adapter piece, it would be possible to use the previously existing interface. The adapter could be fixed to the carriage and then the nut would be pressed against it by a screw, which would be aligned to the direction of the movement.

The brass nut would only require a small slot to be machined; this slot would guarantee some clearance to the screw, to accommodate for manufacturing tolerances and thus eliminate the over definition.

The disadvantage of this design is that while allowing for bearing block width and carriage length dimensions fluctuations it would not allow any significant accommodation to angular deviations between the spindle and the carriage, as it is partially possible to do with the plastic nut. Also, this nut design is not pluggable, thus being inferior in terms of ease of assembly.

Spherical Joint Nut

The intention with the Spherical Joint Nut is improving the translating nut to allow for angular deviation compensation – see Figure 74.

The use of a two-part adapter, slightly offset from the carriage wall, would allow for the fitting of a sphere that would permit the angulation of the nut with the simple tightening/untightening of the nut's axial screw. Again, the clearance between the nut and the screw would compensate for part width/length dimension fluctuation and eliminate over definition.

Giving the same axial screw the possibility to tighten/loosen the nut and spherical joint simultaneously would allow for quick adjustments during the assembly procedure.

The main drawback to the previous design is the increased number of parts and, therefore, complexity. Additionally, for this design to be tested the carriage would have to be reworked to eliminate the previously existing interface and to allow for the installation of a screw with the spherical joint, given the space restrictions of the current, unmodified, design of the TP.

Conclusion

The spherical joint nut design would not be chosen, due to its complexity, when compared to the Translating Nut given that most likely the latter would be capable of solving most of the problems. Comparing between the Plastic nut and the Translating Nut, the first shows an increased capacity to accommodate to angular deviations and is a pluggable component, thus being the superior choice.

The decision was to substitute the current b-LSN with the p-LSN, along with producing new carriages with the required slot. A test system was assembled for performance evaluation of the new solution, which is required since the material and manufacturing process for the nut have been altered. This performance evaluation will be further detailed in the following section (6.3).

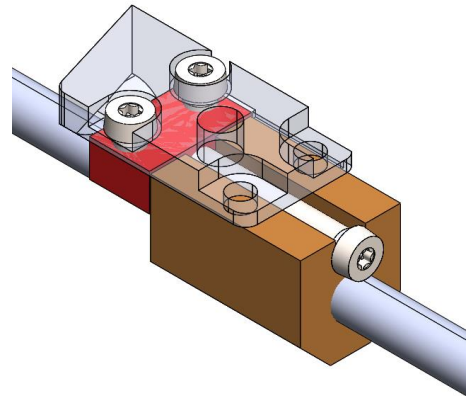


Figure 73 – Translating Nut assembly

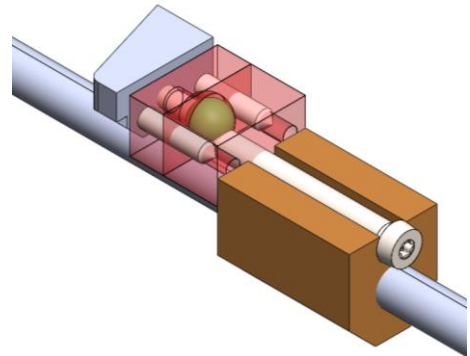


Figure 74 – Spherical Joint Nut assembly

6.3 Linear Encoder and Leadscrew Redesign Testing

The previous sections 6.1 and 6.2 talked about the design changes made to the TP that were aimed at improving the performance of the linear encoder sub-system as well as reducing assembly problems with the leadscrew. In this section, testing activities performed during this project will be explained, for both sub-systems. These testing activities mainly intended to:

- Confirm the linear encoder is providing reliable position readings for the full range of motions of each of the TP's carriages;
- Confirming the linear encoder is not increasing the severity of the "denting effect", and is potentially reducing it;
- Confirming that the Plastic Leadscrew Nut is able to be easily assembled to the system so that motor current problems are diminished;
- Confirming the Plastic Leadscrew Nut is performing adequately when compared to the current grounded Brass Leadscrew Nut.

Past Tests – Denting Effect Root-Cause

As a first step in this activity, past characterization results were analyzed in search for the root cause of the already detected problems with the linear encoder system. As mentioned, it was not known if the "denting effect" was being caused by excessive force of the plunger, given that the system showed almost no deterioration when stored for long periods at room temperature. The effect had been first detected when subjecting the system to 168hrs of temperature and humidity stressing, at 50°C and 95% relative humidity, all part of a leakage current safety requirements testing activity.

Past testing activities were consulted to find evidence of linear encoder lifetime performance and one activity was found to be particularly pertinent. Figure 75 details a partial test setup where the contact force was varied for the foil potentiometer before it was submitted to several hours of temperature and humidity stress.

Although not very concrete information regarding the test procedure was available, test results were present for foil potentiometers subject to parking time at both room conditions as well as at 50°C and 50% relative humidity for two different contact forces – 2N and 3.5N.

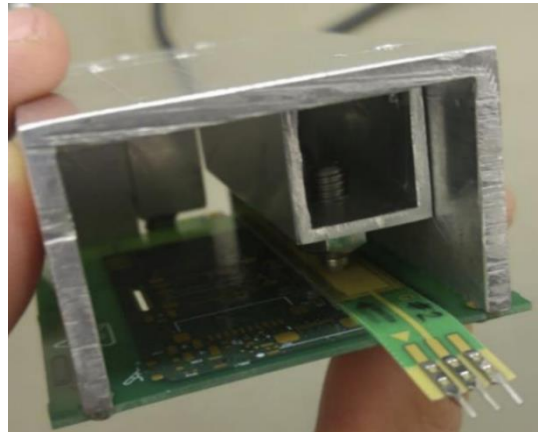


Figure 75 – Testing system construction

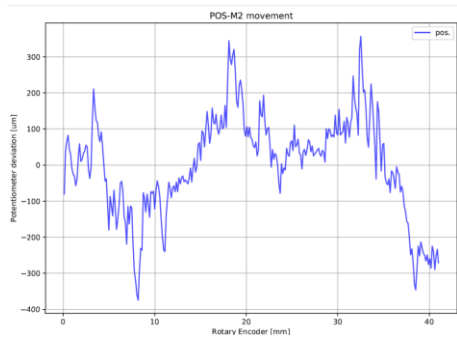
Before any stress test was carried the foil potentiometers were characterized and maximum deviation peaks were around 0.15-0.20mm (considering both components). The characterization results after stress can be consulted in Figure 76, and show substantially higher deviations up to 0.50mm, with no significant difference between the 2N load and the 3.5N load. The characterizations also show that most of the deviations occurred in the first 117hrs of temperature stress.

Unfortunately, the test was not repeated for higher forces acting on the foil potentiometer, nor for relative humidity of 95%, meaning it was not possible to gather data on the performance deterioration evolution for worst-case conditions. Nonetheless, if these results are compared to testing of the system at 50°C and 95% relative humidity of system that should have, for the most part, higher contact forces given the faulty wiper design, these deviation values are significantly lower – in Figure 77 deviations go up to, and slightly beyond, 1mm.

Not knowing if force or humidity, or both, are the main factors potentiating the deviations, it is understood that temperature alone is not the main cause for the problem.

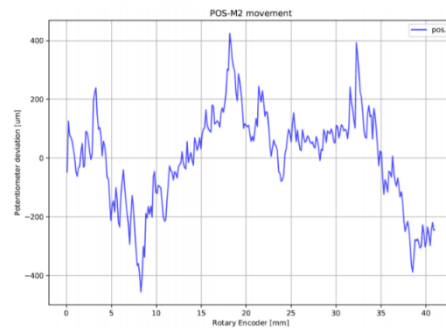
Press Force: 2N

117hrs – 50°C/50% rel. humidity



Max. Absolute Deviation: 0.37mm

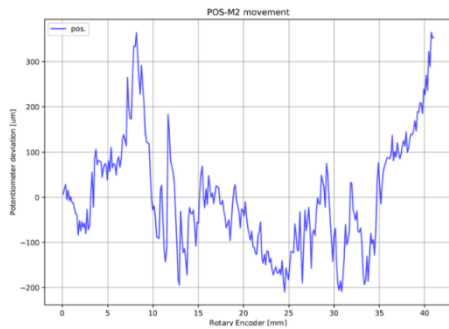
117hrs – 50°C/50% rel. humidity
304hrs – 22°C



Max. Absolute Deviation: 0.45mm

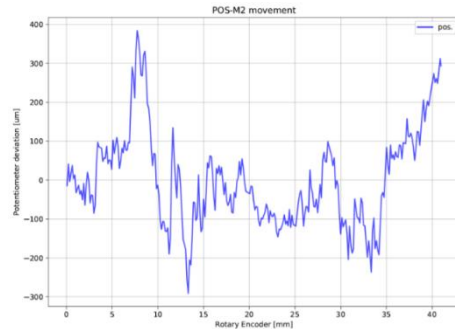
Press Force: 3.5 N

117hrs – 50°C/50% rel. humidity



Max. Absolute Deviation: 0.37mm

200hrs – 50°C/50% rel. humidity
304hrs – 22°C



Max. Absolute Deviation: 0.38mm

Figure 76 – Test results for controlled foil potentiometer forces

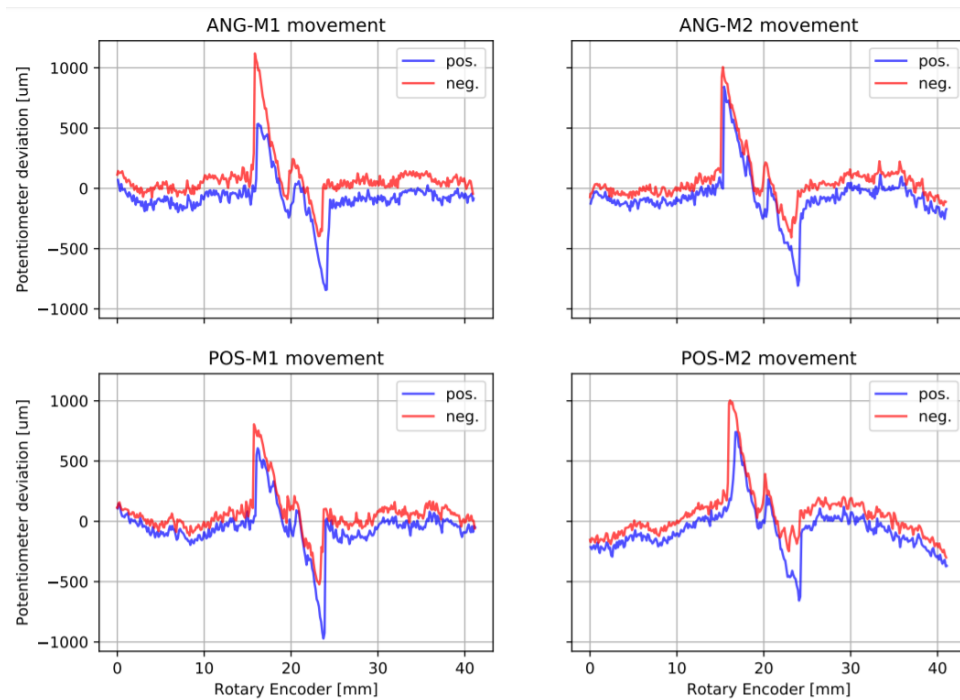


Figure 77 – Test results for 168hrs at 50°C/95% relative humidity

March Tests

The first system test possibility occurred early March and was aimed at further testing the linear encoder system as well as the (new) plastic leadscrew nut (p-LSN). The system used for this test was assembled with newly ordered components and installed with the most recent carriage and p-LSN design, although not with the new wiper (still being developed at the time).

Linear Encoder

To further evaluate temperature and humidity effects on the linear encoder the new system was subjected, following the worst-case use/shipping/storage conditions, to 168hrs of stationary HOME position at 40°C and 80% relative humidity as a first test step.

The results can be seen in Figure 78 and show somewhat lower potentiometer deviations. If the POS module results are compared to the overall previous testing results, in Figure 77, the difference is not so substantial, and most likely that is due to more relaxed testing conditions. However, considering the ANG module potentiometer deviations, these are considerably lower than previous testing, as well as lower than POS module's deviations, not surpassing 0.50mm.

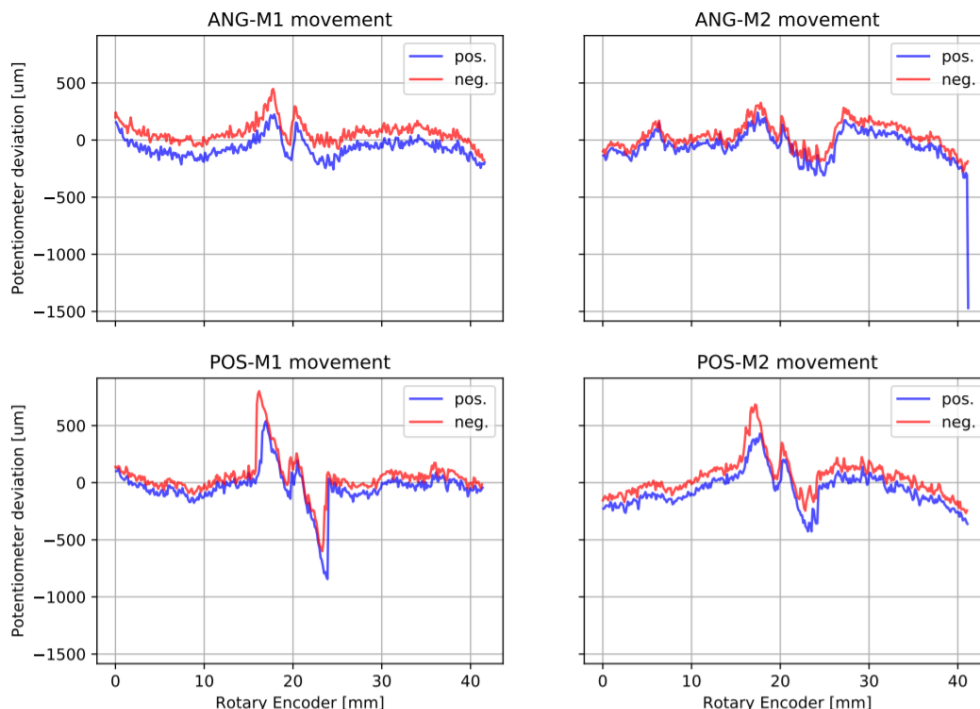


Figure 78 – p-LSN system subject to stationary HOME position for 168hrs at 40°C/80% rel. humidity

The considerable difference between deviations for both modules seems to indicate that the main influencing factor for this problem is in fact the contact force between the wiper and foil, as both modules were subject to the same temperature and humidity stress conditions.

Additionally, it can be seen from the test results that axis M2 from the ANG module showed a failure while trying to read the foil potentiometer's position at the end of the movement. As explained in section 6.1 this is often the case when the wiper cannot exert sufficient pressure on the foil – meaning that the ANG module carriage wiper is most likely being pressed against the foil with a smaller force – this module also showed the least amount of deviation.

All this data is interesting evidence supporting the decision of changing the wiper design, as it seems to flag contact force as the main cause for problems. In addition, the reading failure is further evidence that the design is not capable of accommodating to the tolerance stack. It was understood that further testing should be carried with the new wiper, as it would not be possible to further estimate its performance or main influencing factors; it was necessary to verify if the new design could perform adequately.

Plastic Leadscrew Nut

In addition to the linear encoder specific test, the p-LSN was also targeted for specific tests, as the component would have to be evaluated for the different use conditions of the TP. These conditions were already mentioned in chapter 2 – section 2.3 and include:

- Use Conditions – 10-30°C | 30-70% relative humidity
- Shipping/Storage Conditions – 0-40°C | 20-80% relative humidity

For this reason, after being subject to 168hrs at 40°C and 80% relative humidity, which itself already conditions the p-LSN, characterizations on the system were planned to be executed to evaluate the performance of the p-LSN at different temperatures. The considered parameters to evaluate its performance were the electrical motor currents and the maximum deviation between rotary and linear encoder (measure of the drive chain backlash).

Informal sub-system requirements, obtained based on current design performance, and already questioned in chapter 4.2, were considered as the basis for this evaluation (it should be kept in mind the mechanical performance analysis was not complete by this time). While conscious that these are not hard limits, the performance targets were the following:

- Drive chain backlash within $\pm 30\mu\text{m}$;
- Motor current inferior to 40mA.

With this in mind, a first system characterization was performed at 0°C. This low temperature characterization revealed full jamming of the system, with no axis being able to move at all – characterization data was not obtained, and the system would not be able to operate during real use scenarios. As 0°C is not a use condition for the TP, the characterization was further attempted at 10°C – the results can be found in Figure 79 and revealed heavy performance loss.

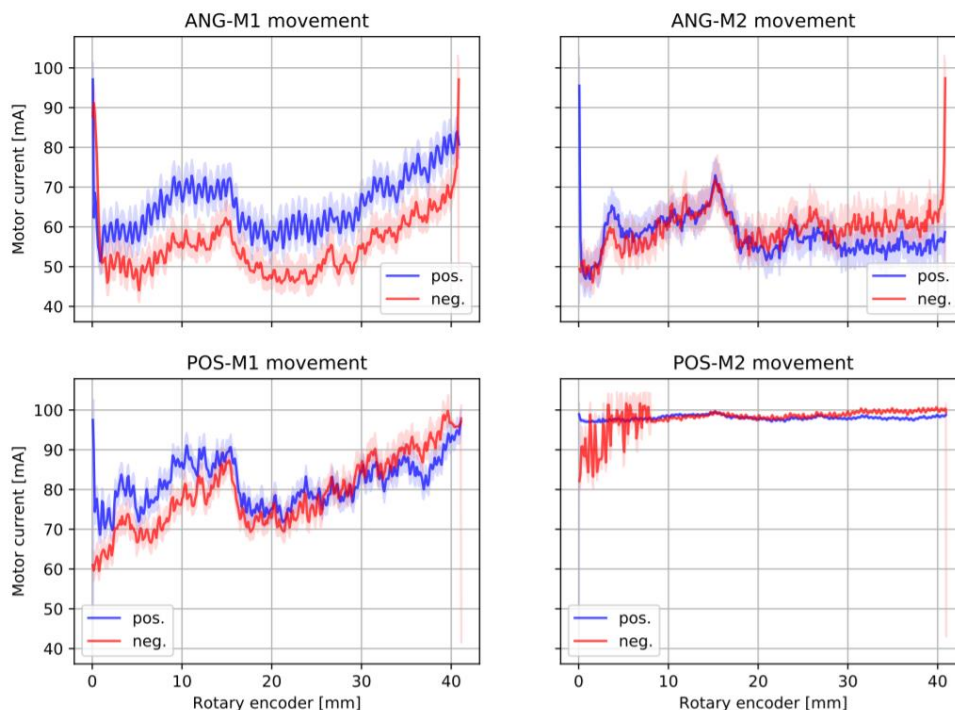


Figure 79 – p-LSN characterization at 10°C

This performance is not at all acceptable for the TP, but it might be understood given that the system used for this test was not assembled by the typical production team, as it was used for a few other independent tests that occurred parallel to this p-LSN tests. It is possible that some assembly mistakes were contributing for these low performance results, as the system is very sensible to the assembly procedure – this is further explored in chapter 7.

Additionally, it is important to understand that the system’s life performance is also conditioned by the initial burn-in cycles, performed after assembly. The standard value for the number of burn-in axial cycles, at the time of this test, was 30. In parallel to this test, and with another system, a cycling-reliability test was being performed, and it showed that systems subject to 700 cycles were actually performing better, in terms of low and stable motor currents, when compared to systems with 30 burn-in cycles – see Figure 80.

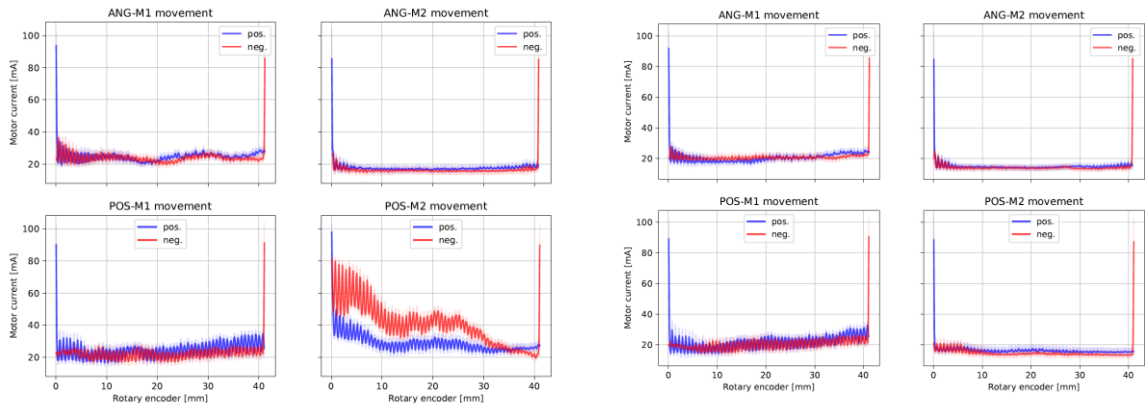


Figure 80 – Example of burn-in impact in motor current; pre-conditioning (left) and post-conditioning (right)

While not necessarily the main impacting factor to the high motor currents, it is possible that the lack of proper cycling is impacting test results – the main factor should be either assembly problems or the nut itself. At this point it was not yet possible to determine if the p-LSN can perform at 10°C or if an alternative design should be pursued.

Not only are motor currents important but also the nut’s influence on the drive chain backlash. The characterization output can be consulted in Figure 81.

Rotary encoder deviation vs linear encoder; S/N 010, 2020-02-13 08:55:54

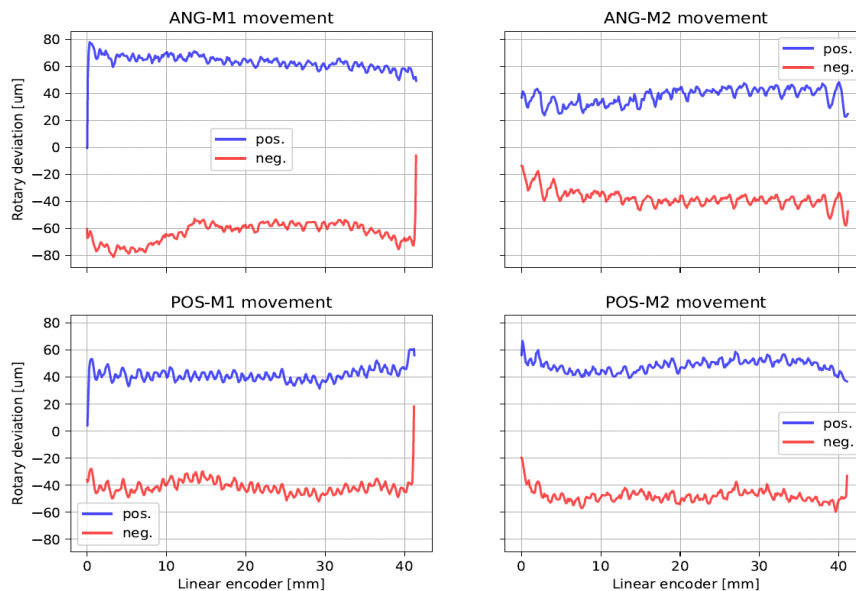


Figure 81 – Drive chain backlash when installed with the p-LSN

These results show a drive chain backlash in the range of ± 40 - $80\mu\text{m}$, which is substantially outside of the informally set requirements. These results were quite unexpected and led to a series of further tests to identify the root-cause of the phenomenon.

The first test tried to evaluate the backlash between the p-LSN and spindle, which was identified as the first potential cause for overall drive chain backlash. The test setup shown in Figure 82 was used to evaluate the maximum displacement of the nut when installed in the spindle and revealed values in the order of $5\mu\text{m}$, which are not high enough to explain the ± 40 - $80\mu\text{m}$ of backlash given that for the b-LSN systems the drive chain backlash is around $\pm 30\mu\text{m}$.

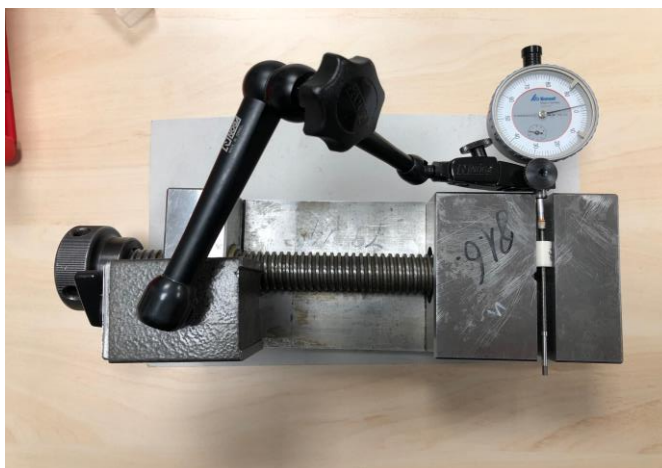


Figure 82 – Test setup to evaluate the LSN backlash

The only other possible explanation would have to be the interface between the p-LSN and the carriages. Inspecting the round, press-fitted, interface it was possible to observe a rectangular-shaped planar surface in locations where contact with the carriages was occurring. This plastic deformation in the nut-carriage interface was thus identified as the root-cause for the increased drive chain backlash and the design was rejected.

Because both problems related with the p-LSN (motor currents and nut-carriage interface backlash) could probably be solved without major reworks, a new p-LSN design was proposed. This reworked design can be seen in Figure 83, making use of a rectangular-shaped planar surface at the contact points with the carriages; the intention would be that of eliminating the stress concentration at the contact points without changing the mounting procedure and making use of the previously existent injection mold.

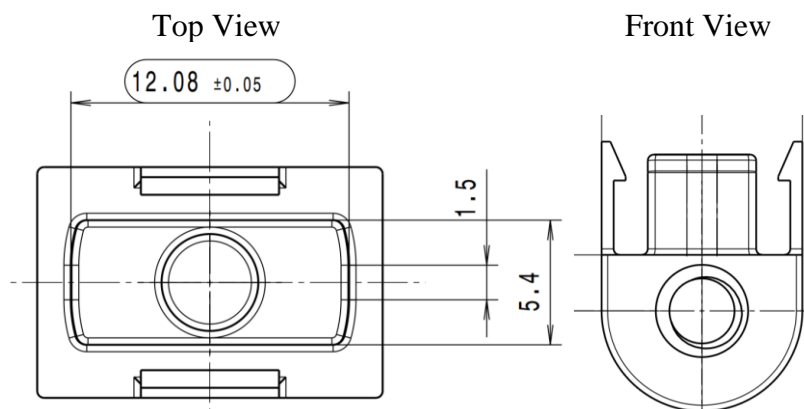


Figure 83 – Reworked p-LSN design

This new design was approved and would be tested again in the next round of tests, together with the new wiper design, to were planned to be carried in April 2020.

April Tests

Having prototype pieces for the new wiper design as well as reworked p-LSNs it was possible to plan for a structured test to both these components using the same test system tested during the previous March tests. This system was planned to be refurbished by the production team to ensure the assembly procedure could be discarded as the cause for poor component performance, however, for reasons external to both the company as well as the testing team, this was not possible; the assembly would end up being done by the testing team.

During this assembly procedure the test team reported several difficulties at getting the motor currents stable and under the informally required 40mA – the cause for these problems will be discussed further in chapter 7. The lack of assembly experience might have influenced this test's results yet again, but either way some interesting conclusions could still be obtained.

The test method was the following:

1. Perform initial characterization;
2. Perform 100 cycles for each axis with a resisting force up to 40N (± 10 N);
3. Characterization;
4. Perform 900 cycles for each axis with resisting force up to 40N (± 10 N);
5. Characterization;
6. Install the system in a thermal chamber;
7. Leave the system for 3 hours at 0°C;
8. Increase the temperature to 10°C and leave for another 3 hours;
9. Characterization at 10°C;
10. Increase the temperature to 30°C and leave for another 3 hours;
11. Characterization at 30°C;
12. Increase the temperature to 40°C, set 80% rel. humidity and leave for 168 hours;
13. Characterization at 40°C.

The test results will be presented and analyzed in the next sub-sections. It should be noted that due to a lapse step 10 was not performed, with system characterization only occurring for step 13. While not invalidating the results, it is unfortunate that data regarding p-LSN performance at 30°C was not possible to collect.

Potentiometer relevant results

Test results for deviation of the potentiometer signal are summarized in Table 7 for the previous March tests, at “Prev. Test – Final Readings” (see also Figure 78), and for April Tests, at “1. Initial Readings” and “13. Final Readings”.

Table 7 – Summarized potentiometer results for April tests

Max. Deviation (mm)	(Old Design)		(New Design)	
	POS M1	POS M2	ANG M1	ANG M2
Prev. Test – Final Readings	0.80	0.70	0.45	0.30
1. Initial Readings	0.40	0.30	0.28	0.38
13. Final Readings	1.00	0.70	0.52	0.61

To understand these results it is necessary to understand that the foil potentiometers were left unchanged from the previous test, and that the new wiper design was only installed at the ANG module, with the POS module using the old design wiper.

The initial characterization results showed that the system was able to recover in between tests, most likely as it was completely disassembled for some days for analysis and installation of the new design – this is evidence that not all deviation is resultant from permanent damage to the foil, meaning that, potentially, storage of the system at different positions could be beneficial to integrity (although this is not necessarily achievable) and comes to reinforce the idea that contact force is the main cause for the detected problems.

Regarding the foil potentiometer’s results, the deviation identified at testing step 13, with the new design, for ANG M1 and M2, was higher than that recorded with the older design, which is especially alarming considering that ANG M2 deviation was doubled. While the overall deterioration was not as pronounced as the one in POS module, comparing it to previous tests shows substantial difference. As the only changed parameter between the tests, contact force seems to be the responsible factor for this finding.

It is possible that the new wiper design, while being able to achieve all the expected improvements, was installed at a certain distance to the foil that would result in a contact force higher than the previous mechanism was achieving – it should be remember that the nominal distance for the new wiper would result in 3.2-4.8N (explained in section 6.1). The deviation results found during testing can thus be representative of new maximum deviation values for the system – this is partially corroborated given that distance measurements between the wiper and the foil potentiometer revealed their relative position was about 0.1mm shorter than nominal – meaning that contact force should be, theoretically, around 4.5N.

Concluding, the new design, besides obvious cost reduction and improvements to the ease of assembly, is most likely also performing better than the old design given that worst-case test results revealed maximum deviation in the order of 0.50-0.60mm, compared to previous 1.00mm (informally, it was reported that other systems with the old design had been tested with higher deviations, in the order 1.20-1.50mm).

Despite this, and because the sample size was small, it would be necessary to repeat this test with another system to confirm the results – this would not be possible in the scope of this work, but is already a planned activity for the company. Additionally, given that the datasheet, as well as experimental results, indicate that reliable results can be obtained for contact forces higher than 0.8mm it is perhaps interesting to define a new nominal position for the wiper so that contact forces may range from 0.8-2.4N or even 1.2-2.8N (to have some safety margin).

p-LSN relevant results

For the nut testing the most important results are, again, the motor currents and the drive chain backlash. The results are detailed in Table 8, which includes also the maximum values obtained in the previous March tests.

Table 8 – Summarized reworked p-LSN backlash results for April tests

Test Step	Max. Absolute Drive Chain Backlash (µm)			
	POS M1	POS M2	ANG M1	ANG M2
1.	24	35	35	41
3.	23	37	32	42
5.	21	42	31	42
9.	24	45	35	44
13.	24	42	40	47
Prev. March Tests	≈60	≈60	≈80	≈60

The results show that the reworked p-LSN has successfully improved the interface with the carriages, no longer showing unacceptable backlash values. The nuts are expected to achieve backlash values in the order of ±40µm (it should be considered that the values in the table are often times those measured at isolated peaks – the 47µm deviation, for example, represents a very contained peak near the end of the carriage stroke) and have shown no deterioration even when subjected to harsh cycling conditions (1000 cycles with a 40N resisting force) or when cycling at lower and/or higher temperatures (10°C and 40°C).

The 40µm backlash is not within the informally specified values, however this limit was not considered as a hard limit and the assembly benefits should outweigh this p-LSN disadvantage.

While the results for the backlash values are acceptable, the motor current characterizations are not so satisfactory. A comparison between the motor currents at room temperature, at test step 5, and at 10°C, test step 9, can be found in Figure 84. These motor currents are significantly better than those found during previous tests, like those shown in Figure 79, but still mostly outside of the informally set requirements.

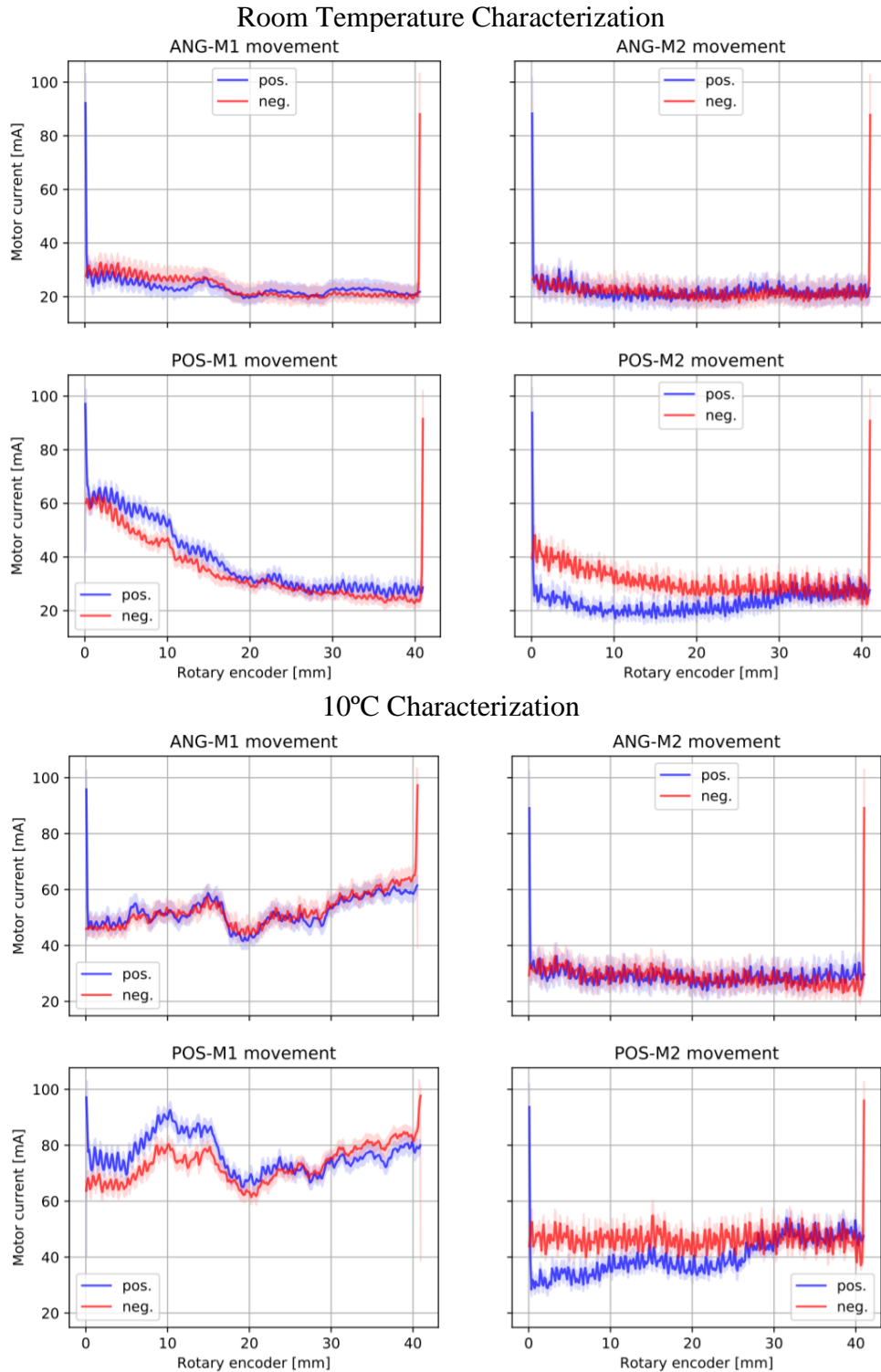


Figure 84 – Reworked p-LSN motor currents at room temperature (top) and 10°C (bottom)

While the 40mA are not a hard limit, the TP should not show much higher currents during no load operation because the motors shutdown at 100mA as a measure to detect system collisions. The high motor currents, verified at 10°C for no load conditions, will possibly lead to the system falsely identifying a collision, thus being unable to operate, when simply installed with a medical instrument (due to the extra effort on the motors caused by the held weight).

Looking with some more depth at the motor currents recorded at 10°C, it is possible to find a substantial difference between the performance of the several axes. While the M1 axes show a very negative performance, the M2 axes are much more stable, with the ANG M2 axis even showing values well within the 40mA specification.

As mentioned previously, the system was, unfortunately, not possible to be assembled by a trained team; this means the performance deterioration results shown in Figure 84 are most likely a measure of the performance of the testers as assemblers rather than a measure of the actual performance of the p-LSN.

If any conclusion can be taken from these results it is that the TP is overly sensible to the assembly procedure. Additionally, because the ANG-M2 axis was able to show good performance the p-LSN is most likely capable of performing adequately at 10°C, even if showing slightly increased friction when compared to the current B-LSN design – this can be inferred by comparing the results of Figure 84 with those shown in Figure 85 for another testing TP system installed with the B-LSN and characterized at 6°C.

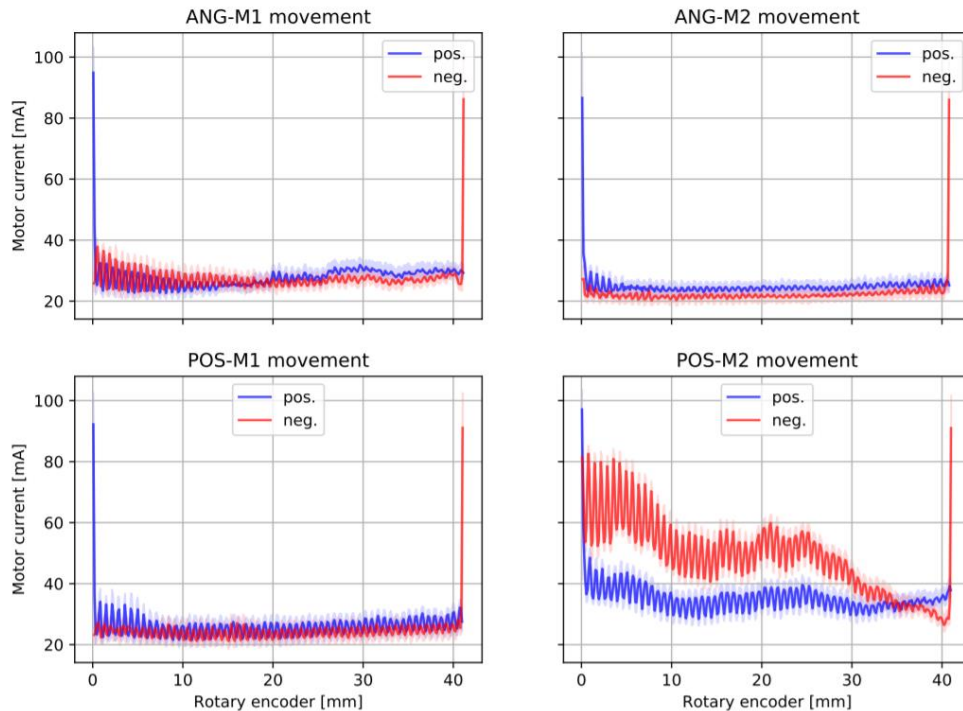


Figure 85 – Characterization at 6°C with current B-LSN

Subject to a lower temperature than the p-LSN, the B-LSN is showing stable motor currents in the order of 20-30mA (POS-M2 axis is, again, reflecting assembly problems and the 80mA were already shown in a previous room temperature characterization – it should, therefore, not be considered), which is slightly better than the 30-40mA with its plastic counterpart.

Despite this slight loss in performance, considering friction and backlash, the p-LSN is able to provide a much simpler assembly procedure than the B-LSN and eliminates the over definition of the TP, which it set out to do. Nonetheless, changing between these designs might not be the best decision at the moment given the increased sensibility of the system’s performance to the assembly procedure when mounted with the p-LSN. Additionally, it is possible to observe that even for an axis showing satisfactory performance at room temperature, like the ANG M1, it is not guaranteed that performance will remain equally satisfactory when subject to lower temperatures – this could mean that assembly errors are not detected during production testing. Unlike what was predicted, the elimination of the over definition did not solve the over sensitivity of the system to the assembly procedure, and until that dependence is solved, or at least minimized, the p-LSN is not a safe choice; one of the reworked B-LSN designs might prove a better short-term alternative.

7 Linear Guides and System Assembly

As mentioned in the previous chapter, the system's performance is heavily conditioned by the assembly of the system, which itself is not a trivial or straightforward process. The assembly procedure requires substantial amounts of manual adjustments until a stable system, with acceptable levels of friction (measured by the motor currents), is achieved and that condition has not been improved by the elimination of the over definition occurring between the Bearing Block, the carriages and the linear guides position. In this chapter the linear guides and their impact on the overall system performance and assembly procedure will be analyzed.

7.1 Linear Guides Position and Assembly

As previously mentioned in chapter 3.1, the linear guides (LGs) are part of the scope of this project and they have had their interactions with other mechanical components, assembly procedure and impact on system performance analyzed as part of the project activities. A first introduction to the overall assembly of these components will be detailed next:

Baseplate-A1 – Two miniature linear guides are installed with the rails screwed on the baseplate and the moving blocks screwed on carriage A1 - Figure 86. These linear guides are first installed in carriage A1 using the reference edges signaled within red circles in Figure 88, and secondly installed in the baseplate making use of a reference edge (signaled with an orange circle) that contacts the back linear guide rail. The back linear guide is the first to be fix and the frontal linear guide follows suit.

A1-A2 – Two identical, miniature, linear guides are also installed but this time with their upwards side facing each other, between carriage A1 and carriage A2 (shown in Figure 87). Similarly to the Baseplate-A1 interface, the linear guides are also installed using reference edges, this time with the first installation occurring at Carriage A2; the alignment here is guaranteed by the edges circled in orange at Figure 89. After the LGs are fixed to A2 this carriage is installed directly on top of carriage A1 with the linear guide rails supported by the red circled edges; the rails are then fixed to A1.

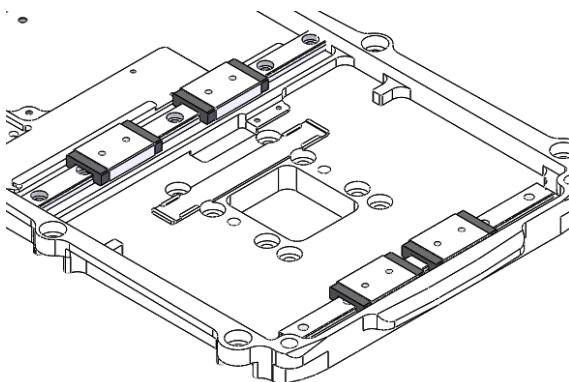


Figure 86 – Baseplate-A1 linear guide assembly

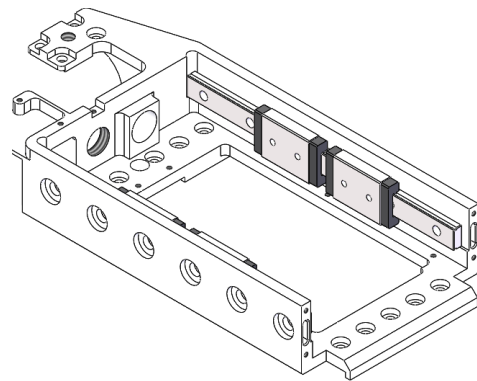


Figure 87 – A1-A2 linear guide assembly

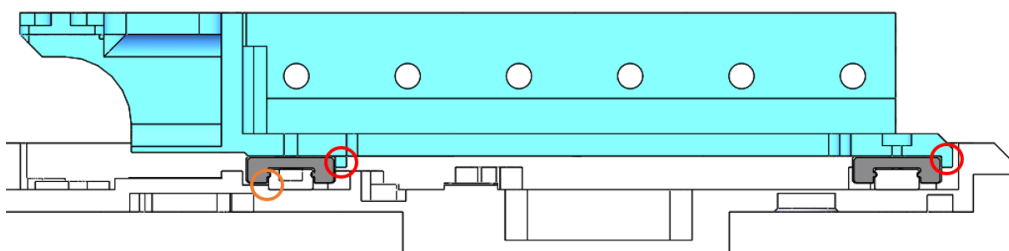


Figure 88 – Baseplate-A1 linear guide assembly – side section view

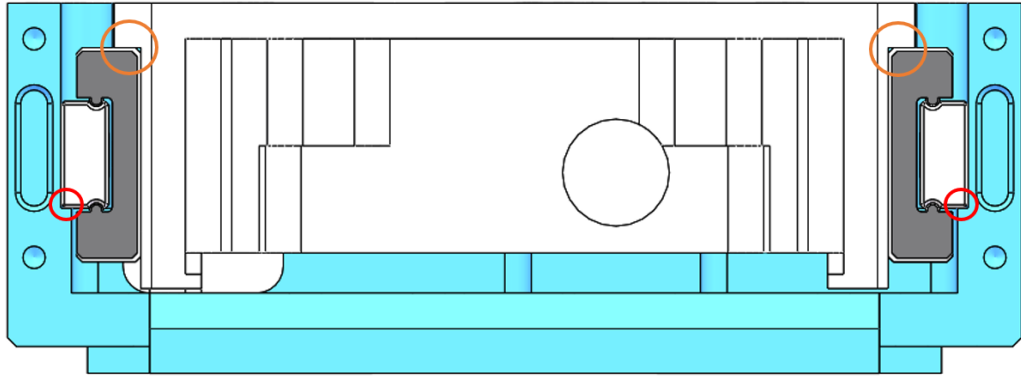


Figure 89 – A1-A2 linear guide assembly front view

In the midst of both procedures the carriages need to be connected to the leadscrew nuts, which, in turn, need to be adjusted for their height, pitch, and yaw. It is almost certain for the freshly assembled setup to jam, with tweaks necessary to be performed to both the linear guides and the LSNs; one of the big problems is thus identifying which component is misaligned and how exactly is it misaligned.

Because of the assembly sequence, and partially due to the miniature nature of the equipment, it is quite difficult to have any indicator on the presence of misalignments before system cycling begins – no relative position control other than reference edges is in place. Therefore, system cycling is usually initiated with the carriages mounted separately (without the linear guides being attached), allowing for the adjustment of the leadscrew nut position (until current is low and stable) before adjusting the linear guides (again, checking for low and stable currents). Despite this, it is often found that while adjusting the linear guides, small position tweaks to the nut are required to be able to fulfill the 40mA specification – this leads to an empiric, long, and iterative procedure.

The system is expected to be produced in small quantities, with orders expected to be of around 60-100 systems/year. For this reason, the assembly time, estimated at 1.0-1.5 days/system, is acceptable. Nonetheless, an improvement of the assembly time is important to reduce assembly costs, freed human resources and to allow for a future increase in the number of assembled systems per year.

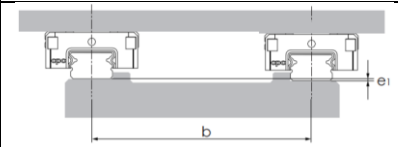
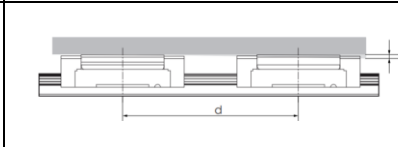
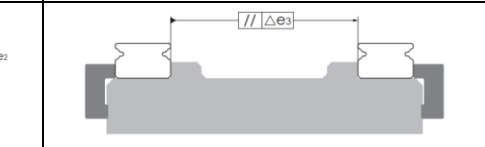
As mentioned in chapter 4.1, an estimated two thirds of the assembly time, or $\approx 0.7-1.0$ days/system, are spent getting the correct internal alignments. The redesign of the LSN, as already explained, was meant to improve this situation by removing the over definition and allowing for self-adjustment, unfortunately, and despite easing assembly, it revealed unable to solve all of the mounting problems, possibly masking some of those problems at room temperatures. It thus became even more important to understand the why the linear guides are so troublesome during TP mounting.

7.2 Tolerance Analysis

A first step towards understanding and solving the linear guides issues was that of checking their installation requirements and comparing that to the used process. The miniature linear guides' datasheet can be found in Figure 100 at Appendix A, for which the important reference is 3WL VS (3mm height rail linear guides, 4.5mm total, with a clearance of 0-1 μ m).

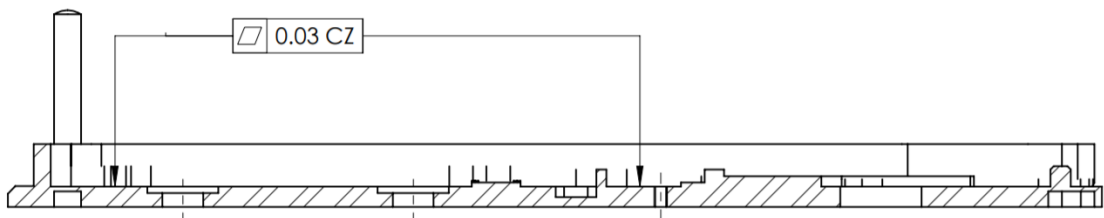
In Table 9 the mounting surface requirements for the linear guides can be consulted – the values are according to the datasheet formulas (15, 16 and 17) and consider the geometry of the TP based on 3D CAD measurements.

Table 9 – Linear Guide mounting surface maximum manufacturing errors

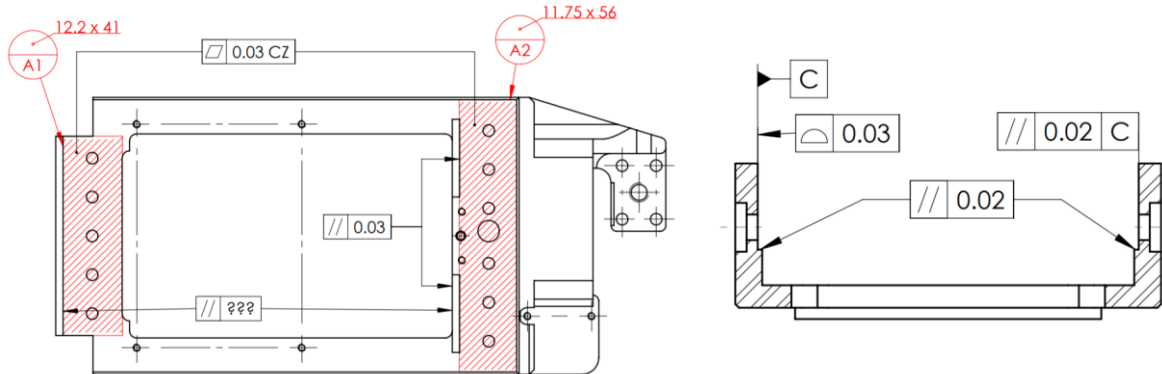
Requirements	Floor Height Difference (e_1)	Floor Flatness (e_2)	Parallelism (e_3)
(μm)	≤ 16	≤ 7	≤ 2
Illustrations (datasheet):			
Floor Height Difference	Floor Flatness	Parallelism	
			

These necessary mounting surface tolerance values were then searched for in the equipment’s technical drawings. A compilation of that activity can be seen in Figure 90 (the drawings + tolerances shown are just as an illustration, they do not correspond the actual component technical drawings).

Baseplate Relevant Tolerances



Carriage A1 Relevant Tolerances



Carriage A2 Relevant Tolerances

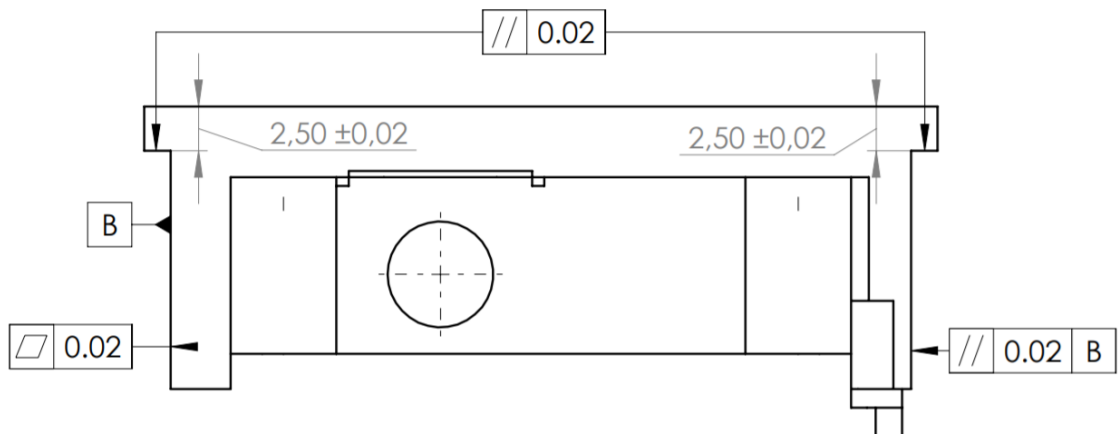


Figure 90 – TP technical drawings LG mounting surfaces relevant tolerances

Taking into account the assembling procedure and the component relative position it is possible to have a comparison between required and actual tolerances – see Table 10.

Table 10 – Comparison between required and actual LG mounting surfaces

	Floor Height Difference (e₁)	Floor Flatness (e₂)	Parallelism (e₃)
Required (μm)	≤16	≤7	≤2
Baseplate-A1 (μm)	30	30	Not specified
A1-A2 (μm)	N/A	20	20

The specified tolerance for the TP components is not within the requirements, and this may potentially be the cause for many of the witnessed assembly troubles. Additionally, it is also possible that the hand pressing of the linear guides against the reference edges is not able to support the wanted repeatability/reproducibility for the process. Despite knowing about these tolerance issues, it was not entirely known if the tolerance values could be tightened or, if not, how significant their impact was in the performance of the system – this is analyzed next.

Lifetime of the LG – Given the small stroke range of the TP, its small speed, and expected number of use cases throughout the lifetime, it is not likely that the linear guides will ever face any sort of deterioration – the tolerances are specified taking into account a minimum lifetime of at least 50 Km of travel distance, which is far exceeding the expected 700m of lifetime travel distance in worst-case scenarios; also, maximum dynamic/static loads are, in worst-case, around 20x inferior to the maximum loads for the configuration. It is important to note that these linear guides have been used extensively during tests and have never shown any problem.

Accuracy – Another typical problem for systems not following the required mounting tolerances, as stated by the manufacturer, is lack of position precision. This could potentially be a topic for improvement, given that high precision positioning is required for the TP; however, the system has no dynamic performance requirements, the medical instrument position relative to the patient is tracked in real time via imaging software and testing has shown that independent of the position tracking mode, the TP fulfills accuracy requirements. It is possible that a reduction of friction, resulting from a more ideal alignment of the linear guides, could lead to higher precision, but then the cost of tolerance tightening needs to be evaluated as a tradeoff.

Motor Currents – Motor currents are certainly the aspect most impacted by the loosened tolerances, given that any misalignment of the linear guides can result in the system jamming or in substantially increased friction. Two different tolerance requirements can be explored:

- Surface Flatness
- Parallelism

Parallelism

The reference edges are aimed at improving the ease of assembly, providing the assemblers with physical touch point where the linear guides can be pressed against – these features should be responsible for guaranteeing proper parallelism between the linear guides and should have a maximum specified parallelism deviation of 2μm.

For the Baseplate-A1 interface, it was found that carriage A1 had no specified parallelism tolerance between the front and back LG edges. For the back LG edge, divided into two small edges which are not possible to machine together given the “pin” feature used for PCB alignment, there is a 30μm specified parallelism tolerance.

Additionally, it is possible to verify that a similar (yet slightly better situation) is present for the A1-A2 interface; carriage A2 has the reference edges specified for a 20μm parallelism deviation. While the reference edges used for this interface in carriage A1 could be used in substitution, these also have a 20μm parallelism specification.

In addition to the unsatisfactory parallelism tolerances, the process states that the alignment of the linear guides should take place by aligning the moving blocks and not the rails. While the blocks do have the necessary precision for this, as the installation is done with the moving blocks around 40mm away from each other, this means that the dealignment at the rail extremities is higher than the actual parallelism deviation between the reference edges, given that the total linear guide length is about 90mm.

The rail installation process is also not ideal because pressing of the rail against the reference edge is not possible while tightening the screws. The tightening torque on the screws, and any potential unintentional user force, will also contribute to further dealignment.

While no information exists from the manufacturer regarding the impact of dealignment on friction, it was possible to find information for linear guides of other suppliers. In Figure 91 it is possible to find the typical impact of dealignment in system friction and rigidity.

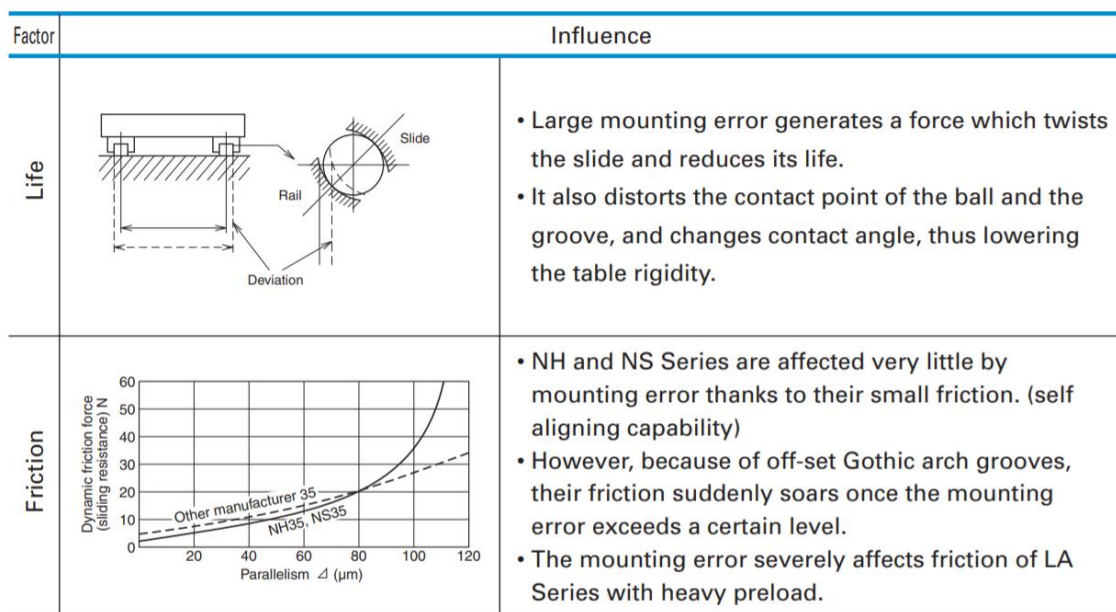


Figure 91 – Impact of mounting deviations on linear guide performance [NSK, 2020]

Flatness

Not only parallelism can cause increased friction problems to the system, but also the lack of proper surface flatness – Figure 92 illustrates the possibly induced deformation. While the requirements here are more relaxed, they are also not achieved (even if by a smaller margin).

As mentioned in section 6.3, a TP was assembled by testing teams, and not production teams, for some of the tests conducted during this project. These unaccustomed assemblers reported a several difficulties and one particular finding was surely due to surface flatness: it was found that while cycling the M1 axis (Baseplate-A1 interface) with the linear guides only lightly pressed against the baseplate (meaning that parallelism deviation was not overly influencing system friction), the motor currents would spike when tightening the screws that would secure the carriage to the moving block. This effect is a possible confirmation of the impact of flatness problems on system friction – when tightening carriage A1 to the moving blocks the latter ones are possibly slightly bending to accommodate height differences and having the roller elements pressed against the rail, increasing friction for the system – this is a possible explanation of the phenomenon.

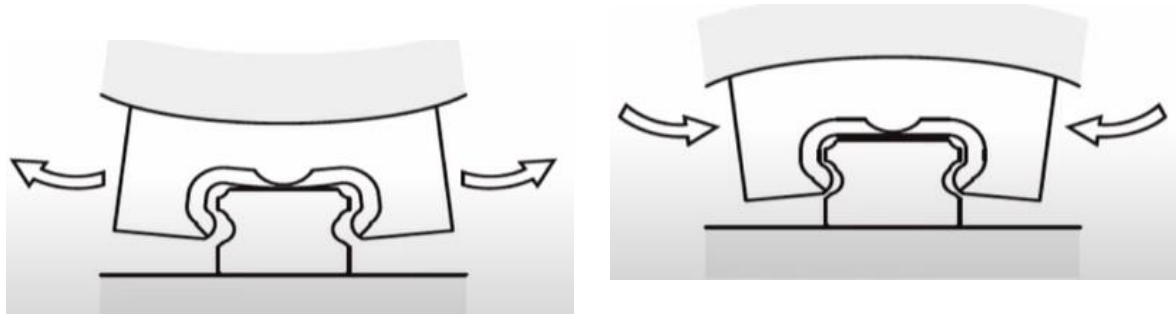


Figure 92 – Illustration on the influence of flatness on the linear guides [MiSUMi, 2014]

While these problems are definitely worrisome, they are not impeding the system from ultimately being assembled and performing adequately. Because of this, it is not imperative that system tolerances are tightened, especially as that could reveal a substantial increase in system cost; the decision was made to assess together with the manufacturers of the linear guides, baseplate and carriages how far the tolerances could/should be tightened and how it would be possible to come up with a cost-effective solution to ensure proper internal alignments while reducing the need for constant assembly tweaking.

7.3 Improvement Solution

Linear Guides Manufacturer

A first step towards better understanding how an improvement could be attained was that of contacting the linear guides manufacturer. The intention here was that of better understanding the tolerance requirements for the mounting surfaces, its impact on rigidity, lifetime, and friction. While a meeting did take place, to advance with a cooperation, and to guarantee the free flow of information, it was necessary that certain business agreements took place. Because this was a long process, it was not possible to achieve any relevant conclusion during the timeline of this project; however, the conditions were set for future cooperation.

Baseplate and Carriages Manufacturer

In parallel, the manufacturer responsible for the baseplate and carriages was contacted with the intention of discussing current vs required mounting surfaces tolerances. It was possible to understand that current tolerance range was the best that could confidently be achievable without incurring into manufacturing R&D, given the susceptibility of the parts to bending – tightening tolerances which would lead to substantial cost increase for the parts. The decision was made not to proceed with tolerance tightening.

Possible Improvement Ideas

Precise Frames – While it would be difficult to machine the baseplate and the carriages with the required tolerances, given their geometry, it would perhaps be possible to cost-effectively machine a frame (simpler geometry). The frame parts could be designed to simultaneously guarantee the necessary tolerances to properly align the LGs and to include a quick attachment feature to both baseplate and carriages. This would result in a cost increase for the system and would require the redesign of the baseplate and carriages but would be more cost-effective than tightening tolerances for the already existing parts.

Switching Linear Guides – Other existing idea was that of changing the type of linear guide being used, to either another roller linear guide or even to a sliding linear guide. This idea was dropped as there are almost no alternative standard linear guides with the same installation height of 4.5mm, and because catalogue consulting showed that manufacturers tend to specify equivalent mounting tolerances; also, sliding linear guides would not be possible to use without performance loss, as their friction is usually higher and their rigidity is not on par with rolling guides for most load solicitations (one direction is typically quite rigid, while the others aren't).

Reducing number of blocks and/or rails – Another way to solve the dealignment problems could be, intuitively, by removing the parts that end up causing dealignment. This idea was almost immediately dropped however, as reducing the number of rails would result in excessive bending momentums for the LGs and reducing the number of moving blocks was detrimental to the rigidity of the overall setup. There was no intention of reducing performance.

Removing the reference edges – It would be possible to remove the current reference edges and simply align the system manually with the use of a comparator to check for proper alignment – this is actually one of the recommended assembly procedures by the manufacturer and is illustrated with more detail in Figure 93. While not improving flatness related problems, it could prove useful to alleviate parallelism problems. Sadly, assembling a system manually without the use of reference edges is difficult, especially when considering the carriage A1-A2 interface where it would be quite difficult to fine adjust the linear guides tilt and especially difficult to control the parallelism between the two sideways linear guides using a comparator. The idea was dropped.

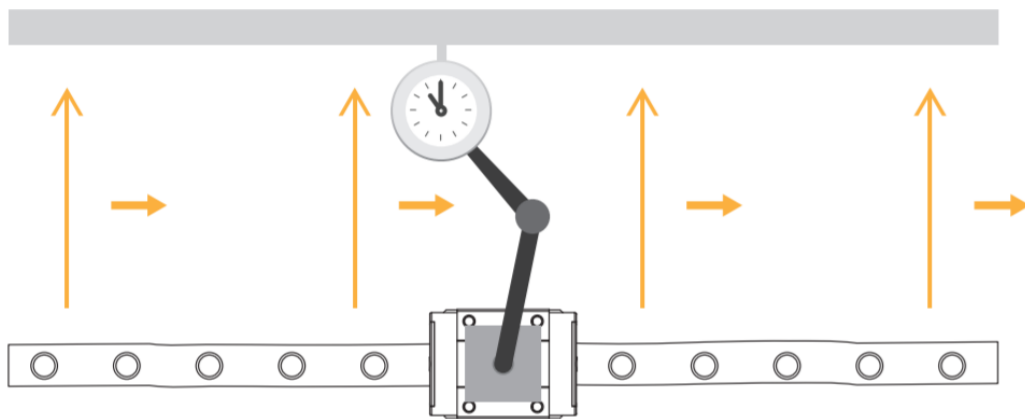


Figure 93 – Recommended assembly procedure w/o reference edges, pins or vises – from Figure 100, appendix A

Mounting Jigs

Given that current reference edges are not anywhere within the necessary tolerances means they are detrimental to proper TP assembly and improvement could probably be achieved if they were removed. To substitute them, a precise frame could be employed; this idea was taken seriously, however, another simpler idea could be that of using a reusable part (jig) to provide precisely aligned reference edges during system assembly.

This external (to the TP) part could improve assembly repeatability/reproducibility and guarantee proper parallelism alignment between the LGs without the need for constant tweaks and without incurring on substantial cost increase. It would need to be designed differently for the Baseplate-A1 and A1-A2 interfaces, would have to possess two parallel (within $2\mu\text{m}$) edges or surfaces, and have some means to ensure proper pressure between the LG and these precise edges/surfaces – the latter to eliminate small bends and guarantee the tightening procedure does not compromise the LG relative position – it would also require the elimination of the current alignment edges at both the baseplate and moving carriages.

This jig idea was selected for further concept exploration, and selected as a first approach to assembly improvement; in case it would prove to be insufficient or incapable of eliminating the majority of assembly problems than the “Precise Frame” idea would necessarily follow. Jigs concepts are detailed in Figure 94 and Figure 95.

Given the manufacturing and development activities occurring in parallel to this proposal, it was decided that the concept phase would not progress into tooling investment and testing, meaning that no final result is available on whether this jig would actually improve system assembly. Despite this, there is confidence in the value of this proposition, and the idea has been selected for future development activities.

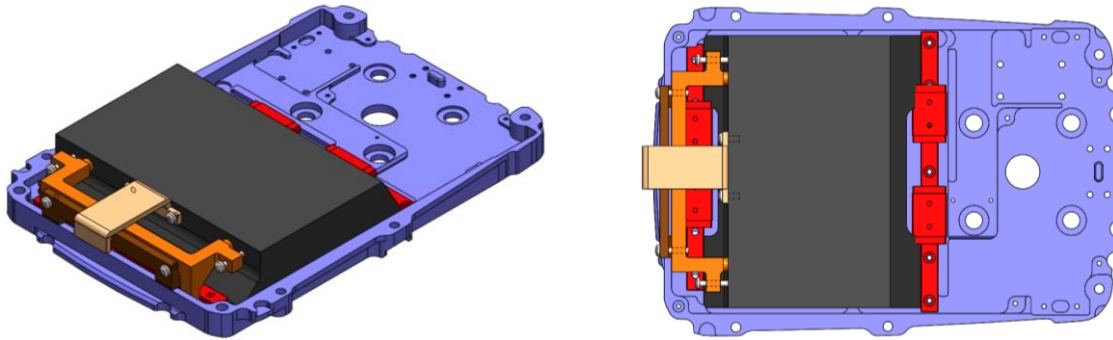


Figure 94 – Concept for Baseplate-A1 mounting jig

Both concepts are based on the linear guide rail alignment, as opposed to the previous moving block alignment. For the Baseplate-A1 interface the back linear guide would still be aligned by the baseplate reference edge – this edge serves as a datum feature and would thus not be subject to manufacturing tolerance; then the front linear guide would be positioned against the precise jig block (black block), which, in turn, would be pressed against the back linear guide rail. This back linear guide + precise block + front linear guide sequence means that as long as the precise block functional edges are machined within a $2\mu\text{m}$ parallelism tolerance, the linear guides will be positioned within a $2\mu\text{m}$ maximum parallelism deviation.

To ensure correct pressing of the precise block against the back linear guide a push system can be adjusted manually by two screws (orange piece) against the baseplate. Additionally, a brown pull system is present to ensure proper pressing of the front LG to the precise block. Recesses in the middle of the precise block allow the linear guide moving blocks to be positioned at the center while the 4 outer screws are tightened.

While the center piece is projected in aluminum, and will require precise machining, the pressing mechanism can easily be manufactured by 3D Printing for cost saving purposes – this mechanism should thus allow for a cost-effective alignment.

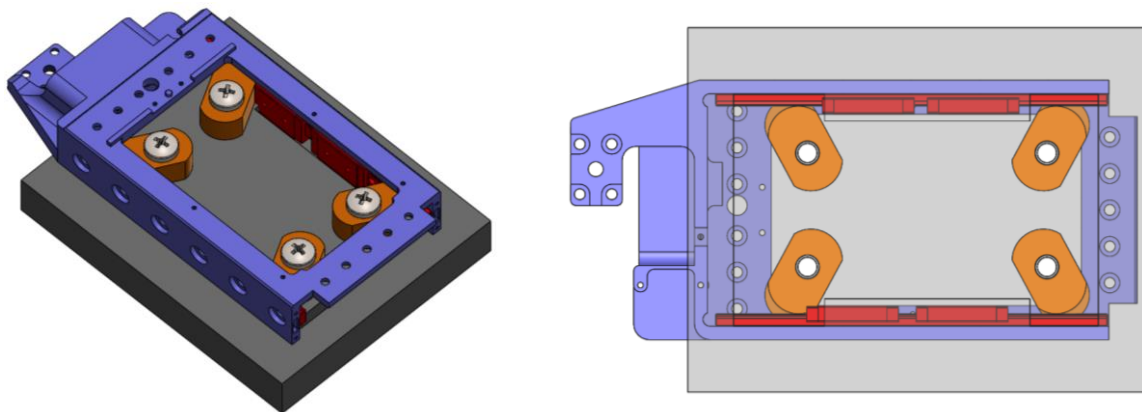


Figure 95 – Concept for A1-A2 mounting jig

A similar concept is presented for the A1-A2 interface. Using the precise (black) block as the reference edge, it would be possible to ensure linear guide alignment within a maximum parallelism deviation of $2\mu\text{m}$ if the top block surface is machined to that precision. The linear guides can be hand placed with the moving block at the center recess and the assembler can use the orange pressers to both press the linear guide against carriage A1 (by turning) as well as against the precise block (by tightening the presser screw). The same aluminum machining + 3D printed pressers' combination is intended with this concept for cost-efficiency.

The use of both these concepts can most likely help improve process repeatability and reproducibility, with only moderate impact on the assembly procedure, however, as mentioned, testing evidence to sustain this claim is still pending.

8 Conclusions and Future Work

The introductory phase of this dissertation presented the company, the system, and introduced product development. Along these initial topics, it was possible to:

- Better understand the iONE system, its development stage, its main functions, the product's mechanical architecture and how an optimization project could provide the company and its customer with additional value;
- Understand the system's main associated challenges and mechanical problems, as well as its self-characterization capabilities and how these could contribute to the current and future optimization efforts;
- Understand the system cost and part number allocation, with the main contribution sub-system and/or components being identified and a rationale being provided on whether or not an optimization could take place on those sub-systems;
- Understand the main contributing factor to the system performance;

The main goal of this project, and the bulk of this dissertation, was the identification of the main optimization opportunities and the proposal of improvement solutions. Several opportunities were found during the activities performed in the context of this project and for most of these opportunities a concept was proposed to exemplify how a design change could take place to improve on the unsatisfying areas. In this project, and for some cases, it was possible to implement these changes; these consisted in:

- Linear Encoder – Possible redesign of the foil potentiometer wiper system to reduce the total number of parts, to ensure successful readings on the full range of motion of the TP and to improve signal reliability (by reducing the “denting effect”);
- Leadscrew – Possible redesign of the nut-carriage interface to eliminate the assembly over definition and to ensure a quicker alignment between the nut and the spindle;
- Linear Guides – Possible improvement on the assembly procedure to ensure the linear guides are repeatably installed within the required position tolerances;
- Small Components – Possible redesign of small custom components used in the blue tape sub-system, as well as the clamping plates used in the PCB cables, to reduce the cost of these parts;
- Bearing Block – Possible replacement of the gears (and fixing clamps, nuts, etc.) used in the drive chain with simpler, and cheaper, alternatives;
- NGE – Possible reevaluation of the material and manufacturing process selection for the Needle Guide Extension sub-system components to improve on cost;

Some of the identified optimization opportunities were already possible to tackle with improvements. In this project, the implemented improvements, and results, were:

- Small Components – Changed the manufacturing process and material selection for these components, they are now supplied 3D Printed in PA12. Cost reduction above 90% for all three components (Pin Holder, Clamping Plate and Cover Tape Bracket);
- Linear Encoder – Redesigned linear encoder wiper system, including a quick prototype/refurbishment design meant to test for performance improvements, and a final implementation design meant to achieve maximum reduction on the number of parts and sub-system cost. The redesigned wiper showed to be capable of providing readings for the full range of motion and to improve the reading's reliability;
- Leadscrew – Changed the nut to a plastic version. This new design, after suffering a small rework from the initial concept, proved to be capable of balancing good performance with ease of assembly (given the plug interface designed to connect with the carriages). The new nut also allowed for the elimination of the assembly over definition;

Some identified optimization opportunities originated concepts with substantial improvement potential but were not possible to implement during this project's timeline given its short duration. The work regarding these improvement opportunities was the following:

- NGE – These sub-system parts were quoted for Vacuum Casting and Plastic Injection Molding in ABS-like PU and PA6, respectively. The results were promising, with cost reduction nearing 50% per component for some VC/PIM suppliers;
- Bearing Block – A concept was presented to swap the current stainless steel gear pair by two acetal gears, with noise and cost reduction benefits. The calculations showed that two plastic gears could safely fulfill the function and result in about 70% cost reduction, despite available standard gears requiring a small redesign of the bearing block to increase the inter-axis distance;
- Linear Guides – It was found that the linear guide mounting surface tolerances were insufficient and detrimental to system assembly. A mounting jig concept was proposed to allow for correct parallel mounting of the linear guides without the need for constant, iterative, position readjustments.

Some possible optimization opportunities were identified by not further analyzed during this project. These opportunities are, anyway, mentioned during the dissertation and could provide themselves to be valuable topics to be tackled in future projects. Future works could tackle the:

- PA connection – Rework the Trajectory Platform to Positioning Arm interface to allow for a quicker setup time of the equipment and to reduce the total number of custom parts (present in the current interface);
- Blue tape – Rework the sub-system to reduce the total number of parts and possibly ensure a tighter seal of the Trajectory Platform's interior;
- NGE – Redesign of the NGE to EEF interface to reduce the existing play and improve on the overall performance of the Trajectory Platform;

In addition to the work activities carried on the improvement possibilities, a FEA analysis was conducted to the EEF to support ongoing development activities. The main conclusions:

- The EEF "single pin" geometry is capable of increased functionality and satisfactory performance, thus being a superior alternative to the "twin pin" configuration, especially if the guiding joint thickness is increased;
- The EEF should be manufactured with a bulkier body to allow for more rigidity and subsequently allow for reduced medical instrument deviations during operation;

Overall, it can be considered that that the main goal of identifying potential improvements aspects for the TP system was achieved with success, with work progressing further and allowing for the implementation of improvements during this project's timeline. Additionally, the system was theoretically characterized. The EEF shows the highest potential for future improvement, especially when considering the NGE-EEF interface.

References

- Interventional-Systems. (2020). *Interventional-Systems*. Retrieved March 02, 2020, from <https://www.interventional-systems.com/>
- Materialise. (2020, May 12). *Materialise*. Retrieved April 01, 2020, from <https://www.materialise.com/en>
- Medtronic. (2020). *Stealth Autoguide*. Retrieved February 03, 2020, from <https://www.medtronic.com/us-en/healthcare-professionals/products/neurological/cranial-robotics/stealth-autoguide.html>
- MiSUMi. (2014, February 05). *Youtube - Introduction to Miniature Linear Guides*. Retrieved June 10, 2020, from <https://www.youtube.com/watch?v=SDUHO7-ghX8>
- Nóvoa, H., & Faria, J. (2019). *Apontamentos da UC de Gestão da Qualidade Total, FEUP*.
- NSK. (2020, April 25). *Precision Machine Components NSK Linear Guide*. Retrieved May 10, 2020, from <https://www.nsk.com/products/precisionmachine/linearguide/index.html>
- Pereira, J. (2019, December 3). *Desenvolvimento de Produto*.
- SPD/SI. (2020). *SPD/SI*. Retrieved May 02, 2020, from <https://www.sdp-si.com/>
- Speer, J. (2018, May 7). *The ultimate guide to Design Controls for Medical Device Companies*. Retrieved March 15, 2020, from <https://www.greenlight.guru/blog/design-controls>
- Speer, J. (2018, November 11). *Ultimate Guide to ISO 13485 Quality Management System (QMS) for Medical Devices*. Retrieved March 15, 2020, from <https://www.greenlight.guru/blog/iso-13485-qms-medical-device>
- U.S. Food & Drug Administration. (1997, March 11). *Design Control Guidance For Medical Device Manufacturers*. Retrieved March 15, 2020, from U.S. Food & Drug Administration: <https://www.fda.gov/regulatory-information/search-fda-guidance-documents/design-control-guidance-medical-device-manufacturers>
- Unknown. (2020, May 20). *conceptdraw*. Retrieved March 23, 2020, from <https://conceptdraw.com/a1739c4/preview>

Appendix A - Datasheets

GEARHEAD DATA	
Reduction	16 : 1
Absolute reduction	16/1
Max. motor shaft diameter	1.2 mm
Number of stages	2
Max. continuous torque	0.03 Nm
Max. intermittent torque	0.05 Nm
Direction of rotation, drive to output	=
Max. efficiency	81 %
Average backlash no load	1.8 °
Mass inertia	0.005 gcm ²
Gearhead length (L1)	14.1 mm
Max. transmittable power (continuous)	2.4 W
Max. transmittable power (intermittent)	3.9 W

Figure 96 – TP Maxon Gearbox GP10A 218416 datasheet extract



HOTPOT



Features

- High Life Cycle
- High Temperature Capability
- Linear Position Sensor
- IP65 Dust Proof, Water Proof (Intense Spray)
- Fiberglass Substrate
- 3M Pressure Sensitive Adhesive (PSA)
- Upon Request
 - Male or Female Nicomatic Connectors
 - Wiper of 1-3 Newton Force to Actuate Part
- Contactless Options Available



Mechanical Specifications

- Life Cycle: >10 million
- Height: ≤0.51mm (0.020")
- Actuation Force (with a 10mm wide active cavity):
 - 40°C 3.0 to 5.0 N
 - 25°C 2.0 to 5.0 N
 - +23°C 0.8 to 2.0 N
 - +85°C 0.7 to 1.8 N

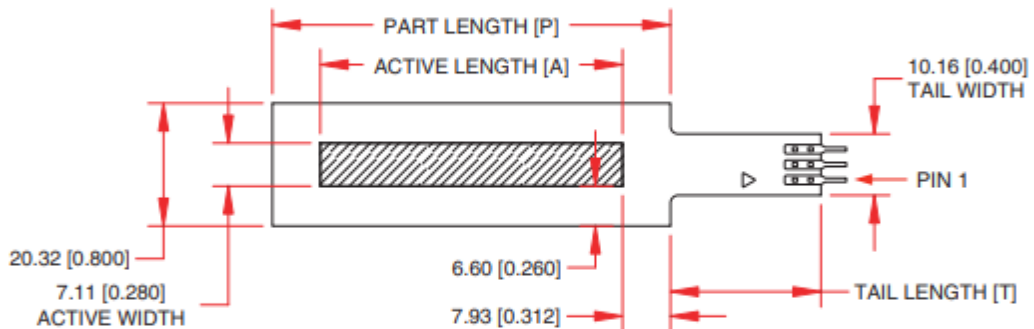
Environmental Specifications

- Operating Temperature: -40°C to +85°C
- Humidity: No affect @ 95% RH, 24hrs 60°C
- IP Rating of Active Area: IP65

Electrical Specifications

- Resistance - Standard: 10k Ohms (lengths >300mm = 20k Ohms)
- Resistance - Custom: 5k to 100k Ohms
- Resistance Tolerance: ±20%
- Effective Electrical Travel: 10 to 1200mm
- Linearity (Independent): Linear ±1% or ±3% Rotary ±3% or ±5%
- Repeatability: No hysteresis, but with any wiper looseness some hysteresis will occur
- Power Rating (depending on size, varies with length and temperature): 1 Watt max. @ 25°C, ≤0.5 Watt recommended
- Resolution: Analog output theoretically infinite; affected by variation of contact wiper surface area.
- Dielectric Value: No affect @ 500VAC for 1 minute

Dimensional Diagram - Stock Linear HotPots



A	12.50mm 0.492"	25.00mm 0.984"	50.00mm 1.969"	100.00mm 3.937"	150.00mm 5.906"	170.00mm 6.693"	200.00mm 7.874"	300.00mm 11.811"	400.00mm 15.748"	500.00mm 19.685"	750.00mm 29.528"	1000.00mm 39.370"
P	28.36mm 1.117"	40.86mm 1.609"	65.86mm 2.593"	115.86mm 4.562"	165.86mm 6.531"	185.86mm 7.318"	215.86mm 8.499"	315.86mm 12.436"	415.86mm 16.373"	515.86mm 20.310"	765.86mm 30.153"	1015.86mm 39.995"
T	12.70mm 0.500"						24.89mm 0.980"					

Figure 97 – Datasheet for the foil potentiometer

K0333

Federnde Druckstücke glatte Ausführung, Edelstahl



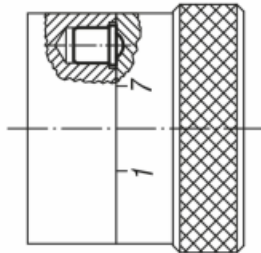
Artikelbeschreibung/Produktabbildungen



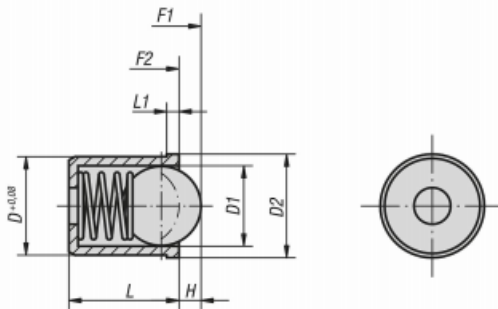
Beschreibung

Werkstoff:
Hülse und Feder Edelstahl.
Kugel Edelstahl oder POM.

Ausführung:
Hülse blank. Kugel gehärtet, blank.



Zeichnungen



Artikelübersicht

Federnde Druckstücke glatte Ausführung, Edelstahl

K0333

Federnde Druckstücke glatte Ausführung, Edelstahl



Artikelübersicht

Bestellnummer	Material Komponente	D	D1	D2	L	L1	H	Federkraft Anfang F1 ca. N	Federkraft Ende F2 ca. N
K0333.02	Edelstahl	2	1,5	2,5	3	0,6	0,4	1,2	2,5
K0333.03	Edelstahl	3	2,5	3,5	4	0,8	0,65	1,7	3,4
K0333.04	Edelstahl	4	3	4,6	5	1	0,8	3	7
K0333.05	Edelstahl	5	4	5,6	6	1	1	4	7
K0333.06	Edelstahl	6	5	6,5	7	1	1,5	6	12
K0333.08	Edelstahl	8	6,5	8,5	9	1	1,8	6	12
K0333.10	Edelstahl	10	8	12	13,5	2,5	2,7	10	20
K0333.12	Edelstahl	12	10	14	16	2,5	3,5	15	25
K0333.304	POM	4	3	4,6	5	1	0,6	3	7
K0333.305	POM	5	4	5,6	6	1	0,8	4	7
K0333.306	POM	6	5	6,5	7	1	1,3	6	12
K0333.308	POM	8	6,5	8,5	9	1	1,5	6	12
K0333.310	POM	10	8	12	13,5	2,5	2,6	10	20
K0333.312	POM	12	10	14	16	2,5	3,3	15	25

Figure 98 – Datasheet for the OTS wiper

NONMETALLIC SPUR GEARS • MODULE 0.4

ISO CLASS 8
5 mm FACE WIDTH
20° PRESSURE ANGLE

> **MATERIAL:**
Acetal

PHONE: 516.328.3300 • FAX: 516.326.8827 • WWW.SDP-SI.COM

QUALITY CLASS

METRIC COMPONENT CATALOG NUMBER
A 1P 2MY04

No. of Teeth Code

No. of Teeth Code	No. of Teeth	P.D.	D Dia.	d Bore H8	d Tolerance	D ₁ Hub Dia.
012	12	4.8	5.6	3	+0.014/0	4.5
015	15	6	6.8	3	+0.014/0	5.5
016	16	6.4	7.2	3	+0.014/0	5.5
020	20	8	8.8	3	+0.014/0	6
024	24	9.6	10.4	4	+0.018/0	8
025	25	10	10.8	4	+0.018/0	8
030	30	12	12.8	4	+0.018/0	8
032	32	12.8	13.6	4	+0.018/0	8
035	35	14	14.8	4	+0.018/0	10
036	36	14.4	15.2	4	+0.018/0	10
040	40	16	16.8	4	+0.018/0	10
045	45	18	18.8	4	+0.018/0	10
048	48	19.2	20	4	+0.018/0	10
050	50	20	20.8	4	+0.018/0	10
055	55	22	22.8	4	+0.018/0	10
060	60	24	24.8	6	+0.018/0	15
064	64	25.6	26.4	6	+0.018/0	15
065	65	26	26.8	6	+0.018/0	15
070	70	28	28.8	6	+0.018/0	15
072	72	28.8	29.6	6	+0.018/0	15
075	75	30	30.8	6	+0.018/0	15
080	80	32	32.8	6	+0.018/0	15
084	84	33.6	34.4	6	+0.018/0	15
085	85	34	34.8	6	+0.018/0	15
090	90	36	36.8	6	+0.018/0	15
095	95	38	38.8	6	+0.018/0	15
096	96	38.4	39.2	6	+0.018/0	15
100	100	40	40.8	6	+0.018/0	15
108	108	43.2	44	6	+0.018/0	15
120	120	48	48.8	6	+0.018/0	15

1

2

3

4

5

6

7

8

9

10

11

12

13

14

15

A

1-97

Figure 99 – Datasheet for SPD/SI 0.4 modulus acetal gears

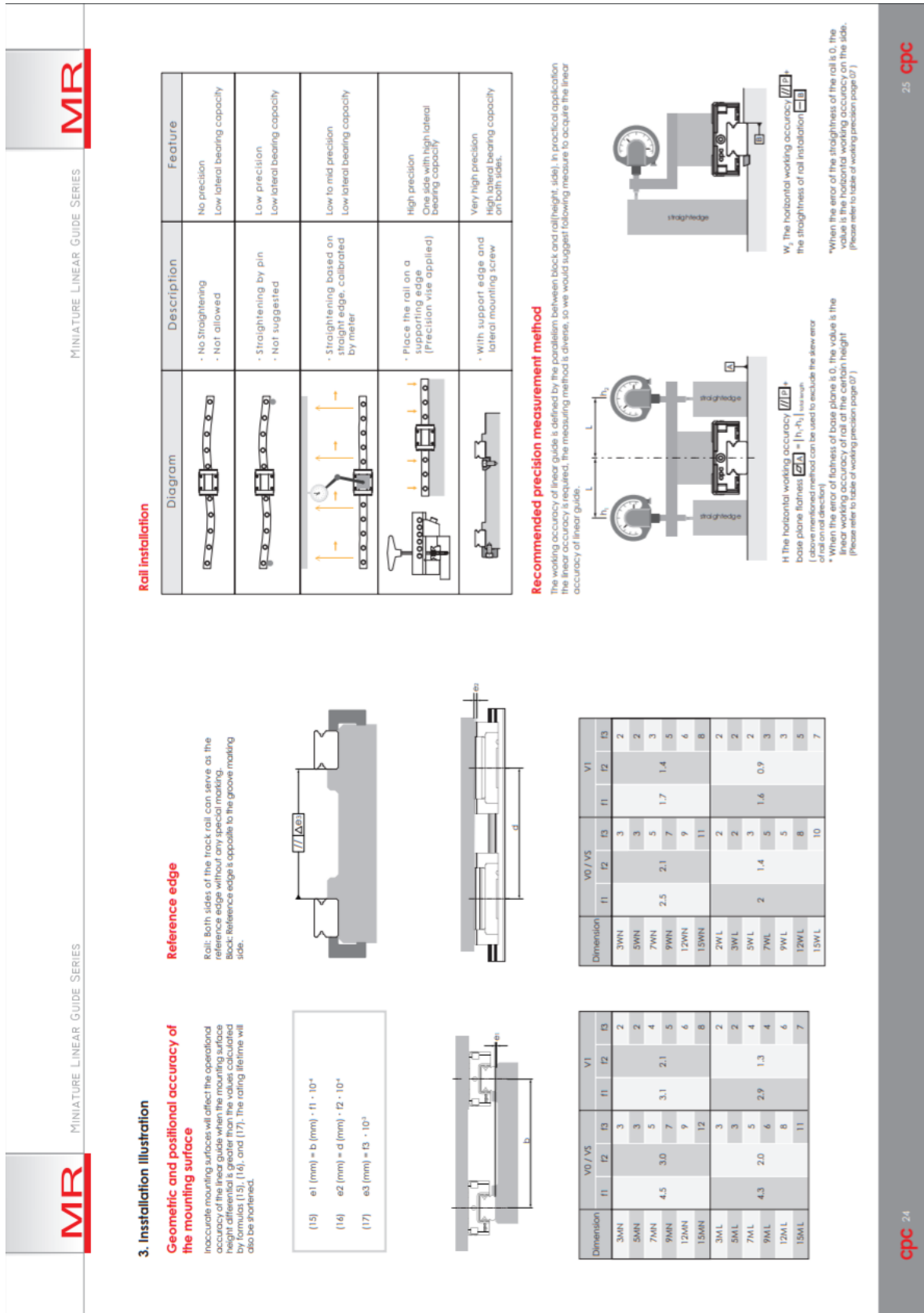


Figure 100 – Linear Guides Datasheet extract - installation

Appendix B - Calculation results according to VDI 2736

The following results have been obtained following calculations for two acetal/POM gears intended to be used in the TP – the calculations are according to VDI 2736 as well as the nomenclature. All calculations were done considering worst-case values for the running conditions as well as the strictest values of allowable stress, wear, and deformation. All values are displayed as necessary for calculating according to the VDI.

Table 11 – Calculations according to VDI 2736

Color Code:			
Input/Consideration	VDI table/graph	Calculation	Final Result
Calculations:			
Parameter	Pinion		Gear
General Parameters			
T_d	0.0140		0.0183
n	850		600
m_n	0.4		0.4
z_i	24		35
b	5		5
d	4.8		7
ω	89		63
F_t	0.0058		0.0052
v_t	214		220
E	3200		3200
ν	0.44		0.44
Z_ε	25.13		25.13
K_A	1.25		1.25
u	1.458		1.458
Tooth/Flank Temperature			
g_0	30		30
P	1.2		1.2
μ	0.28		0.28
d_a	5.2		7.4
d_b	1.959		2.857
ε	0.848		0.850
H_V	0.164		0.164
k_g	2100		2100
ED	1		1
Permitted Temp	80		80
Tooth Temp	30.04		30.02
Tooth Root Load Carrying Capacity			
K_F	1.25		1.25
Y_{Fa}	2.75		2.5
Y_{Sa}	1.65		1.75
Y_ε	0.692		0.692
Y_β	1		1
σ_{FlimN}	47		47

S_{Fmin}	2	2
Y_{St}	2	2
σ_{FG}	94	94
Permitted Stress	47	47
Actual Stress	0.011	0.010
Frictional Wear Load Capacity		
N_L	285000	285000
k_W	0.0005	0.0005
L_{Fl}	0.8	0.8
Permitted Wear	0.04	0.04
Actual Wear	0.0214	0.0193
Deformation		
Permitted Deformation	0.028	0.028
Deformation	5.5×10^{-6}	5.5×10^{-6}

N_L was calculated with basis on a worst-case scenario case study by product management for the total number of interventions and expected platform movements during lifetime. 7000 cycles were considered in the worst-case scenario of 20mm displacement.